ISTANBUL TECHNICAL UNIVERSITY ★ INFORMATICS INSTITUTE

ELUCIDATION OF CYCLOPROPENIUM ACTIVATED S_N2 REACTION MECHANISMS: A COMPUTATIONAL APPROACH

M.Sc. THESIS

Muammer Melin DEMİRKIZAK

Computational Science and Engineering Department

Computational Science and Engineering Programme

DECEMBER 2015

ISTANBUL TECHNICAL UNIVERSITY ★ INFORMATICS INSTITUTE

ELUCIDATION OF CYCLOPROPENIUM ACTIVATED S_N2 REACTION MECHANISMS: A COMPUTATIONAL APPROACH

M.Sc. THESIS

Muammer Melin DEMİRKIZAK
702121015

Computational Science and Engineering Department

Computational Science and Engineering Programme

Thesis Advisor: Assoc. Prof. Fethiye Aylin SUNGUR

DECEMBER 2015

İSTANBUL TEKNİK ÜNİVERSİTESİ ★ BİLİŞİM ENSTİTÜSÜ

SİKLOPROPENYUM AKTİVASYONLU S_N2 TEPKİME MEKANİZMALARININ AYDINLATILMASI: HESAPSAL BİR YAKLAŞIM

YÜKSEK LİSANS TEZİ

Muammer Melin DEMİRKIZAK
702121015

Hesaplamalı Bilim ve Mühendislik Anabilim Dalı

Hesaplamalı Bilim ve Mühendislik Programı

Tez Danışmanı: Doç. Dr. Fethiye Aylin SUNGUR

ARALIK 2015

Muammer Melin DEMİRKIZAK, a **M.Sc.** student of ITU **Informatics Institute** student ID **702121015**, successfully defended the **thesis** entitled "**ELUCIDATION OF CYCLOPROPENIUM ACTIVATED S_N2 REACTION MECHANISMS: A COMPUTATIONAL APPROACH**", which she prepared after fulfilling the requirements specified in the associated legislations, before the jury whose signatures are below.

Thesis Advisor :	**Assoc. Prof. Fethiye Aylin SUNGUR** İstanbul Technical University	....
Jury Members :	**Assoc. Prof. Adem TEKİN** İstanbul Technical University	....
	Assoc. Prof. Nurcan TÜZÜN İstanbul Technical University	....

Date of Submission : 27 November 2015
Date of Defense : 25 December 2015

To my family and love,

FOREWORD

This thesis is the result of my two years studying in a scientific research project. It has been totally an eye-opening and instructive period of my life. Therefore, I would like to thank my advisor Assoc. Prof. Fethiye Aylin Sungur for giving me valuable advice and support always when needed. This study would not be possible without her belief in me. She always encouraged me to strive for more and helped me to overcome any diffuculties I encountered. In addition, I'd like to thank Ayla Başaran Kınalı for her all contributions during the project. In conclusion, I greatly acknowledge TUBITAK 113Z218 for the financial support and the ITU-National High Performance Computing Center for the cpu time provided.

December 2015 Melin Demirkızak

TABLE OF CONTENTS

Page

FOREWORD ix
TABLE OF CONTENTS xi
ABBREVIATIONS xiii
LIST OF TABLES xv
LIST OF FIGURES xvii
SUMMARY xix
ÖZET xxi
1. INTRODUCTION 1
2. LITERATURE REVIEW 3
3. METHODOLOGY 11
  3.1 Density Functional Theory 11
    3.1.1 The Hohenberg- Kohn existence theorem 12
    3.1.2 The Hohenberg- Kohn variational theorem 12
    3.1.3 The Kohn-Sham method 13
    3.1.4 The Kohn-Sham energy expression 14
  3.2 Basis Set 15
  3.3 Intrinsic Reaction Coordinate 16
  3.4 Computational Details 17
4. FINDINGS AND DISCUSSION 19
  4.1 The Beckmann Rearrangement 19
    4.1.1 The Beckmann rearrangement reactions at room temperature 20
      4.1.1.1 The initiation step 20
      4.1.1.2 The self-propagating mechanism 26
      4.1.1.3 The organocatalytic mechanism 28
      4.1.1.4 The alternative organocatalytic mechanism 29
      4.1.1.5 The relationship between the experimental yield and energy barrier of the rate-determining step 33
      4.1.1.6 Benchmark study 34
    4.1.2 The Beckmann rearrangement reactions at elevated temperature 35
  4.2 Chlorodehydration of Alcohols 42
    4.2.1 Mechanism A 44
      4.2.1.1 Chlorodehydration reaction in the presence of p-methoxy-phenyl cyclopropenone 44
      4.2.1.2 Chlorodehydration reaction in the presence of m-nitro-phenyl cyclopropenone 49
      4.2.1.3 Benchmark study 52
    4.2.2 Mechanism B (alternative mechanism) 53
      4.2.2.1 Alternative chlorodehydration reaction in the presence of p-methoxy-phenyl cyclopropenone 53
      4.2.2.2 Alternative chlorodehydration reaction in the presence of m-nitro-phenyl cyclopropenone 56
      4.2.2.3 Benchmark study 59
5. CONCLUSIONS 63
CURRICULUM VITAE 71

ABBREVIATIONS

BKR **:** Beckmann Rearrangement
DFT **:** Density Functional Theory
GGA **:** Generalized Gradient Approximation
GTO **:** Gaussian Type Orbital
HF **:** Hartree Fock
HF SCF **:** Hartree Fock Self - Consistent Field
IRC **:** Intrinsic Reaction Coordinate
KS **:** Kohn-Sham
LDA **:** Local Density Approximation
LSDA **:** Local Spin Density Approximation
N/A **:** Not Available
NBO **:** Natural Bond Orbital
PES **:** Potential Energy Surface
RDS **:** Rate Determining Step
TS **:** Transition Structure

LIST OF TABLES

Page

Table 2.1 : Product distributions of chlorodehydration reaction with different catalysts 10
Table 4.1 : NBO charge values of the atoms structures located on or near the reaction coordinate in the initiation step 25
Table 4.2 : NBO charge values of the atoms structures located on or near the reaction coordinate in the self-propagating mechanism........ 27
Table 4.3 : NBO charge values of the atoms structures located on or near the reaction coordinate in the alternative organocatalytic mechanism 31
Table 4.4 : Experimental yield values and relative free energies of transition structure TS3 (Vanos and Lambert, 2010). 34
Table 4.5 : Relative electronic energy values of self-propagating and alternative organocatalytic mechanisms in the rate determining step ($\Delta E^{\#}$: Relative electronic energy values kcal/mol) 34
Table 4.6 : Experimental results of cyclopropenone catalyzed chlorodehydration reaction (Vanos and Lambert, 2011)........ 43
Table 4.7 : NBO charge values of structures located on the reaction coordinate or atoms near to reaction coordinate of chlorodehydration mechanism in the presence of p-methoxy-phenyl cyclopropenone........ 49
Table 4.8 : NBO charge values of structures located on the reaction coordinate or atoms near to reaction coordinate of chlorodehydration mechanism of m-nitro-phenyl substituted cyclopropenone........ 52
Table 4.9 : Energy values ($\Delta E^{\#}$: Relative electronic energy values kcal/mol) of the rate determing steps of chlorodehydration mechanisms in the presence of m-nitro-phenyl and p-methoxy-phenyl cyclopropenones........ 52
Table 4.10 : NBO charge values of structures located on the reaction coordinate or atoms near to reaction coordinate of Mechanism B in the presence of p-methoxy-phenyl cyclopropenone 56
Table 4.11 : NBO charge values of structures located on the reaction coordinate or atoms near to reaction coordinate of Mechanism B in the presence of m-nitro-phenyl cyclopropenone........ 59
Table 4.12 : Energy values ($\Delta E^{\#}$: Relative electronic energy values kcal/mol) of the rate determing steps of alternative chlorodehydration mechanisms in the presence of m-nitro–phenyl and p-methoxy-phenyl cyclopropenones……..60

LIST OF FIGURES

Page

Figure 2.1 : Cyclopropenium activated BKR reaction mechanisms by Lambert and co-workers. a. Organocatalytic mechanism b. Self-propagating mechanism (Vanos and Lambert, 2010) 5
Figure 2.2 : Modeled reactions by Lambert and co-workers (Vanos and Lambert, 2010) 7
Figure 2.3 : BKR reaction mechanism by Yadav and co-workers (Srivastava et al, 2010) 8
Figure 2.4 : Products of chlorodehydration reactions (Kelly and Lambert, 2009) 9
Figure 2.5 : Suggested mechanisms for chlorodehydration reactions (Vanos and Lambert 2011) 10
Figure 4.1 : Initiation step of the Beckmann rearrangement 20
Figure 4.2 : Three dimensional structures of the possible conformermers of 1,1-dichloro-2,3-4 methoxydiphenylcyclopropene and their relative energies in kcal/mol 21
Figure 4.3 : Three dimensional structures of the transition states on the initiation path 22
Figure 4.4 : Relative free energy profile of the initiation step 23
Figure 4.5 : The proposed intermediates for the self-propating mechanism 26
Figure 4.6 : Three dimensional structures of the transition states for the self-propagating mechanism 27
Figure 4.7 : Relative free energy profile of self-propagating mechanism 28
Figure 4.8 : The proposed intermediates for organocatalytic mechanism 28
Figure 4.9 : Three dimensional structures of the transition states for organocatalytic mechanism 29
Figure 4.10 : Relative free energy profile of organocatalytic mechanism.(Note: * : 4_Methoxy_DCP is determined as a starting point) 29
Figure 4.11 : The proposed intermediates for alternative organocatalytic mechanism ... 30
Figure 4.12 : Three dimensional structures of the transition states for alternative organocatalytic mechanism 31
Figure 4.13 : Relative free energy profile of alternative organocatalytic mechanism 32
Figure 4.14 : Compared relative free energy profile of self-propagating and alternative organocatalytic mechanism 33
Figure 4.15 : The proposed intermediates for organocatalytic BKR proceeding via Meisenheimer complex (Srivstava et al, 2010) 36
Figure 4.16 : Relative free energy profile of the organocatalytic mechanism proceeding via Meisenheimer complex 37
Figure 4.17 : Three dimensional structures of intermediates and transition states of the organocatalytic mechanism proceeding via Meisenheimer complex at elevated temperature. 38
Figure 4.18 : Three dimensional structures of intermediates and transition states

for the BKR turning back to self-propagating mechanism during the R-migration at elevated temperature.. 41
Figure 4.19 : Relative free energy profile of the BKR turning back to self-propagating mechanism during the R-migration at elevated temperature....................... 42
Figure 4.20 : Proposed chlorodehydration mechanism in the presence of oxalyl chloride to obtain PRODUCT I 45
Figure 4.21 : Three dimensional structures of intermediates and transition states for chlorodehydration mechanism in the presence of p-methoxy-phenyl cyclopropenone 46
Figure 4.22 : Relative free energy profile of chlorodehydration mechanism in the presence of p-methoxy-phenyl cyclopropenone 48
Figure 4.23 : Three dimensional structures of the possible conformers of m-nitro-phenyl cyclopropene and their relative energies in kcal/mol................ 49
Figure 4.24 : Three dimensional structures of intermediates and transition states for chlorodehydration mechanism in the presence of m-nitro-phenyl cyclopropenone 50
Figure 4.25 : Relative free energy profile of chlorodehydration mechanism in the presence of m-nitro-phenyl cyclopropenone 51
Figure 4.26 : The proposed intermediates for Mechanism B.................................. 53
Figure 4.27 : Three dimensional structures of intermediates and intermediates for Mechanism B in the presence of p-methoxy-phenylcyclopropenone.......... 54
Figure 4.28 : Relative free energy profile of Mechanism B in the presence of p-methoxy-phenylcyclopropenone... 56
Figure 4.29 : Three dimensional structures of intermediates and intermediates for Mechanism B in the presence of m-nitro-phenylcyclopropenone 57
Figure 4.30 : Relative free energy profile of Mechanism B in the presence of m-nitro-phenylcyclopropenone 58
Figure 4.31 : Charge distribution of I-6 and m-nitro-I6 structures 59
Figure 4.32 : Relative free energies of Mechanism A and Mechanism B in the presence of p-methoxy-phenylcyclopropenone 60
Figure 4.33 : Relative free energies of Mechanism A and Mechanism B in the presence of m-nitro-phenylcyclopropenone 61

ELUCIDATION OF CYCLOPROPENIUM ACTIVATED S_N2 REACTION MECHANISMS: A COMPUTATIONAL APPROACH

SUMMARY

Nucleophilic substitution of alcohols has a strategic importance in organic chemistry due to their wide usage in pharmaceutical industry. Despite the importance of these reactions, the traditional reagents used in the experimental studies suffer several problems including poor reactivity, hazardous by-product formation, narrow scope product formation. In 2009, as a powerful alternative to the established methods, Lambert et al. whom provides a support from a pharmaceutical industry, developed a new method for the nucleophilic substitution of alcohols. The new method based on the formation of cyclopropenium cation in situ and the activation of alcohol containing substrates through the usage of this reagent. They have demonstrated the effectiveness of this new methodology in a number of dehydration reactions including, chlorodehydration, diolcyclodehydration and Beckmann Rearrangement reactions.

Cyclopropenones were first prepared by Breslow and Volpin in 1959 which are stable precursor to cyclopropenium ions. These compounds have a number of useful qualities for applications in catalysis, which include the ability to be polarizable due to aromatic resonance form and to tune their physical and electronic properties. Despite being widespread usage, the mechanisms that they involved are not clarified yet. In this project, comprehensive density functional theory calculations were carried out to explain the experimentally proposed reaction mechanisms for chlorodehydration and Beckmann rearrangement reactions. The geometrical structures of all stationary points in the energy profile were optimized by employing the M062X functional and the 6-31+G(d,p) basis. In addition, benchmark studies were done with different functionals, methods and basis sets to validate the methodology used in the study.

The results pointed out that temperature factor takes an important role in determination of Beckmann rearrangement reaction mechanisms. Further, the alterations in the oxime and cyclopropene ring substitutents have an impact on the efficiency of the reaction. In conclusion, in chlorodehydration reactions, preferred mechanism depends on the substituents on the phenyl ring of the cyclopropenone and the results enabled us to explain the product distribution in that reactions.

SİKLOPROPENYUM AKTİVASYONLU S_N2 TEPKİME MEKANİZMALARININ AYDINLATILMASI: HESAPSAL BİR YAKLAŞIM

ÖZET

Yoğunlukla ilaç üretiminde kullanılması nedeniyle, alkollerin nükleofilik yer değiştirme tepkimeleri organik kimya içinde en çok çalışılan ve stratejik öneme sahip konulardan biridir. Bugüne kadar yapılan deneysel çalışmalarda geleneksel tepkenler kullanıldığında düşük verimle ürün elde edilmektedir. Aynı zamanda bu tepkimeler çok miktarda zararlı yan ürünün oluşumuna da sebebiyet vermektedir. Lambert ve arkadaşları yeşil kimya başlığı altında değerlendirilebilecek yeni bir sentez yöntemi ile siklopropenon varlığında alkollerin klorodehidrasyonu, Beckmann Yeniden Düzenlenmesi gibi alkollerin nükleofilik yer değiştirme tepkimelerini kapsayan bir dizi deney gerçekleştirmişlerdir. Ürünler, yüksek verim ve enantioseçicilik ile oluşmuştur. Deneyler kapsamında kullanılan siklopropenonlar ilk olarak Breslow ve Volpin tarafından 1959'da hazırlanmışlardır. Siklopropenonlardan elde edilen kararlı siklopropenyum iyonları aromatik rezonans formlarından dolayı polarize olabilmektedir. Siklopropenyum iyonu, iki pi elektronunun üç adet 2p orbitali üzerinde delokalizasyonu sonucunda pozitif yüklü ve yüksek termodinamik stabiliteye sahip bir moleküldür. Bunun yanısıra çeşitli sübstitüyelerle elektronik ve sterik ayarlanabilirliklerinin yüksek olması nedeniyle son zamanlarda oldukça yaygın olarak kullanılmaktadırlar. Yaygın kullanımlarına karşın henüz tepkime mekanizmaları aydınlatılamamış olup her iki tepkime için de deneysel veriler ışığında birden fazla mekanizma önerisi bulunmaktadır. Tez kapsamında hem Beckmann Yeniden Düzenlenmesi hem de alkollerin klorodehidrasyonu tepkimelerine ait mekanizmaların hesapsal yöntemlerle aydınlatılması amaçlanmıştır. Bunun için G09 paket programı ile yoğunluk fonsiyonel teorisi kullanılarak M062X/6-31+G** seviyesinde modellemeler gerçekleştirilmiştir. Ayrıca deneysel koşullara uygunluk sağlanması amacıyla Beckmann yeniden düzenlenmesi tepkimeleri için asetonitril çözücüsü ve klorodehidrasyon tepkimeleri için dimetilen klorür çözücüsü içinde hesaplamalar gerçekleştirilmiştir. Ayrıca farklı fonksiyonel, yöntem ve baz setleri ile kıyaslama çalışmaları yapılarak metodolojinin uygunluğu sorgulanmıştır.

Tez kapsamında, siklopropenyum varlığında gerçekleşen iki farklı tepkime modellenerek mekanizmaları aydınlatılmaya çalışılmıştır. Bunlardan ilki oksim yapısının amid yapısına düzenlenmesi olarak bilinen Beckmann Yeniden Düzenlenme tepkimesidir. Alman kimyacı Ernst Otto Beckmann'ın siklohekzanondan ara ürün olarak siklohekzanonoksim oluşturması ve sonucunda kaprolaktam elde etmesi ile tepkime literatürde yerini almıştır. Kaprolaktamın endüstride önemli bir rol oynayan Nylon 6'nın öncüsü olması Beckmann Yeniden Düzenlenme tepkimelerinin önem kazanmasını sağlamıştır. İlk bölümdeki çalışma da Lambert ve arkadaşlarının 2010 yılında yayımlamış olduğu Beckmann yeniden düzenleme tepkimesinin deneysel verileri baz alınarak modellemeler

gerçekleştirilmiştir. Üç farklı deney seti ile çalışılmıştır. İlk iki deney seti aynı oksimi içerirken, siklopropen yapılarında farklılık vardır. Son deney setinde ise kullanılan oksim farklıdır. Deneylerin verimliliği kullanılan tepkenlere göre farklılık göstermektedir. Modelleme çalışmalarımızda, bağıl serbest enerji değerlerinin azalması ile deneysel verimin artışı arasında kalitatif bir uyum görülmüştür. Literatürde oda sıcaklığında gerçekleşen deneyler için üç farklı mekanizma önerilmektedir. Kendinden ilerleyen ve organokatalitik mekanizmalarının öncesinde gerçekleşen başlangıç aşamasının hız belirleyici adımı R-göçü olup 40.9 kkal/mol bağıl serbest enerji değerine sahiptir. Başlangıç aşaması sonucunda nitrilyum katyonu ve siklopropenyum türevi oluşur. Bu aşamadan sonra kendinden ilerleyen ve organokatalitik mekanizmaları üzerinden dallanma yaşanmaktadır. Dolayısı ile nitrilyum katyonunun eldesi önceliklidir. Kendinden ilerleyen ve organokatalitik mekanizmaları için serbest enerji profilleri karşılaştırıldığında, hız belirleyici adımı daha düşük bağıl serbest enerji değerine sahip olan organokatalitik mekanizmanın daha olası olduğunu görülmüştür. Çalışmaların devamında Yadav ve arkadaşlarının 2010 yılında yüksek sıcaklıkta gerçekleştirdikleri Beckmann yeniden düzenlemesi tepkimesinin deney sonucunda önerdikleri ve Meisenheimer kompleksinden ilerlediğini öne sürdükleri mekanizma modellenmiştir. Modelleme çalışmaları sırasında önerilen mekanizma harici farklı mekanizmaların olasılığı ortaya çıkmıştır. Elde edilen veriler tepkimenin hem Meisenheimer kompleksi üzerinden ilerleyebileceğini hem de R-göçü adımı sonrasında kendinden ilerleyen mekanizmaya dönebileceğini göstermiştir. Ayrıca başlangıç aşaması için önerilen alternatif yol ile hız belirleyici adımın bağıl serbest enerji değeri hem oda sıcaklığında hem de yüksek sıcaklıkta yaklaşık 20 kkal/mol değerinde bulunmuştur. Bu da Lambert'in önermiş olduğu R-göçü adımı değerinden yaklaşık 20 kkal/mol daha düşük bir değerdir. Ayrıca, çalışmalar sırasında asidik ortamın Meisenheimer kompleksinin oluşumunu kolaylaştırdığını ve geçiş konumu sonrasında HCl'in desteklediği kompleks yapısı ile geçiş konumu yapısı arasında 0.8 kkal/mol olduğu görülmüştür. Fernandez ve arkadaşlarının söylediğinin aksine ara ürün yapısısından HCl'in ayrılmasını takiben Meisenheimer kompleksi lokal minima olarak elde edilebilmiştir.

Tezin ikinci bölümünde Lambert ve grubu tarafından 2011 yılında deneyleri gerçekleştirilen siklopropenon katalizörlü klorodehidrasyon tepkimesine ait çalışmadaki ürün dağılımını ve tepkime mekanizmasını aydınlatmak üzere hem p-metoksidifenilsiklopropenon hem de m-nitro-difenilsiklopropenon varlığında modelleme çalışmaları gerçekleştirilmiştir. Literatürde oda sıcaklığında gerçekleşen deneyler için iki farklı mekanizma önerilmektedir. Elde edilen sonuçlar, p-metoksidifenilsiklopropenon ile gerçekleştirilen klorodehidrasyon tepkimesinde ÜRÜN I eldesi için A mekanizmasından ilerlemesinin olasılığının daha yüksek olduğunu ancak B Mekanizmasının hız belirleyici adımının bariyer yüksekliğinin de oda sıcaklığında aşılamayacak bir değere sahip olmadığını göstermiştir. Deneylerde m-nitrodifenilsiklopropenon kullanıldığında gözlemlenen ÜRÜN II artışı, B Mekanizmasında ÜRÜN II eldesine kadar olan mekanizmanın gerçekleşme olasılığının ÜRÜN I'in oluşumuna olanak tanıyan A Mekanizmasına göre daha fazla olmasından kaynaklandığı gösterilmiştir.

Kullanılan yöntem ve baz setlerinin kıyaslanabilmesi için post HF yöntemlerinden MP2 olmak üzere BMK ve wB97XD gibi farklı yoğunluk fonksiyonel teorisine ait fonksiyoneller ve de yüksek bir seviyeye sahip 6-311+G** baz seti ile tek nokta enerji hesabı yapılmıştır. Bu hesaplamaların sonucunda, tez kapsamında tercih edilen

yoğunluk fonksiyonel teorisi yönteminin ve kullanılan M062X fonksiyoneli ile 6-31+G** baz setinin uyumlu olduğuna karar verilmiştir.

Elde edilen sonuçlar, Beckmann Tepkimelerinde sıcaklık faktörünün tepkime mekanizmalarında etkin rol oynadığını göstermektedir. Klorodehidrasyon tepkimelerinde deneysel olarak önerilen mekanizmaların siklopropenon üzerindeki sübstitüyeye bağlı olarak tercih edilirliğinin değiştiği gösterilmiş ve sonuçlar ürün dağılımındaki farklılıkların açıklanabilmesini sağlamıştır. Son olarak, Beckmann yeniden düzenlenmesi ve klorodehidrasyon tepkimelerinin siklopropenon varlığında yüksek egzergonisiteye sahip olduğu görülmüştür.

1. INTRODUCTION

Nucleophilic substitution of alcohols has a strategic importance in organic chemistry due to their wide usage in pharmaceutical industry. Despite the importance of these reactions, the traditional reagents used in the experimental studies suffer several problems including poor reactivity, hazardous by product formation, narrow scope product formation. In addition, traditional methods show a poor enantioselectivity in the presence of catalyst. In 2005, the ACS Green Chemistry Institute and the pharmaceutical industry representatives came together to declare their support for "Green Chemistry" studies.

In their list of key research areas, OH activation for nucleophilic substitution of alcohols is in the first place. These reactions have been used since many years due to their cheapness and easier conductance. However, they caused formation of hazardous byproducts (Constable et al. 2007).

In 2009, as a powerful alternative to the established methods, Lambert et al. whom provides a support from a pharmaceutical industry, developed a new method for the nucleophilic substitution of alcohols (Lambert and Kelly, 2009). The new method based on the formation of cyclopropenium cation in situ and the activation of alcohol containing substrates through the usage of this reagent. They have demonstrated the effectiveness of this new methodology in number of dehydration reactions including, chlorodehydration, diolcyclodehydration and Beckmann Rearrangment reactions. The reactions ended up with a good yield and high stereoselectivity under mild and convenient conditions. During the cyclopropenium activation process, cyclopropene is prone to degrade to cyclopropenium ion with loss of chloride ion due to the aromatic stabilization of the resulting cyclopropenium ions. The electron deficient cyclopropenium is combined with an hydroxylic substrate to produce the activated intermediates. Cyclopropenium activated alcohol intermediate is used both for the chlorodehydration and Beckmann reactions via nucleophilic displacement mechanism.

Yadav et al. have also studied the cyclopropenium activated Beckmann Rearrangement reaction of alcohols (Srivastava et al. 2010). Two researchers have published their works simultaneously. Yadav could not observe an imidoyl chloride intermediate during the course of this work. Therefore he suggested an organocatalytic mechanism for the Beckmann rearrangement. However, Lambert stated that the reaction may be self-propagating rather than organocatalytic (Vanos and Lambert, 2010).

Based on an experimental study by Lambert et al. related to the chlorodehydration of alcohols, it is stated that, alcohols react with an activating agent oxalyl chloride and provide formation of byproduct (Kelly and Lambert, 2011; Vanos and Lambert, 2011). In this regard, two different reaction mechanisms were proposed in the presence of cyclopropenone.

The mechanism is still unidentified for both reactions. In the scope of the thesis, experimentally proposed reaction mechanisms for chlorodehydration and the Beckmann rearrangement reactions were studied computationally in order to elucidate mechanisms. The geometrical structures of all stationary points in the energy profile are optimized at the M062X/6-31+G(d , p) level of theory including solvent effects. The elucidation of the reaction mechanisms will give an idea to synthetic chemists those are working with electron deficient cyclopropenium ions and the Beckmann rearrangement and chlorodehydration reactions of alcohols.

2. LITERATURE REVIEW

Cyclopropenones are precursors of cyclopropenium ions which are the smallest member of Hückel aromatic systems. Cyclopropenones were synthesised for the first time by Breslow and Volpin nearly 50 years ago. (Zhao et al, 2011; Breslow et al, 1959; Breslow and Peterson 1960; Kursanov et al, 1959). These three membered ring structures, namely cyclopropenium ions, have marvellous physical and chemical properties like the stability derived from the delocalization of the two-pi electrons over three 2p orbitals and possessing an ionic charge that leads to high reactivity towards anions. Therefore, cyclopropenium ions are widely used in many reactions, recently. Beckmann rearrangement and chlorodehydration reactions are the examples of this situation (Srivastava et al, 2010; Vanos and Lambert, 2010; Vanos and Lambert, 2011).

In 2009, Lambert and co-workers used cyclopropenium ion as an organocatalyst to convert alcohols into the corresponding alkylchlorides in which the stability of cyclopropenium ion is explained by the delocalization of two pi electrons over three 2p orbitals (Kelly and Lambert, 2009). Despite the apparent molecular strain inherent in such a small ring, this type of cation is known to have considerable thermodynamic stability and ionic charge. Thus, such aromatic cations readily combine with an anion or a Lewis basic heteroatom causing reversible generation of the corresponding neutral carbocycles species (Kelly and Lambert, 2009). Since then, these thermodynamically highly stable, electron deficient ions are used for various nucleophilic substitution reactions. (Kelly and Lambert, 2009; Vanos and Lambert, 2010; Vanos and Lambert, 2011).

Scientists tend towards new strategies under the scope of green chemistry. The first organocatalytic BKR reaction was carried on by Ishihara et al. in which cyanuric chloride (2,4,6-trichloro-1,3,5-triazine) was used as an organocatalyst for the conversion of acetophenone oxime to the corresponding amide. The proposed mechanism proceeds over a Meisenheimer complex in the solvent acetonitrile at reflux temperature (Furuya et al, 2005).

In this continuation, attracted by the unique reactivity profile of the cyclopropenium ion and knowing the fact that liquid phase BKR usually proceeds under the conditions of electrophilic activation of the oxime hydroxyl group, Yadav et al. reasoned that cyclopropenium ion is a well-suited electrophic species for activation of the oxime hydroxyl group facilitating the transformation of ketoximes into amides/lactams. In their study, cyclopropenones are used as an organocatalyst that are the precursors of the cyclopropenium ions. In the experiment, 1,1-dichloro-1,2-diphenylcyclopropene and $ZnCl_2$ were added to a solution of ketoxime in dry acetonitrile. Then, the reaction mixture was heated. Yadav et al. could not observe neither imidoyl chloride nor 2,3-diphenylcyclopropenone intermediate during the course of that work. An organocatalytic mechanism via formation of a Meisenheimer complex was suggested based on their observations in the experiment (Srivastava et al, 2010).

After a short while Lambert et al. published a study similar to Yadav et al. based on the organocatalyzed BKR with cyclopropenium ion and its products (Vanos and Lambert, 2010). In the study, experiments were conducted at room temperature and in the presence of nitromethane or acetonitrile solvents. A better yield was observed when 1,1-dichloro-1,2-dixylylcyclopropene or p-methoxy-phenyl substituted cyclopropene were used. Lambert et al. proposed two different mechanisms based on experimental results : organocatalytic and self-propagating mechanisms as distinct from the previous study by Yadav et al. (Vanos and Lambert, 2010) (Figure 2.1).

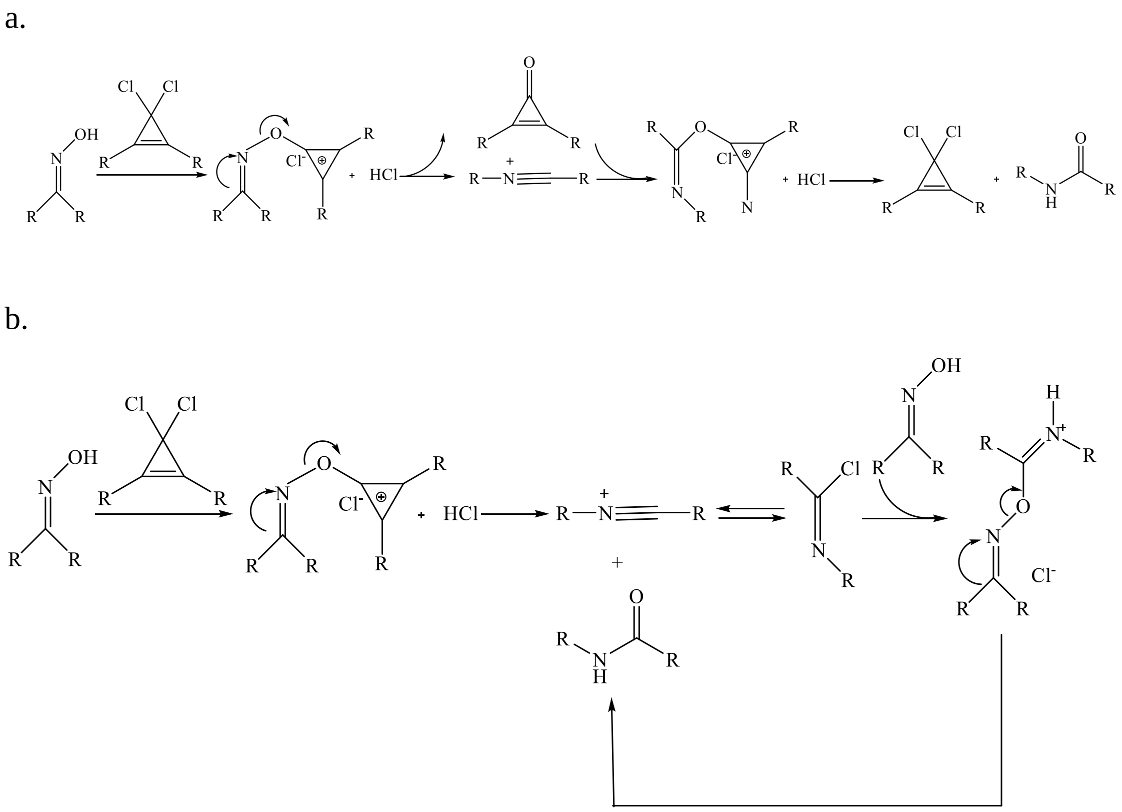

Figure 2.1 : Cyclopropenium activated BKR reaction mechanisms by Lambert and co-workers. a. Organocatalytic mechanism b. Self-propagating mechanism (Vanos and Lambert, 2010).

The organocatalytic mechanism proposed by Lambert starts with the nucleophilic attack of the oxime to cyclopropenium ion and cyclopropeniumoxime is obtained as an intermediate. As R migration of cyclopropeniumoxime turns to nitrilium cation and cyclopropenone moves away. In the next step, cyclopropenium imidate can occur in the consequence of alkylation of expelled cyclopropenone of nitrilium cation. Imidate converts to amide after some changes on it. The structure of this mechanism is in accord with the mechanism that Ishihara has proposed an organocatalytic mechanism for the cyanuric chloride. According to another situation, nitrilium cation or imidoyl chloride can alkylate the oxime directly and get a midproduct. Subsequently, the midproduct can turn to amide and provide the regeneration of nitrilium ion. This mechanism is called self-propagating mechanism.

Two more experiments were made in order to find the most propabable mechanism. In the first experiment, acetophenone oxime, 2,3-dimesitylcyclopropenone and oxalyl chloride were used. However, only oxalate ester occured, none of the BKR products were observed. It means that cyclopropenone can not compete with the oxime nucleophilically. The second experiment which was tried on 50°C, it was observed a high yield in the presence of HCI and imidoyl chloride in the conversion of benzophenone oxime to the BKR product. In addition to that, the imidoyl chloride was detected with ^{1}H NMR in the presence of cyanuric chloride. According to the results of these experiments, Lambert et al. suggested a self-propagating mechanism instead of an organocatalytic mechanism. Nevertheless, some suspicions remain due to the fact that Yadav realized his BKR study at elevated temperatures (Vanos and Lambert, 2010).

Eriksson et al. modeled the Beckmann rearrangement reaction with the benzophenoneoxime and p-toluenesulfonyl chloride structures (An et al, 2013). In this work, they proposed a new self-propagating mechanism similar to Lambert and Chapman's self-propagating mechanism (Vanos and Lambert, 2010; Chapman, 1935). In their second study, they used five organocatalyts such as cyanuric chloride (CNC), triphosphazene (TAPC), bis(2-oxo-3-oxozolidinyl) phosphinic chloride (BOP-Cl), TsCl and 1,1-dichloro-1,2-diphenylcyclopropene (CPI-Cl) to investigate probable reaction mechanisms. However, effect of temperature was not included to calculations. It should be noticed that the complete understanding of the reaction mechanism based on the reaction conditions. Thus, there are still doubts on the reaction mechanism.

NMR experiments have demonstrated that Meisenheimer complexes may only be formed as stable species if a very nucleophilic reagent attacks to the very electron-deficient substrates (Boga et al, 2005). Previous computational studies have shown that formation of Meisenheimer complexes in basic medium were dependent on how much an aryl halide was activated by electronwithdrawing substituents (Jones et al, 2013). It has been also stated that Meisenheimer complexes exist in shallow minima, and ether formation is a fast process where the computed stationary points on potential energy surfaces may be identified as a transition state rather than a local energy minima (Fernandez et al, 2010; Glukhotsev et al,1997) A debate on Meisenheimer complexes still continues.

In the thesis, all of the experimentally proposed paths either at room or at elevated temperatures are investigated in detail for the cyclopropenium activated Beckmann rearrangement mechanism. Organocatalytic and self-propagating mechanisms are modeled with the compounds studied during the Lambert et al.'s experiments in 2009 (Figure 2.2). The first experimental set, in other words, the reaction of p-methoxy-phenyl substituted cyclopropenium and acetophenone oxime is choosen in order to elucidate the mechanism (Figure 2.2 A). Other oximes and cyclopropenes that are taken into consideration during the course of this computational work enable us to explain the impact of the alterations in the oxime and cyclopropene ring substitutents on the efficiency of the reaction. BKR via Meisenheimer complex formation suggested by Yadav et al. is also modeled in the presence of acetophenoneoxime and p-methoxy-phenyl substituted cyclopropenium at elevated temperature to fulfill the scope of this study (Figure 2.3).

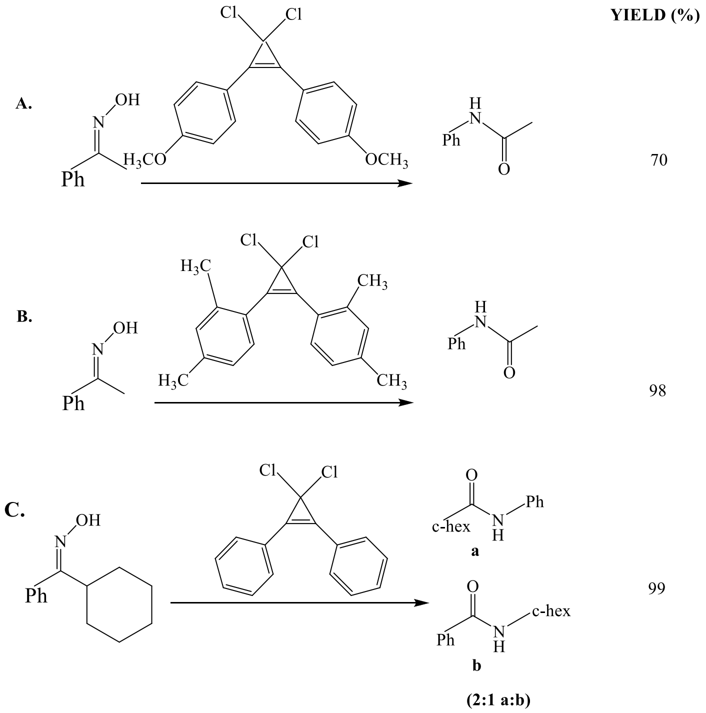

Figure 2.2 : Modeled reactions by Lambert and co-workers (Vanos and Lambert, 2010).

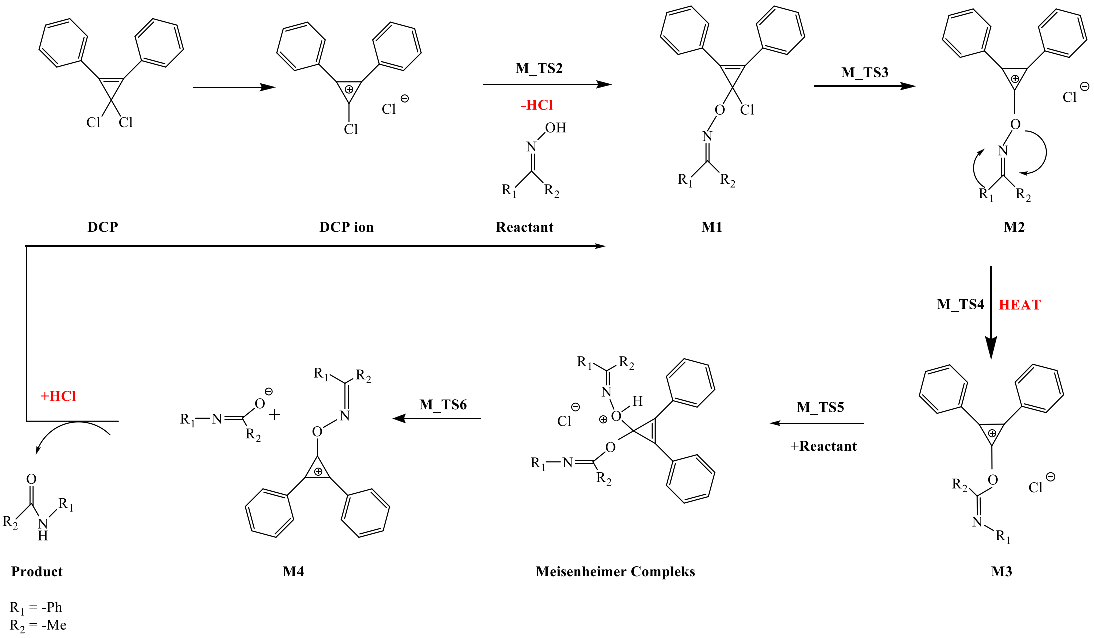

Figure 2.3 : BKR reaction mechanism by Yadav and co-workers (Srivastava et al, 2010).

In the second part of the thesis, chlorodehydration of alcohols reactions were modeled based on the experimental studies by Lambert et al. (2011). The nucleophilic substitution of alcohols has an important place in the field of organic synthesis. A great amount of products could be obtained via these reactions. The most flexible and efficient method is Mitsunobi reactions for the nucleophilic transformations of alcohols (Mitsunobu and Yamada, 1967). This reaction proceeds via alkoxy phosphonium and provides usage of different nucleophiles such as carboxylic acid, phenol, amide and azide. Although different phosphine reactives can be used, triphenylphosphine is usually preferred. The necessity of separating byproducts from the last product creates the biggest disadvantage of this method. Hence, Denton and co-workers developed a new method in order to separate the phosphine oxide from mixture of reaction (Denton et al, 2010). They showed that, phosphine which is the undesirable byproduct of Mitsunobi reaction could be used to catalyze the chlorodehydration reaction. Recently, alternative methods have been developed due the fact that byproducts cause the formation of environmental waste. Firstly, in 2009, Lambert et al. performed a quite similar study to Denton's phophine oxide activated nucleophilic substitution reaction. They offered a new approach for dehydration reactions based on the facile formation of cyclopropenium ions. They activated chlorodehydration of alcohols reactions with cyclopropenones (Kelly and Lambert, 2009). In recent studies, $AlCl_3$ has been used for the chlorination of aromatic primary and secondary alcohols and it has been reported that, a high yield is obtained as a consequence of it (Ma et al, 2012). However, Lambert’s study has milder conditions. In 2014, a similar study was done by Bekensir et al. in the presence of chloro tropylium chloride for the formation of alkyl and acyl chloride (Nguyen and Bekensir, 2014).

The first experiment which was done by Lambert et al. in 2009 is substantial for chlorodehydration reactions, as well as Beckmann rearrangement reactions (Kelly and Lambert, 2009). As a result of performed studies, many patents have been received and cyclopropenones began to be called as organocatalysts. According to the proposed mechanism, a cyclopropene (Figure 2.4, Structure 1) with two geminal substitutents (X) exists in equilibrium with cyclopropenium salt (Figure 2.4, Structure 2) and cyclopropenyl ether occurs with the addition of alcohol substrate to cyclopropenium salt (Figure 2.4, Structure 3). Finally, a cationic ether (Figure 2.4, Structure 4) provides formation of product (Figure 2.4, Structure 5) and cyclopropenone (Figure 2.4, Structure 6) with the nucleophilic substitution.

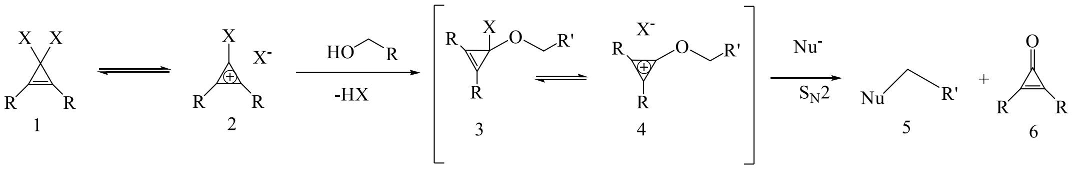

Figure 2.4 : Products of chlorodehydration reactions (Kelly and Lambert, 2009).

In the next study by Lambert and his group, cyclic ether is obtained from the cyclopropenium ion activated diol cyclodehydration reaction too (Kelly and Lambert, 2011). In the same year, another experimantal study by Lambert et al. related to the chlorodehydration of alcohols has reported that by-products form as a consequence of the reaction between oxalyl chloride as activation reagent and alcohol (Figure 2.5) (Kelly and Lambert, 2011).

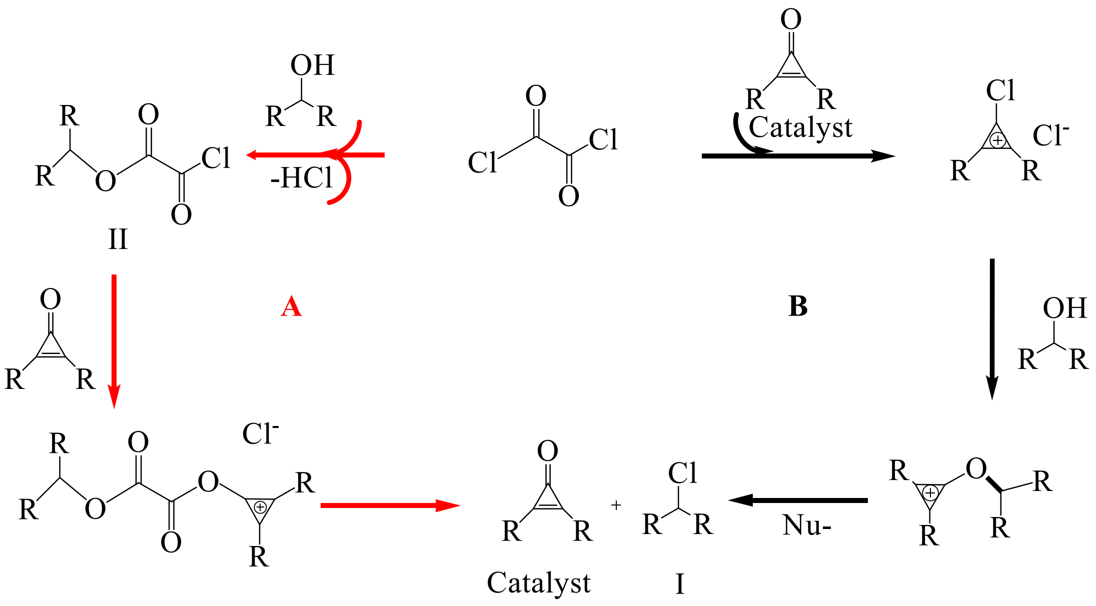

Figure 2.5 : Suggested mechanisms for chlorodehydration reactions(Vanos and Lambert, 2011).

In the experiments, product distribution was also investigated by changing the substituents on the phenyl rings of cyclopropenones. When an electron-withdrawing substituent was added, efficiency of the catalyst decreased and structure II formed as an intermediate. On the other hand, the presence of an electron-donating substituent increased the ratio of I: II (Table 2.1).

In the second part of the thesis, elucidation of chlorodehydration reaction mechanism of alcohols was aimed. In this regard, the structures belonging to Mechanism A and B as shown in Figure 2.5 were optimized at the M06-2X/6-31+G** level of theory including dichloromethane as a solvent.

Table 2.1 : Product distributions of chlorodehydration reaction with different catalysts.

R	I(%)	II(%)
No catalyst	0	100
p-MeO-Ph	>98	<2
m-NO_2Ph	14	86

3. METHODOLOGY

3.1 Density Functional Theory

In Density Functional Theory (DFT), electron density is the quantity of interest. The total energy is a unique functional of the electron density. Pierre Hohenberg and Walter Kohn that states that *the energy and all other properties of a ground-state molecule are uniquely determined by the ground-state electron probability density ρ(r).* The ground-state electronic energy E_0 is a functional of ρ. Then, it can be written as

$$E_0 = E_0 \ [\rho\ (\vec{r})] \qquad \textbf{(3.1)}$$

Kohn and Sham developed this theory and formulated a method called Kohn-Sham orbitals. Kohn-Sham orbitals are expressed within a basis set of functions and a determinant is formed from these functions.

While Hartree-Fock calculations depend on spatial and spin coordinates of all N electrons which scale as N4, DFT is only interested in a single function of a single spatial coordinate. Thus, computations are faster than HF calculations. In addition, DFT incorparates electron correlation that will lead to the more accurate results.

The problem behind of DFT is that energy functional is not known. A simple approach is local density approximation (LDA). The main idea of LDA is the assumption that the density locally can be treated as a uniform electron gas and total ensemble is electrically neutral. Local spin density approximation (LSDA) is used for high-spin systems. A more complex set of functionals depend on the electron density and also the first derivative of electron density. These method is called generalized gradient approximation (GGA). Non-uniform gas is used to improve LDA. There are also hybrid methods that were introduced by Becke combine functionals Hartree-Fock exact exhange functional and exchange-correlation density functionals. GGA and hybrid approximations have a higher accuracy (Computational chemistry: a practical guide for applying tehniques to real-world problems, 2001, p.42, 43).

3.1.1 The Hohenberg- Kohn existence theorem

In DFT, electrons interact with eachother and with an external potential $V_{ext}\ (\vec{r})$. *The external potential $V_{ext}(r)$ is uniquely determined within a trivial additive constant by the ground state electron density $\rho(r)$.*

Proof : Let's think two external potential $V_{ext}\ (\vec{r})$ and $V'_{ext}(\vec{r})$, both of them gives the same $\rho(\vec{r})$ for its ground state. Two different Hamiltonians are $\widehat{H}$ and $\widehat{H}'$ and each Hamiltonian will be associated with different a ground-state wave functions Ψ and Ψ'. Taking Ψ' as a trial wave function for the $\widehat{H}$ problem,

$$\begin{aligned} E_0 < \langle \Psi' | \widehat{H} | \Psi' \rangle &= \langle \Psi' | \widehat{H}' | \Psi' \rangle + \langle \Psi' | \widehat{H} - \widehat{H}' | \Psi' \rangle \\ &= E'_0 + \int \rho(\vec{r})\ [V_{ext}\ (\vec{r}) - V'_{ext}(\vec{r})]\ d\vec{r} \end{aligned} \tag{3.2}$$

where E_0 and E'_0 are the ground-state energies for $\widehat{H}$ and $\widehat{H}'$, respectively. If Ψ is taken as a trail function for the $\widehat{H}'$,

$$\begin{aligned} E'_0 < \langle \Psi | \widehat{H}' | \Psi \rangle &= \langle \Psi | \widehat{H} | \Psi \rangle + \langle \Psi | \widehat{H}' - \widehat{H} | \Psi \rangle \\ &= E_0 + \int \rho(\vec{r})\ [V_{ext}\ (\vec{r}) - V'_{ext}(\vec{r})]\ d\vec{r} \end{aligned} \tag{3.3}$$

Adding equation (3.2) and equation (3.3), $E_0 + E'_0 < E'_0 + E_0$ is obtained. It creates a contradiction. This is an evidence for existence of a unique $V_{ext}\ (\vec{r})$ that gives the same $\rho\ (\vec{r})$ for their ground state (Essentials of Computational Chemistry, 1961, p. 252, 253).

3.1.2 The Hohenberg- Kohn variational theorem

The second Hohenberg and Kohn theorem states that the expectation energy value must be greater than or equal to the true ground-state energy. A variational principle is satisfied by the density. The variational principle can be applied to the ground state (Essentials of Computational Chemistry, 1961, p. 254).

$$E_{cand} \geq E_0 \tag{3.4}$$

3.1.3 The Kohn-Sham method

Hohenberg and Kohn proved that ground-state electronic energy of a molecule is a functional of electron density ρ. However, $E_0\,[\rho]$ is not known. Thus, Kohn and Sham developed approximations to find $E_0\,[\rho]$. According to the Kohn-Sham method, an unreal reference system should be built. (to refer the unreal reference system, *s* subscript will be used as a notation) In this system, there are some important rules:

The system has the same number of electrons (*n*) with the molecule it is studied. Electron- nuclei attraction is ignored and it is assumed that electrons do not interact eachother. Each electron has a potential energy, $v_s\,(x_i, y_i, z_i)$ *i=1,2,...,n*. The real form of v_s is unknown. Electron density of the reference system is the same as electron density of the real system.

In the scope of these rules, the Hamiltonian s of the reference system is the sum of Hamiltonians of the individual electrons:

$$\begin{gathered}\hat{H}_S = -\frac{\hbar^2}{2m_e}\sum_{i=1}^{n}\nabla_i^2 + \sum_{i=1}^{n} v_s\,(x_i, y_i, z_i) \equiv \sum_{i=1}^{n}\hat{h}_i^{KS} \\ \hat{h}_i^{KS} \equiv -\frac{\hbar}{2m_e}\nabla_i^2 + v_s\,(x_i, y_i, z_i)\end{gathered} \tag{3.5}$$

Here, $\hat{h}_i^{KS}$ is the one-electron Kohn–Sham Hamiltonian. The Kohn–Sham orbitals θ_i^{KS} are eigenfunctions of $\hat{h}_i^{KS}$

$$\hat{h}_i^{KS}\,\theta_i^{KS} = \varepsilon_i^{KS}\,\theta_i^{KS} \tag{3.6}$$

where ε_i^{KS} is the Kohn–Sham orbitals of θ_i^{KS}.

Probability density ρ can be expressed as a sum of the probability densities $|\theta_i^{KS}|^2$ of the individual orbitals. Thus,

$$\rho = \rho_s = \sum_{i=1}^{n} |\theta_i^{KS}|^2 \tag{3.7}$$

3.1.4 The Kohn-Sham energy expression

The ground-state energies of the molecules and the unreal reference system are different. Kohn and Sham express the energy as the sum of five terms shown in the following equation, respectively the average electronic kinetic energy in the reference system, the average potential energy of attractions between the electrons and the nuclei in the molecule, classical energy of electrical repulsion, the internuclear repulsion energy and exchange–correlation energy functional which is is a functional of electron probability density.

$$E_e =< K_{e,s} > +< V_{ne} > +J + V_{NN} + E_{xc}[\rho] \tag{3.8}$$

Here, V_{NN} is a constant term that depends on the nuclear charges and the internuclear distances.

$E_{xc}[\rho]$ can be expressed like that,

$$E_{xc}[\rho] \equiv < K_e > - < K_{e,s} > + < V_{ee} > - J \tag{3.9}$$

As it can be understood from the equation (3.9) the difference of the average electronic kinetic energy in the molecule and in the reference system is added to the difference of the average potential energy of interelectronic repulsion and the classical repulsion energy. In shortly, exchange–correlation energy term is the difference of between the non-interacting system and the real system. If equation (3.9) is written in equation (3.8), the following equation is obtained:

$$E_e =< K_e > +< V_{ne} > +< V_{ee} > +V_{NN} \tag{3.10}$$

Thus,

$$\widehat{H}_e = \widehat{K}_e + \widehat{V}_{ne} + \widehat{V}_{ee} + \widehat{V}_{NN} \tag{3.11}$$

Finding molecular electronic ground state energy depends on the Kohn-Sham orbitals θ_i^{KS}.

In one electron Kohn-Sham Hamiltonian is defined as the sum of one-electron kinetic energy operator and potential energy. The potential energy v_s includes the potential energy of electron-nucleus attraction, the potential energy of electron-electron repulsion and v_{xc} exchange- correlation potential terms. Exchange-correlation potential is functional derivative of exchange-correlation energy functional.

$$v_{xc}(x, y, z) = \frac{\delta E_{xc}}{\delta \rho} \quad \textbf{(3.12)}$$

When $E_{xc}[\rho]$ is known, exchange- correlation potential can be obtained easily.

(Physical Chemistry, 2009, p. 711,712,713, 714, 715).

3.2 Basis Set

A basis set is expressed as a set of mathematical functions (basis functions). A linear combination of these basis functions which their coefficients are determined by the HF SCF calculation create molecular orbitals. Increasing number of basis functions enable to represent the wavefunction better. However, in practice use of an infinite basis set is not possible and use of an infinite complete set of functions cause to approach the HF limit (Essentials of Computational Chemistry, 1961, p.166).

There are a list of basis sets: minimal basis sets, Pople basis set, correlation consistent basis sets, double, triple, and quadruple zeta basis sets, plane wave basis sets (Computational Chemistry and Molecular Modeling, 2008, p.124).

The Pople basis sets are one of the most used basis sets in the field of computational chemistry and are indicated by the notation X-YZG. This notation means that each core orbital is described by a single contraction of X GTO primitives and each valence shell orbital is described by two contractions, one with Y primitives and the other with Z primitives. 3-21G, 3-21G*, 3-21+G*, 6-31G, 6-31G**, 6-31+G* are the examples of Pople basis sets. These basis sets are a split-valence double-zeta basis sets since they include two numbers after the hyphens. Moreover, split-valence triple basis sets that have three numbers of the hyphens exist such as 6-311+G, 6-311+G** and etc.

Polarization functions can be added to the Pople basis sets. They denote by one or two asterisks. The meaning of one asterisk is that a set of d primitives have been added to atoms heavy atoms. Two asterisks mean that a set of p primitives have been also added to light atoms like hydrogen and helium. s orbitals can polarize if it is mixed with p orbitals and p orbitals can polarize if it is mixed with d orbital. Thus, polarization functions should be used be included in all calculations. As they gain flexibility to wave functions, they provide to obtain more accurate computed geometries and vibrational frequencies.

Diffuse functions can be also added to the Pople basis sets by a plus sign. According to the the notation, one or two plus signs can be used. A single plus sign means that one set of s and p type gaussian with the same exponents have been added on heavy atoms. The second plus sign indicates that diffuse functions are used for all atoms by adding one diffuse s and p type gaussian on heavy atoms and one diffuse s type gaussian on hydrogens. Diffuse functions that have very small exponents are used to hold the electron far away from the nucleus. Use of diffuse functions are necessary for anions, Rydberg states, very electronegative atoms like fluorine.Moreover, they are used to obtain accurate description of weak bonds such as hydrogen bonds and binding energies of van der Waals complexes. Basis sets are also called augmented basis sets when they are used with diffuse functions (Computational chemistry: a practical guide for applying tehniques to real-world problems, 2001, p.81,82).

3.3 Intrinsic Reaction Coordinate

The intrinsic reaction coordinate (IRC) has a widespread usage in the field of quantum chemistry since it provides to have an opinion about the mechanism of the reactions. IRC traces the reactant and product from the transition structure. It builds a unique reaction path.

Intrinsic reaction coordinate is defined as the path of steepest descent in mass-weighted Cartesian coordinates. The IRC approach proposed by Fukui is based on the classical equations of motion. Fukui noted that the IRC represents the vibrationless–rotationless motion path of the reacting system (Fukui, 1970, 1981).

IRC tries to solve the following differential equation:

$$\frac{dq(s)}{ds} = -\frac{g(s)}{|g(s)|} \tag{3.13}$$

Here q is the mass-weighted Cartesian coordinates, s is the direction of IRC and g is the mass-weighted gradient vector (Maeda et al, 2015).

3.4 Computational Details

The geometry optimizations and the frequency calculations was performed with the M062X functional and the 6-31+G(d,p) basis set (Zhao and Truhlar; 2006, 2008). The transition states are ascertained by vibrational analysis with only one imaginary frequency mode. The pathway for the reaction was obtained at the M06-2X/6-31+G(d,p) level by using the intrinsic reaction coordinate (IRC) with mass-weighted coordinates (Gonzales and Schlegel; 1989, 1990).

The solvent used in the experimental works were acetonitrile for Beckmann rearrangement reactions and dichloromethane for chlorodehydration reactions. Therefore, the dielectric constants were used 37.5 for acetonitrile and 8.93 for dichloromethane.

The study is conducted using Gaussian'09 (G09) program package on a cluster with 32 computation nodes, AMD Opteron(tm) Processor 6380 (Frisch et al, 2009). The solvation effect of acetonitrile is considered by using the polarizable continuum model (PCM) of the Tomasi group as implemented in G09 (Miertus et al, 1981). The energies that are reported in the text are the thermal free energies obtained with solvent optimization calculations unless otherwise stated. Charges of atoms are calculated with NBO (Reed et al, 1998).

Single point energy calculations with M062X/6-311+G(d,p), BMK/6-31+G(d,p), MP2/6-31G+(d,p) and wB97XD/6-31G+(d,p) were done to analyze suitability of the basis set and the methodologies for the systems studied (Frisch et al, 1990; Boese and Martin, 2004; Chai and Head-Gordon, 2008). The graphical representations were obtained using CYLview program.

4. FINDINGS AND DISCUSSION

4.1 The Beckmann Rearrangement

Since the discovery of the Beckmann rearrangement (BKR) in 1886, the reaction has become a powerful tool in the syntheses of amides and lactams from their corresponding oximes. The high industrial impact of BKR came from the caprolactam production which is a precursor of Nylon 6. The conventional reaction conditions are severe which require high temperatures and strongly acidic and dehydrating media leading to the formation of the large amounts of byproducts (Kopple and Katz, 1959). Scientists tend towards new strategies under the scope of green chemistry. In a recent study on BKR by Yadav et al., the product was obtained with a better yield and high stereoselectivity with an efficient organocatalysis process (Srivastava et al, 2010). In their study, cyclopropenones are used as an organocatalyst that are the precursors of the cyclopropenium ion. The experiment was realised by Yadav et al. in the presence of 1,1-dichlorodiphenylcyclopropene, acetophenoneoxime, $ZnCl_2$ as a co-catalyst for the optimum yield and acetonitrile solvent at reflux temperature (80 °C). Yadav et al. could not observe neither imidoyl chloride nor 2,3-diphenylcyclopropenone intermediate during the course of that work. Based on the hypothesis for organocatalytic Beckmann Rearrangement by Ishihara et al., an organocatalytic mechanism via formation of a Meisenheimer complex in the presence of cyclopropenium ion was suggested.

After a short while Lambert et al. published a study similar to Yadav et al. based on the organocatalyzed BKR with cyclopropenium ion and its products (Vanos and Lambert, 2010). In the study, experiments were conducted at room temperature and in the presence of nitromethane or acetonitrile solvents. A better yield was observed with 1,1-dichloro-1,2-dixylylcyclopropene relative to p-methoxy-phenyl substituted cyclopropene. Lambert et al. proposed three different mechanisms based on experimental results : organocatalytic and self-propagating mechanisms as distinct from the previous study by Yadav et al. (Vanos and Lambert, 2010).

Depending on the experimental and computational studies in the literature, BKR was studied at room temperature at three main titles: Self-propagating, organocatalytic and alternative organocatalytic mechanisms. BKR was studied at elevated temperature via formation of Meisenheimer complex.

4.1.1 The Beckmann rearrangement reactions at room temperature

4.1.1.1 The initiation step

The proposed mechanisms either self propagating or organocatalytic start with an initiation step, where 1,1-dichloro-2,3-4-methoxydiphenylcyclopropene (4-Methoxy DCP) readily loses Cl^- to form 4-Methoxy DCP ion. The reaction then proceeds with the nucleophilic attack of the oxime to the 4-Methoxy DCP ion forming a cationic intermediate, Structure I2 (Figure 4.1). The formation of a nitrilium ion via R migration step completes the initiation step. The reaction path is then branched off into three depending on the proposed role of the cyclopropenium ion.

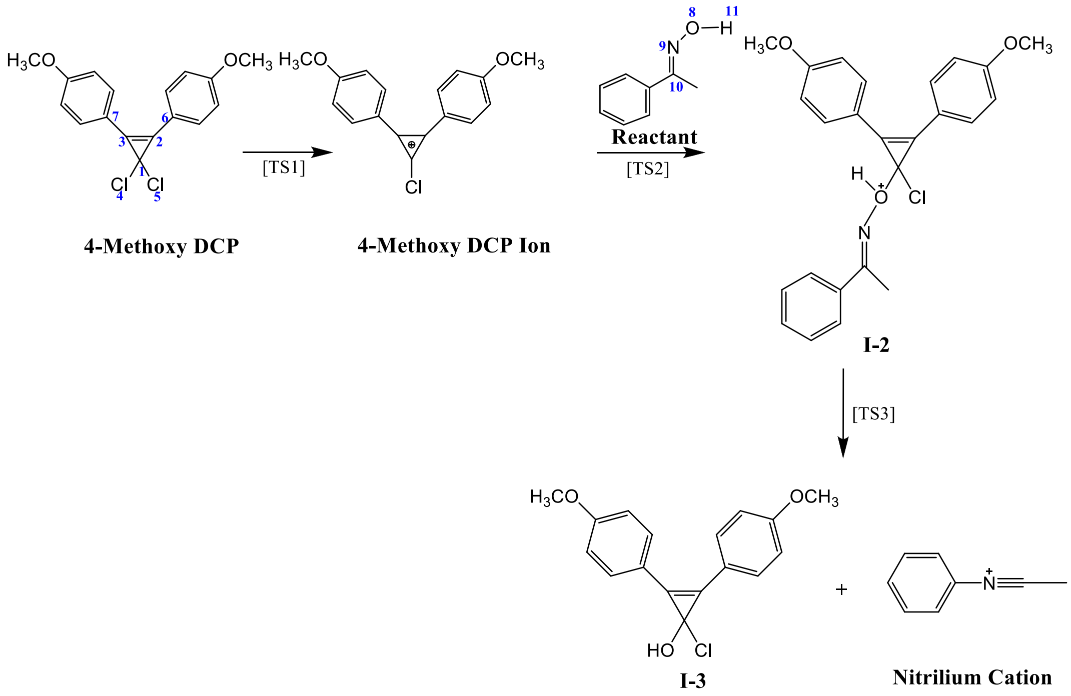

Figure 4.1 : Initiation step of the Beckmann rearrangement.

The possible conformers of 1,1-dichloro-2,3-4-methoxydiphenylcyclopropene (4-Methoxy_DCP) were scanned at M062X level of theory using 6-31+G** basis set to identify the lowest energy conformer which will be used in the proceeding reaction steps. The conformers and their relative energies are shown in Figure 4.2. The lowest energy conformer is structure C1. Other possible conformers have relative energies of +0.50 and +0.75 kcal/mol with respect to the lowest energy conformer. Despite the fact that the small energy differences will raise almost equally populated conformers, structure C1 is chosen as the reacting conformer. In structure C1, the length of the two identical bonds of cyclopropene ring is 1.44 Å where the C2-C3 bond length is 1.32 Å (Figure 4.2).

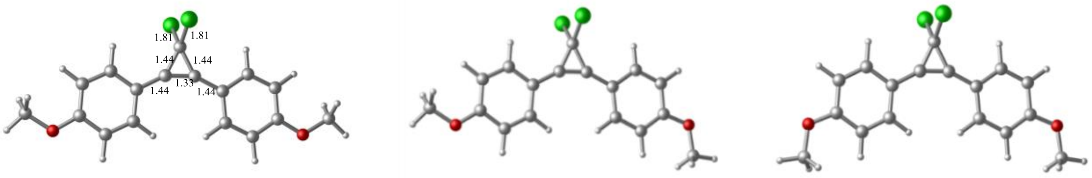

C1 (0.00) C2 (+0.50) C3(+0.75)

Figure 4.2 : Three dimensional structures of the possible conformers of 1,1-dichloro-2,3-4 methoxydiphenylcyclopropene and their relative energies in kcal/mol.

The formation of a cyclopropenium ion with C1-Cl5 bond breaking is modeled via structure TS1 having a relative free energy of 11.3 kcal/mol. (Figure 4.3, Figure 4.4) The distance between C1 and Cl5 is elongated to 2.47 Å as chlorine leaves and the length of C-C bonds within the three membered ring became almost equal (C-C = 1.37 Å) in structure TS1 (Figure 4.3a). Product-like transition state structure TS1 supports Hammond’s Postulate (Hammond, 1955).

The formation of a cyclopropenium ion (4-MethoxyDCP ion) is an endothermic process having a reaction energy of 5.4 kcal/mol (Figure 4.4). The stability of 4-MethoxyDCP ion is derived from the delocalization of the two-pi electrons over three 2p orbitals. There are two identical C-C bonds having a length of 1.36 Å in the ion and the length of the third C-C bond is 1.40Å (Figure 4.3b**)**. The geometrical parameters are an indication of delocalized electrons on the three membered ring system. The NBO charge results are tabulated in Table 4.1. As chlorine, Cl5, leaves the Cl4 which is bound to C1 becomes positively charged in the 4-MethoxyDCP molecule. Not only the chlorine, positive charges on the ring atoms are also increased. As chlorine leaves, the hybridization scheme of C1 turns out to be sp^2 facilitating the delocalization on the ring thereby enhancing the stabilization of the cyclopropenium ion (4-MethoxyDCP ion). The delocalization on the ring can be also deduced from the NBO second order perturbation energies. Pi electrons of C1 atom of 4-MethoxyDCP ion create stabilization energy over C2 and C3 atoms. The stabilization energy of cyclopropenium ion is higher than the stabilization energy that transition structure TS1 has**.** The delocalization from C2-C3 bonding orbitals to C1-Cl4 antibonding orbitals with a value of 41.2 kcal/mol is the highest stabilization within the molecule.

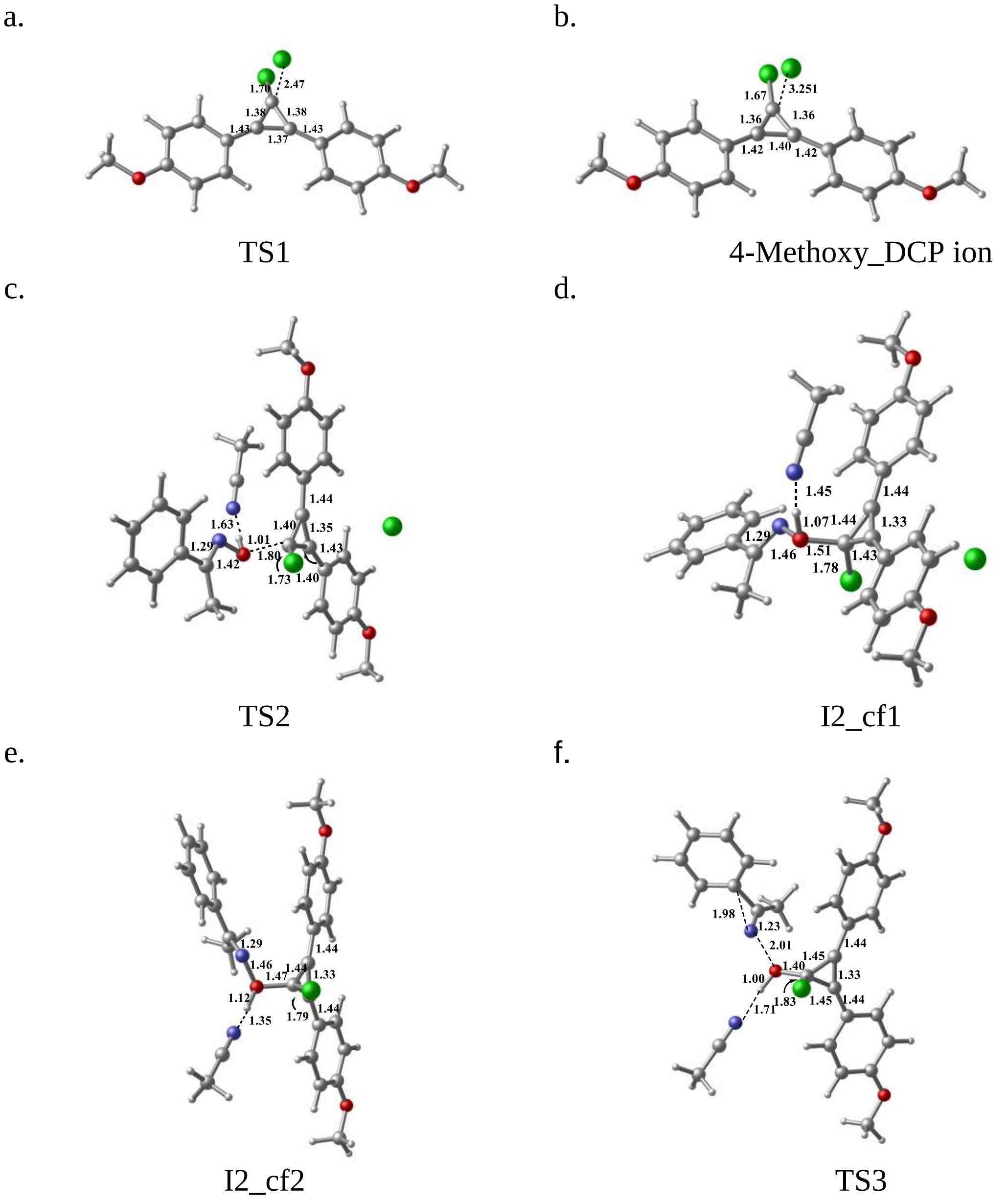
1.70
2.47
1.38
1.38
1.43
1.37
1.43
1.67
3.251
1.36
1.36
1.42
1.40
1.42
1.44
1.63
1.40
1.35
1.01
1.29
1.80
1.43
1.42
1.73
1.40
1.45
1.44
1.07
1.44
1.33
1.29
1.46
1.51
1.43
1.78
1.29
1.44
1.46
1.47
1.44
1.33
1.12
1.44
1.35
1.79
1.98
1.23
2.01
1.44
1.45
1.00
1.40
1.33
1.71
1.83
1.45
1.44

a.

TS1

b.

4-Methoxy_DCP ion

c.

TS2

d.

I2_cf1

e.

I2_cf2

f.

TS3

Figure 4.3 : Three dimensional structures of the transition states on the initiation path.

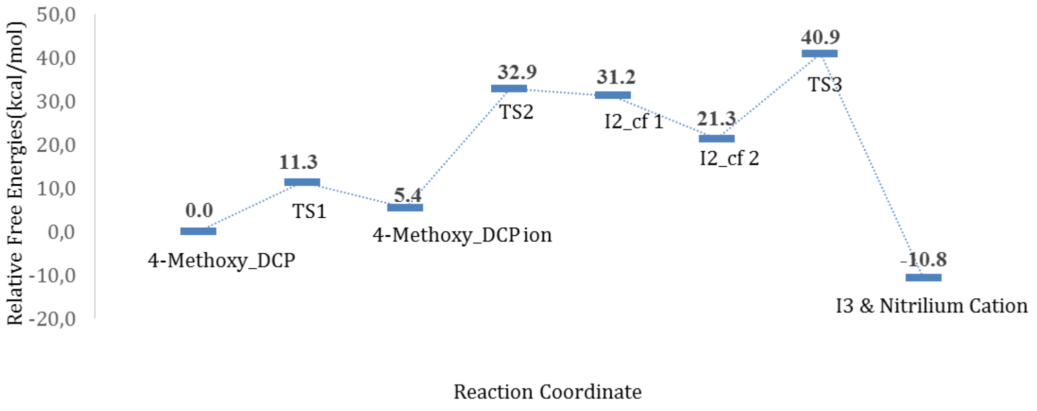

Figure 4.4 : Relative free energy profile of the initiation step.

The second step is the S_N2 like substitution reaction between the acetophenoneoxime; reactant, and the cyclopropenium ion to form the cationic species (Figure 4.3c). The oxygen of the acetophenoneoxime (O8) attacks to the C1 of 4-Methoxy DCP ion with a distance of 1.80 Å (Structure TS2**)**. The presence of a solvent molecule, MeCN, creates an extra stabilization over the transition state structure TS2 by the formation of a long range interaction between H11 and N12 of the MeCN leading to the formation of I2_cf1 with an energy barrier of 27.5 kcal/mol. A lower energy conformer, I2_ cf2 is obtained with a rotation around C2C1O8N9 (ϕ) dihedral angle from 153° to -72°. The intermediate structure I2_cf2 has a relative free energy of 21.3 kcal/mol. The stabilization of the I2_cf2 comes from the pi-pi interactions between the two phenyl rings. Further stronger hydrogen bondings occur as solvent molecule gets nearer (1.35 Å).

The initiation step is completed by the migration of the R group to the N9 (phenyl group) and the cleavage of N9-O8 bonds which leads to the formation of the nitrilium cation and I3. The rate determining step of the initiation step has a relative free energy of 40.9 kcal/mol. This barrier is 6.7 kcal/mol higher relative to the computational study by Eriksson et al. on the reaction between acetophenone and 1,1-dichloro-1,2-dihenylcyclopropene (Tian et al, 2013). The difference may stem from the presence of methoxy groups on the para position of the phenyl rings on the catalyst. Since methoxy groups on the para position is far to the reaction center, it is not possible to raise the energy barrier by steric effect. If the charges are investigated, it can be seen that, negative charges on the atoms has increased. For the NBO charges of C6 atom vary from -0.139 to -0.199 and the NBO charges of C7 atom from -0.135 to -0.182. The differences on O8 and C1 atoms draw the attention.It is clear that, electronic effect has caused an increase in energy barriers The initiation step as a whole is an exergonic process.

Eriksson and co-workers studied the BKR reaction mechanism in the presence of acetonitrile as well as Yadav. Lambert et al. conducted their study in the presence of nitromethane. Since acetonitrile is used explicitly, proton transfers supported by acetonitrile are realised with the interactions of probable hydrogen bond. Although the dielectric constants of the solvents (acetonitrile 37,5 and nitromethane 35.6) are close to eachother, much lower energy barriers could be obtained by use of acetonitrile explicitly. Therefore, transition state structure TS3 which is found to be a rate determining step in the initiation part of the mechanism modeled in the presence of nitromethane solvent, too. The obtained relative free energy value is 42.8 kcal/mol and it is only 1.9 kcal/mol higher than TS3 in the presence of acetonitrile. It will not cause a dramatic effect on the ultimate results. In conclusion, to be able to cite to the values of Eriksson et al. and model the mechanism proposed by Yadav et al., acetonitrile was used during the studies.

Table 4.1 : NBO charge values of the atoms structures located on or near the reaction coordinate in the initiation step.

	C1	C2	C3	Cl4	C6	C7	Cl5	O8	H11	N9	C10	N12
4-Methoxy_DCP	-0.124	0.053	0.059	-0.079	-0.143	-0.159	-0.079					
TS1	0.039	0.134	0.127	0.125	-0.186	-0.170	-0.758					
4-Methoxy_DCP ion	0.035	0.183	0.176	0.178	-0.199	-0.182	-0.989					
Acetophenone oxime								-0.637	0.538	-0.174	0.225	
TS2	0.108	0.101	0.105	0.077	-0.169	-0.173		-0.558	0.563	-0.187	0.305	-0.465
I2_cf1	0.168	0.055	0.063	-0.020	-0.163	-0.163		-0.503	0.555	-0.186	0.335	-0.465
I2_cf2	0.178	0.057	0.043	-0.044	-0.144	-0.163		-0.503	0.543	-0.181	0.330	-0.458
TS3	0.213	0.037	0.034	-0.119	-0.140	-0.140		-0.721	0.563	-0.040	0.325	-0.464

4.1.1.2 The self-propagating mechanism

In the proposed self-propagating mechanism, dimerization step between reactant and nitrilium cation (I4) is followed by the deformation of the intermediate structure (I4) where the corresponding ketone is formed as a product as a final step (Figure 4.5). The role of the cyclopropenium ion is limited with the formation of the nitrilium cation in the initialization step of the whole process and that is why the mechanism is called as self-propagating mechanism.

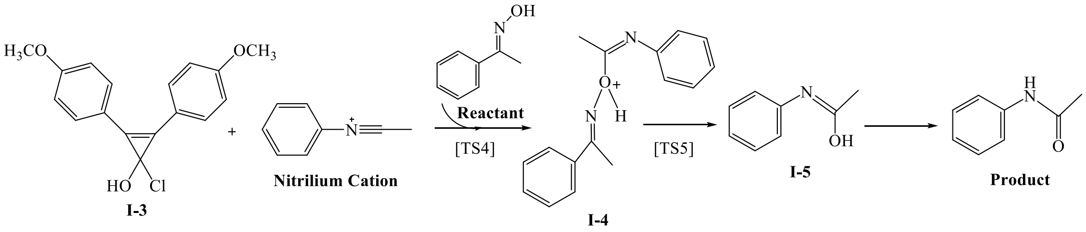

Figure 4.5 : The proposed intermediates for the self-propagating mechanism.

The reaction starts with the attack of partially negatively charged (-0.665) O8' on acetophenoneoxime to positively charged (+0.705) C10 of nitrilium cation (Figure 4.6a). The attack is modeled via the transition state structure TS4. In structure TS4, the presence of strong hydrogen bond interactions between H11 atom on the substrate and the nitrogen atom on the solvent facilitate the formation of transition state structure TS4 which energy barrier is calculated to be 13.5 kcal/mol (Figure 4.7). In the obtained intermediate I4, the length of C10-O8' bond is 1.40 Å . The positive charges on H11 atom and negative charges on O8' atom decrease after transfer of the proton (H11) to the nitrogen of the solvent (Table 4.2).

In the last step, the N9' and O8' bond is broken and a transfer of the phenyl group to the N9' and a reverse transfer of the proton (H11) to the O8' is seen simultaneously to obtain the nitrilium cation. The step, which consists of a bond cleavage and a formation of two bonds is found to be rate determining step having an energy barrier of 19.1 kcal/mol (Figure 4.7). The obtained products are nitrilium cation and the iminol (I-5). It is stated that the the conversion of iminol into amide occur easily and rapidly in room temperature. The self-propagating path has high exergonicity and an irreversible process at room temperature. The obtained activation energies are in harmony with a study by Eriksson et al. (Tian et al, 2013).

Table 4.2 : NBO charge values of the atoms structures located on or near the reaction coordinate in the self-propagating mechanism.

	N9	C10	H11’	N12	O8’	N9’	C10’
R			0.538		-0.637	-0.174	0.225
R and Nitrilium Cation	-0.237	0.705	0.549	-0.459	-0.665	-0.177	0.225
TS4	-0.359	0.664	0.562	-0.466	-0.600	-0.179	0.291
I4	-0.510	0.648	0.500	-0.440	-0.489	-0.167	0.294
TS5	-0.493	0.628	0.564	-0.479	-0.688	-0.037	0.320

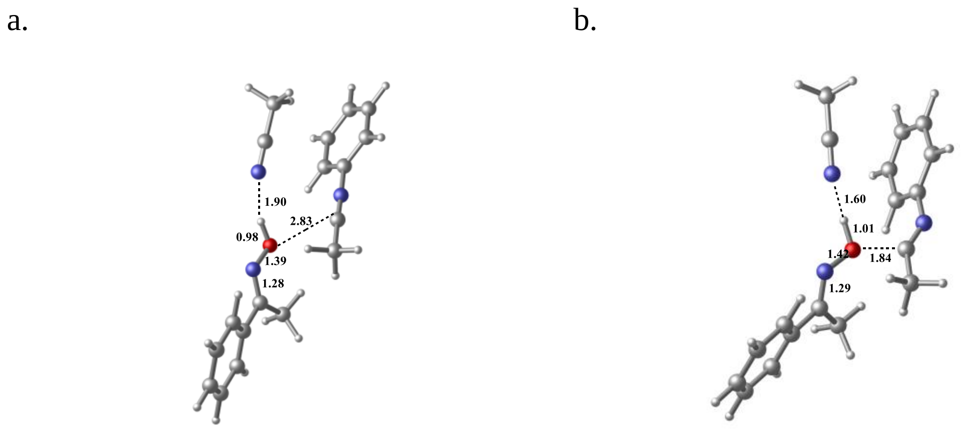
a.
b.
1.90
2.83
0.98
1.39
1.28
1.60
1.01
1.42
1.84
1.29

R and Nitrilium Cation

TS4

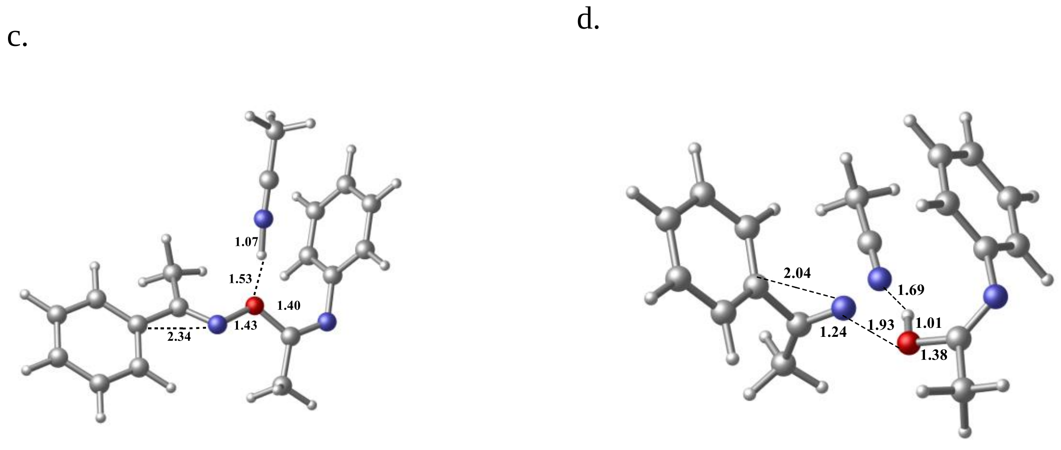
c.
d.
1.07
1.53
1.40
1.43
2.34
2.04
1.69
1.93
1.01
1.24
1.38

I4

TS5

Figure 4.6 : Three dimensional structures of the transition states for the self-propagating mechanism.

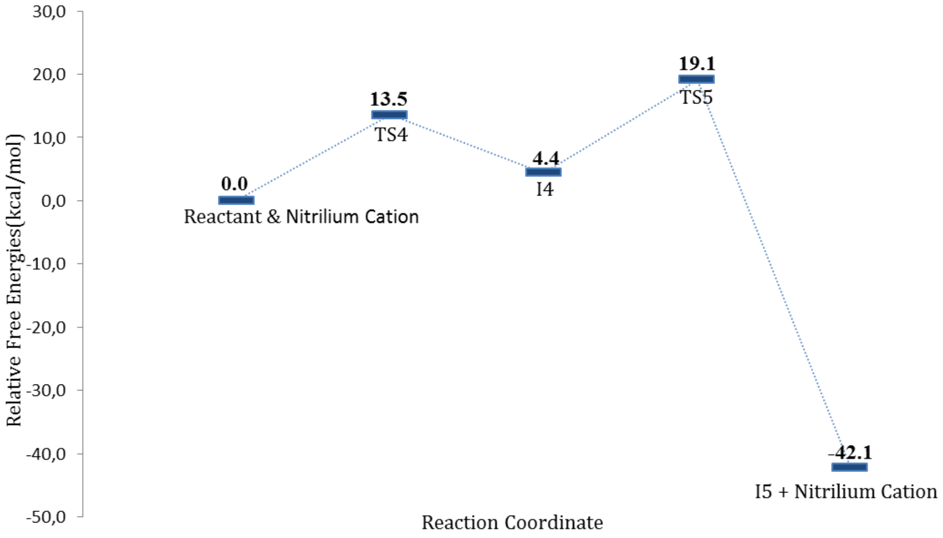

Figure 4.7 : Relative free energy profile of self-propagating mechanism.

4.1.1.3 The organocatalytic mechanism

One of the proposed organocatalytic mechanisms proceeds with the intermediate, structure I-2 that occured by the nucleophilic attack of the hydroxyl group on the reactant in the initialization step. I-2 readily loses its proton for the formation of II-2 which should occur barrierless in the presence of the solvent molecule (Figure 4.8). In the obtained structure II-2, C1-Cl bond is elongated to 3.14 Å (Figure 4.9a). The cyclopropenone intermediate (II-6) and nitrilium cation are obtained via transition state structure TS6 in which N-O covalent bond is broken and R migration occurred simultaneously. TS6 has a high relative free energy of 49.0 kcal/mol (Figure 4.10). Further steps in the reaction path were not modeled since it is not possible to overcome such a high energy barrier at room temperature.

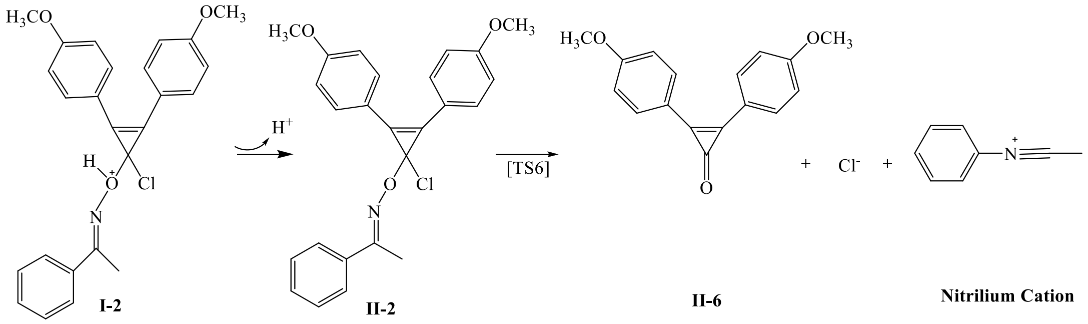

Figure 4.8 : The proposed intermediates for organocatalytic mechanism.

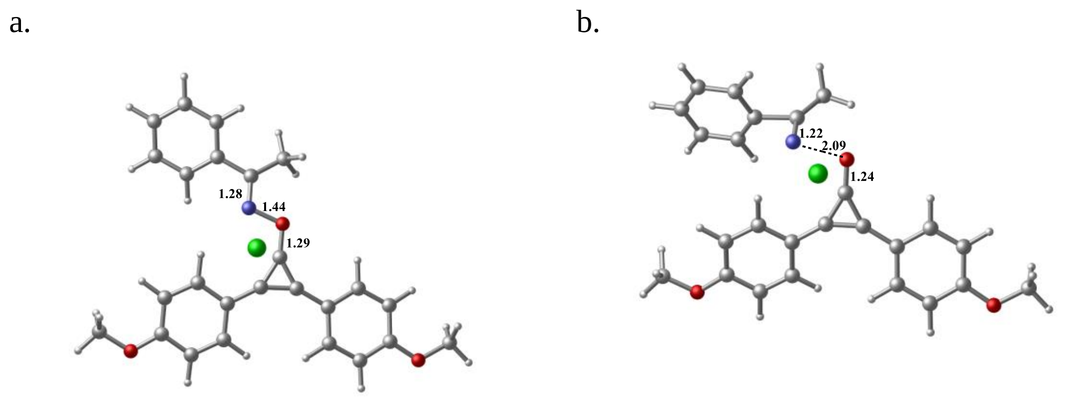

II-2 TS6

Figure 4.9 : Three dimensional structures of intermediates and transition states for organocatalytic mechanism.

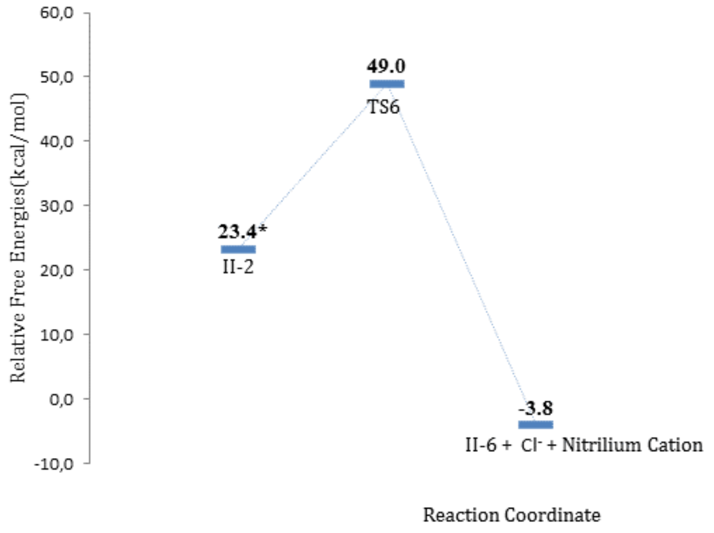

Figure 4.10 : Relative free energy profile of organocatalytic mechanism. (Note: * : 4_Methoxy_DCP is determined as a starting point)

4.1.1.4 The alternative organocatalytic mechanism

The alternative organocatalytic mechanism starts with the nucleophilic attack of negatively charged oxygen on I-3 to positively charged carbon on nitrilium cation which is ended up with the structure III-7. The reaction proceeds with the formation of intermediate I-5 which then converted into a lactam hence the organocatalyst is recovered (Figure 4.11).

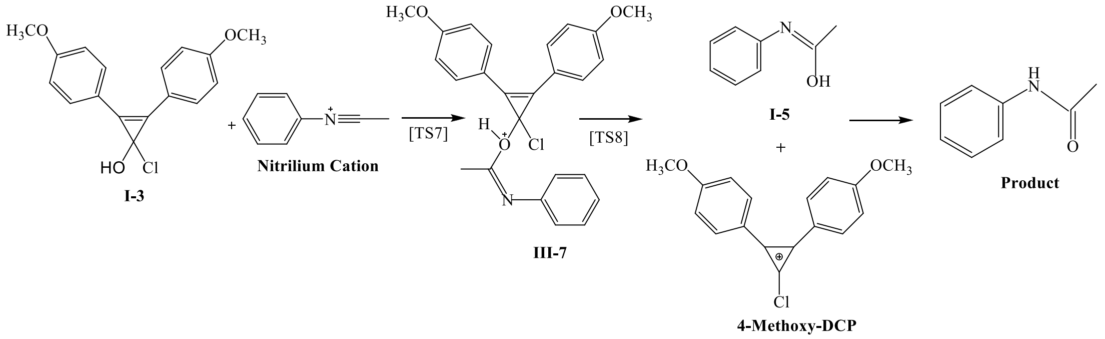

Figure 4.11 : The proposed intermediates for alternative organocatalytic mechanism.

In the pre-reaction complex, the presence of π-π interaction between phenyl ring of nitrilium cation and structure I-3 and the delocalization of charges over aromatic rings resulted in a relative free energy of -10.8 kcal/mol (Figure 4.12a, Figure 4.13). The presence of π-π interaction is supported by the NBO second order perturbation energy values, too. In the pre-reaction complex, C10 and O8 atoms react and the distance between atoms are calculated to be 2.93 Å (Figure 4.12a). The electrostatic interactions between negatively charged O8 atom (-0.812) and positively charged C10 atom (0.699) in the pre-reaction complex contributes to the stabilization of the structure. Further contribution to the stabilization of the pre-reaction complex comes from the electrostatic interaction between nitrogen of the acetonitrile and H11. The bond formation between C10-O8 atoms a distance of 1.80 Å is modeled via transition state structure TS7 having an energy barrier of 13.9 kcal/mol. Further stabilization due to the interaction between lone pair orbitals of O8 atom and orbitals of C10 atom is supported by the NBO second order perturbation energy values. The bond distance decrease from 1.87 Å to 1.62 Å between H11 and acetonitrile and the hydrogen bond interactions in structure TS7 gain strength (Figure 4.12b). Following the transition state, an intermediate structure III-3 occures with an energy barrier of -1.5 kcal/mol. Bond length between C11 and O8 is now 1.45 Å. Meanwhile, bond length between O8 and C1 increased from 1.38 Å to 1.52 Å.

In the modeled transition state structure TS8 for the last step of organocatalytic mechanism, the bond length of O8-C1 elongate to 1.71 Å and the bond breaks. The bond cleavage requires 1.7 kcal/mol energy and the step is concluded with the formation of I5 and 4-MethoxyDCP ion. The reaction has a low relative free energy profile and is highly exergonic (Figure 4.13).

Table 4.3 : NBO charge values of the atoms structures located on or near the reaction coordinate in the alternative organocatalytic mechanism.

	C1	C2	C3	Cl4	C6	C7	O8	H11	N9	C10	N12
I3 and Nitrilium Cation	0.242	0.012	0.020	-0.176	-0.159	-0.161	-0.812	0.547	-0.227	0.699	-0.464
TS7	0.200	0.031	0.039	-0.074	-0.170	-0.159	-0.735	0.562	-0.360	0.656	-0.477
III7	0.169	0.055	0.048	-0.010	-0.161	-0.172	-0.664	0.548	-0.440	0.607	-0.472
TS8	0.128	0.079	0.074	0.058	-0.168	-0.180	-0.694	0.558	-0.463	0.605	-0.475

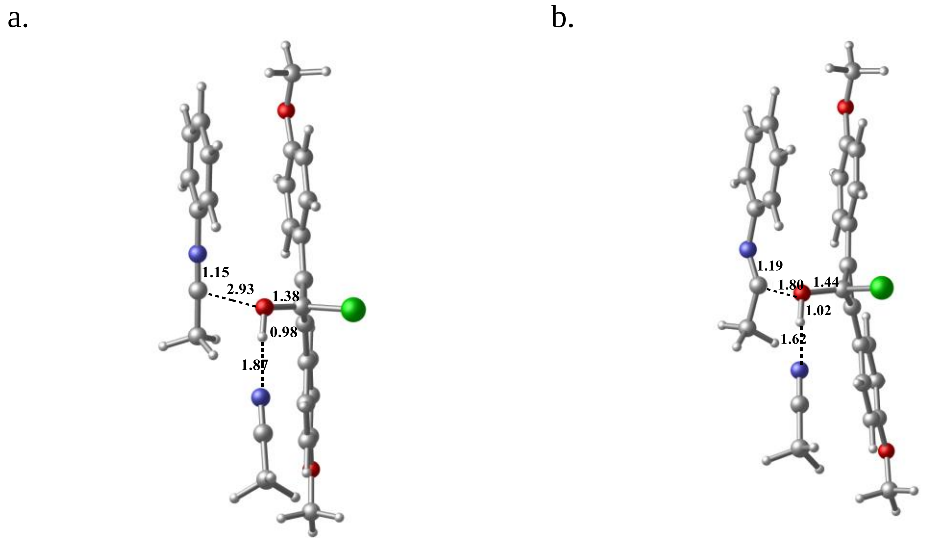
a.
1.15
2.93
1.38
0.98
1.87
b.
1.19
1.80
1.44
1.02
1.62

I3 and Nitrilium Cation

TS7

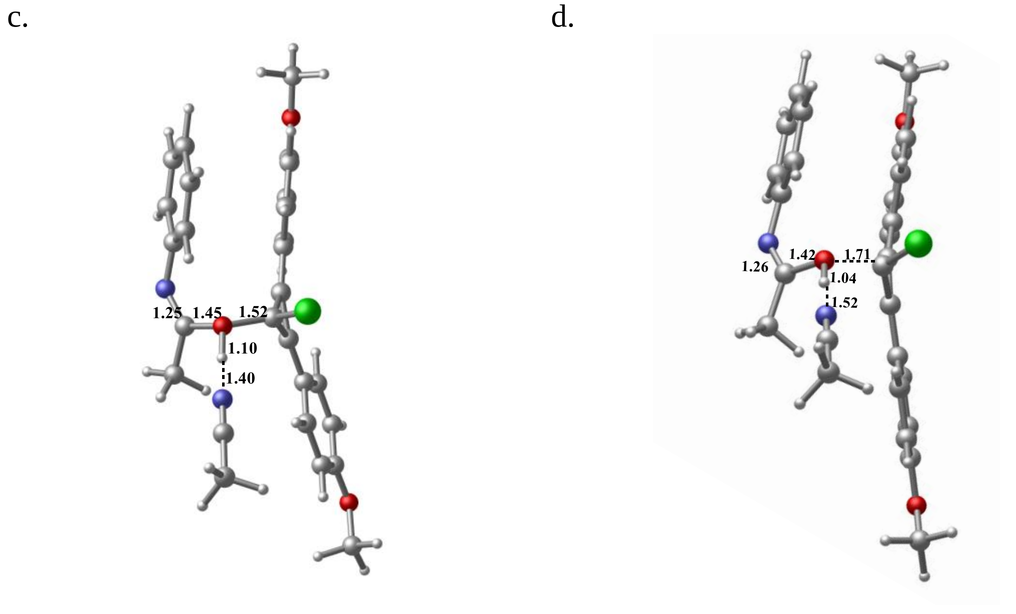
c.
1.25
1.45
1.52
1.10
1.40
d.
1.26
1.42
1.71
1.04
1.52

III7

TS8

Figure 4.12 : Three dimensional structures of the transition states for alternative organocatalytic mechanism.

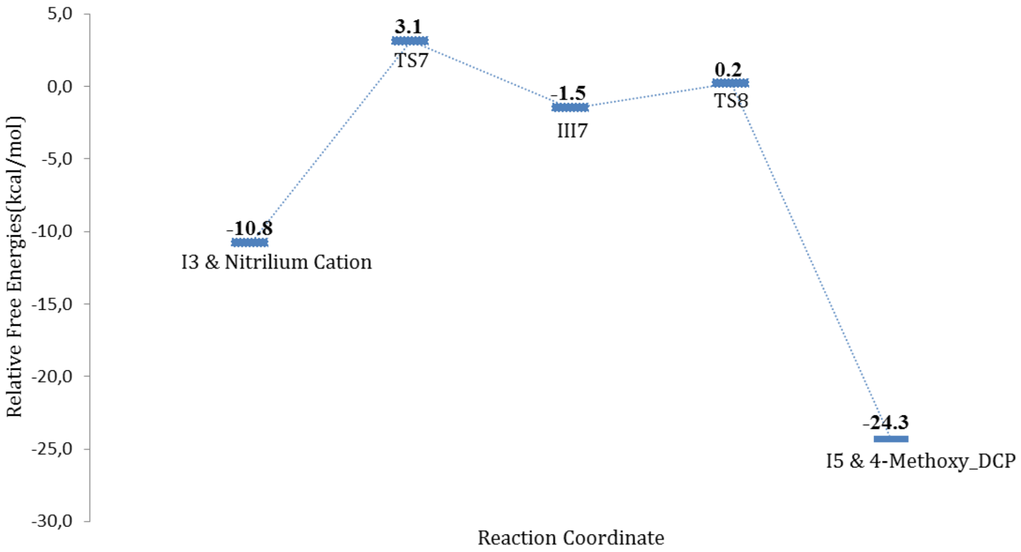

Figure 4.13 : Relative free energy profile of alternative organocatalytic mechanism.

When relative free energy profiles of the proposed mechanisms are compared, organocatalytic mechanism is unlikely to occur due to having the highest energy barrier. In the literature, the rate determining steps of the self-propagating and alternative organocatalytic mechanisms are transition structure TS5 and transition structure TS3, respectively (Tian et al, 2013). In the scope of the thesis, the relative free energy values are found to be 19.1 kcal/mol for TS5 and 40.9 kcal/mol for TS3 where 1,1-dichloro-2,3-4-methoxydiphenylcyclopropene used as a catalyst. According to these results, self-propagating mechanism seems more likely to occur. Nevertheless, formation of nitrilium cation is necessary to finish the initiation part and to be able to continue with self-propopagating or alternative organocatalytic mechanism. Thus, a new relative free energy profile should be formed and analyzed values based on the necessity of the formation of nitrilium cation. For this comparison, energy profiles of self-propagating and alternative organocatalytic BKR has been drawn again after the formation of nitrilium cation (Figure 4.14). As the rate determining step is transition structure TS5 whose relative free energy is 19.1 kcal/mol, now the rate determining step is transition structure TS7 whose relative free energy is 13.9 kcal/mol. The new aspect related to the formation of nitrilium cation has been taken into consideration, the reaction may enter an alternative organocatalytic mechanism.

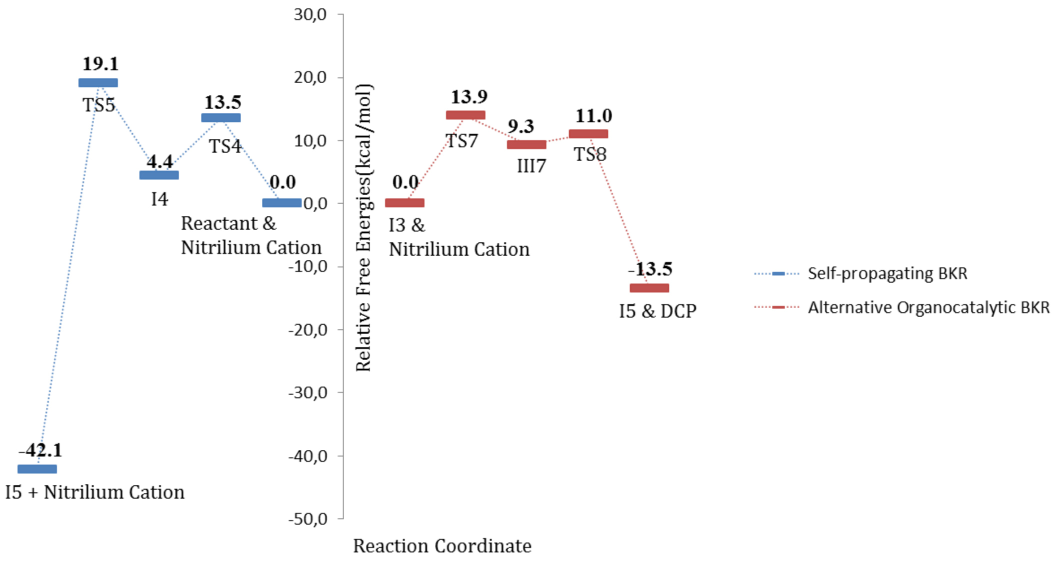

Figure 4.14 : Compared relative free energy profile of self-propagating and alternative organocatalytic mechanism.

4.1.1.5 The relationship between the experimental yield and energy barrier of the rate-determining step

A further investigation of cyclopropenium activated Beckmann rearrangement was reported by Lambert et al. in the same article published in 2010. It was claimed that use of xylyl-substituted cyclopropenes with acetophenoneoxime and use of cyclopropenes with cyclohexanonoxime provided the formation of product in high yield (Figure 2.2). Thus, the reactions were modeled with these structures too. As the rate determining step is to be found transition structure TS3 for both of the self-propagating and alternative organocatalytic mechanisms, yield values were compared with its relative free energies. In the reaction of p-methoxy-phenyl substituted cyclopropene and acetophenoneoxime, the relative free energy of the rate determining step is found to be 40.9 kcal/mol as in the reaction of xylyl-substituted cyclopropenes with acetophenoneoxime, the relative free energy of the rate determining step is 37.4 kcal/mol. At last, in the reaction of cyclopropenes with cyclohexanonoxime, the relative free energy of the rate determining step is found to be 34.4 kcal/mol. The obtained results are in harmony with the experimental yield qualitatively. As the relative free energy values of structure TS3 decrease, experimental yield values increase (Table 4.4).

Table 4.4 : Experimental yield values and relative free energies of transition structure TS3 (Vanos and Lambert, 2010).

	$\Delta G^{\#}$(kcal/mol)	Yield (%)
TS3	40.9	70
Xyl-TS3	37.4	98
Hex-TS3	34.4	99

4.1.1.6 Benchmark study

Single point energy calculations with different methods and higher basis sets were done in order to compare the efficiency of the chosen method and basis set. Relative electronic energy values were calculated for both of self-propagating and alternative organocatalytic mechanisms in the rate determining step.

The utilization of 6-311+G(d,p) basis set with M062X functional, had no effect on relative electronic energy values (Table 4.5). The similar results were obtained by using BMK which was developed for kinetics (Boose and Martin,2004). The studies for wB97XD functional which were repeated, too. (Grimme, 2011). Although, the transition structure TS5 identified as the rate determining step of the self-propagating mechanism has energy of 2 kcal/mol lower than the energy value calculated with M06-2X functional. This difference stem from dispersion effects that were taken into the consideration in wB97XD functional. However, the energy difference between TS5 and TS7 that is found to be the rate determing step of the alternative organocataltic mechanism is still 3.7 kcal/mol (Table 4.5). Similar values were found when MP2 method of post-HF methods were used. Hence, M062X functional is an appropriate functional for the calculation of energy barriers for this type of molecules.

Table 4.5 : Relative electronic energy values of self-propagating and alternative organocatalytic mechanisms in the rate determining step ($\Delta E^{\#}$: Relative electronic energy values kcal/mol).

	Self-propagating (TS 5)	Alternative Organocatalytic (TS 7)
	$\Delta E^{\#}$	$\Delta E^{\#}$
M062X/6-31+G(d,p)	18.6	13.2
M062X/6-311+G(d,p)	18.7	14.3
BMK/6-31+G(d,p)	19.0	14.9
MP2/6-31+G(d,p)	19.0	12.3
wB97xD/6-31+G(d,p)	16.6	12.9

4.1.2 The Beckmann rearrangement reactions at elevated temperature

The experimental study belongs to Yadav et al. and it has been conducted at 80° C. The proposed mechanism by Yadav et al. starts with loss of chloride ion of 1,1-dichloro-2,3-4-methoxydiphenylcyclopropene (p-methoxy DCP) to form p-methoxy DCP ion. The reaction then proceeds with the nucleophilic attack of the oxime to the p-methoxy DCP ion as HCl leaves to form an intermediate structure M1 (Figure 4.15). After loss of a chloride ion from structure M1, structure M2 is formed. Subsequently, intermediate structure M3 is obtained with a R migration. Formation of Meisenheimer complex defined as an intermediate structure is observed as the consequence of a nucleophilic attack of oxime (Reactant) to the intermediate structure M3 as HCl leaves. At the end of the mechanism, the bond between C1 and O8 is broken providing the formation of product and regeneration of structure M2. Moreover, an alternative pathway to the formation of Meisenheimer complex following to the formation of intermediate structure M2 in the absence of chloride ion, which are not proposed experimentally, are proposed and modelled. Accordingly, nitrilium cation and cyclopropenone form in the absence of chloride ion with a R migration. The pathway can turn to self-organocatalytic mechanism due to a reaction between obtained nitrilium cation and reactant (Figure 4.15 - Red arrow). This second pathway has not been proposed experimentally. The existence of the second path turning to self-propogating mechanism after R-migration is discovered in computational studies.

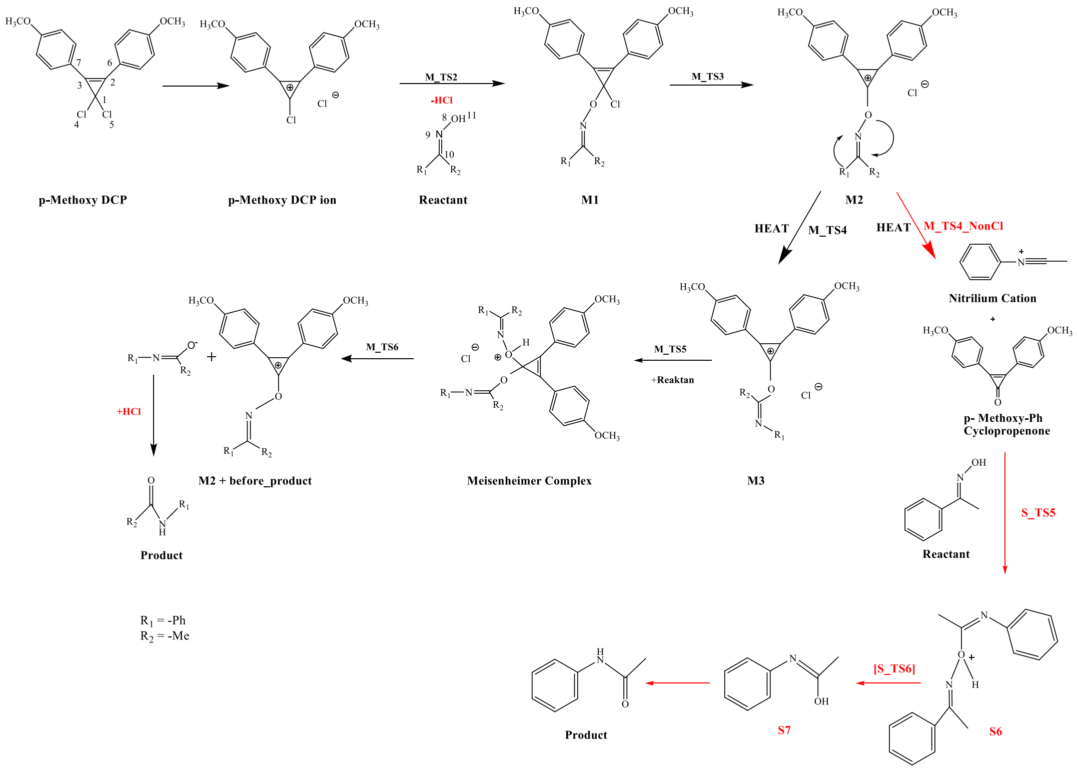
p-Methoxy DCP
p-Methoxy DCP ion
M_TS2
-HCl
Reactant
M1
M_TS3
M2
HEAT
M_TS4
HEAT
M_TS4_NonCl
Nitrilium Cation
p- Methoxy-Ph Cyclopropenone
M_TS6
M_TS5
+Reaktan
+HCl
M2 + before_product
Meisenheimer Complex
M3
Product
Reactant
S_TS5
R$_1$ = -Ph
R$_2$ = -Me
[S_TS6]
S6
S7
Product

Figure 4.15 : The proposed intermediates for organocatalytic BKR proceeding via Meisenheimer complex (Srivastava et al, 2010).

Formation of p-methoxy-DCP ion requires a relative free energy barrier of 11.4 kcal/mol at elevated temperature (Figure 4.16). Although the relative free energies are not affected by the alterations in temperature, free energy of the transition structure is 8 kcal/mol lower than free energy of the related transition structure which is calculated at room temperature. In addition, geometric parameters remain the same at elevated temperature (Figure 4.3a-c, Figure 4.17a-c).

The first step is an endergonic process having 5.2 kcal/mol reaction energy (Figure 4.16). Reaction continues with the nucleophilic attack of oxime to the cyclopropenium ion where HCl dissociates as opposed to the Lambert's mechanism. The distance between the attacker O8 and C1 is calculated to be 1.85 Å as the C1 carbon atom.Similar nucleophilic attack in Lambert's pathway at room temperature has a relative free energy of 32.9 kcal/mol in which dissociation of HCl was not observed (Structure TS2). The calculated relative free energy of TS2 is approximately 14.0 kcal/mol higher than the relative free energy of transition structure M_TS2 (Figure 4.4). The free energy activation barrier for the formation of M1 intermediate is equal to 13.5 kcal/mol (Figure 4.16). In addition, the formed M1 intermediate is more stable than I2_cf2 intermediate due to HCl dissociation

(Figure 4.3, Figure 4.15). Structure M1 has a quite lower relative free energy than structure I2 that is proposed by Lambert et al. and modeled by Ericksson et al. Similar relative free energies are acquired without temperature effect. The path which is proposed for the initiation has not been modeled before.

In the next step, the intermediate, Structure M1 loses its chloride to form Structure M2. The formation of intermediate M2 is modeled via structure TS3 having a relative free energy of 5.0 kcal/mol. M2 has a relative free energy of -1.4 kcal/mol. To be able to complete the initiation part of the path, the next step is R-migration. In addition to the experimentally proposed mechanism, a second path is modeled for the R-migration in which chloride ion does not exist (Figure 4.15). Firstly, the mechanism will be analyzed that realised in the presence of chloride ion and providing formation of Meisenheimer complex.

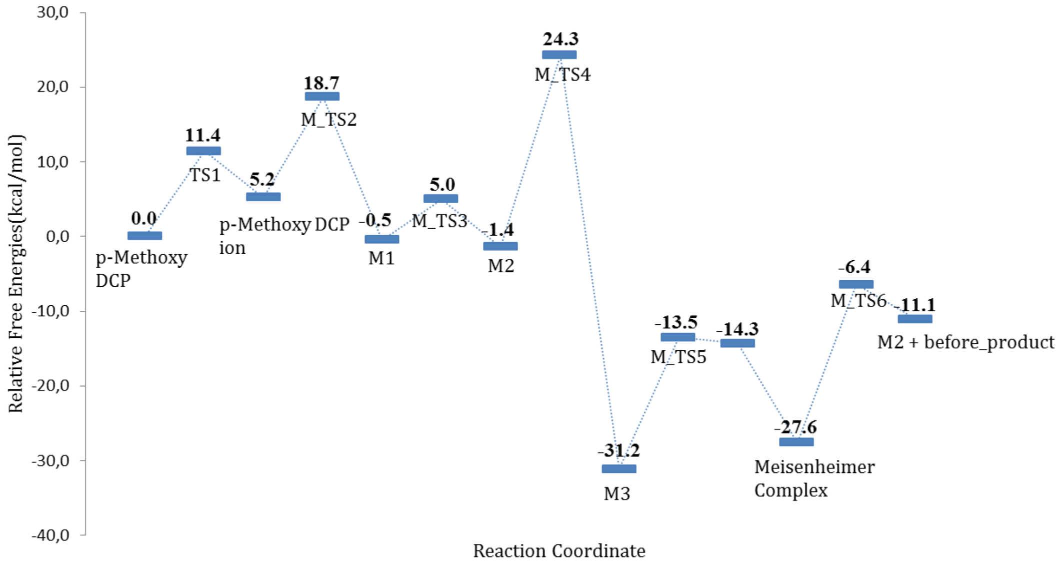

Figure 4.16 : Relative free energy profile of the organocatalytic mechanism proceding via Meisenheimer complex.

R-migration in the presence of chloride ion is modeled with transition structure M_TS4 and following this, M3 forms as an intermediate. When structure of M_TS4 (Figure 4.17h) is compared to the structure TS3 (Figure 4.3) which is modeled for R-migration at room temperature, it is seen that, the main difference between two transition structures comes from the bonding or nonbonding of chloride ion to C1 atom. Since there is not a bonding with chloride ion in transition structure M_TS4, p-methoxy-phenyl substituted cyclopropenium maintains its planarity and electron delocalization between aromatic rings occurs in a high level. On the other hand, having sp^3 hybridization of C1 atom prevent electron delocalization which the structure could enable. TS3 has a relative free energy of 40.9 kcal/mol while M_TS4 has a relative free energy of 24.3 kcal/mol. Both of the transition structures have the highest free energies in their whole energy profiles. Herein, TS3 and M_TS4 can be considered as the rate - determining steps. The forming intermediate, namely, M3 has a high stability due to the same reasons and has a relative free energy of -31.2 kcal/mol. In the next step, O8 atom of the reactant molecule attack nucleophilically to the C1 atom having sp^2 hybridization of M3 intermediate in order to form Meisenheimer complex. Transition from M3 to Meisenheimer complex is modeled through a structure M_TS5. The distance between O8' and C1 atoms are found to be 1.76 Å as the distance between Cl4 - H11' atoms decreases from 2.06 Å to 1.79 Å in M_TS5 (Figure 4.17j). In the obtained new structure, HCl dissociate and formation of Meisenheimer complex as a consequence of interactions between Cl4 and H11' atoms is seen Figure 4.17k. The relative free energy value of Meisenheimer complex is -27.6 kcal/mol. Meisenheimer complex exist in shallow minima according to the computational studies in the literature. Thus, the structure could be modeled as a transition structure more easily instead of local minima (Fernandez et al.; 2010). However, our studies show that, acidic medium facilitates the formation of Meisenheimer complex and then, a free energy difference of 0.8 kcal/mol occurs between the transiton structure and the obtained complex supported by HCl after the transition state (Figure 4.16). Contrary to the views of Fernandez et al. (2010), Meisenheimer complex could be obtained as a local minima following separation of HCl.

a.

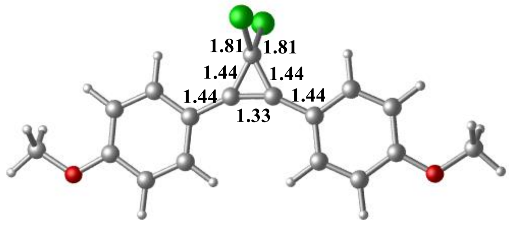

4_Methoxy_DCP

b.

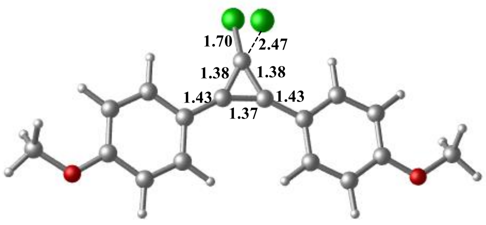

TS1

c.

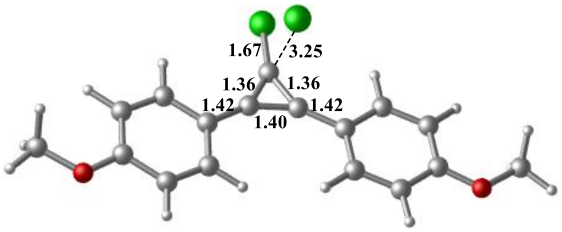
1.67
3.25
1.36
1.36
1.42
1.40
1.42

4_Methoxy_DCP ion

d.

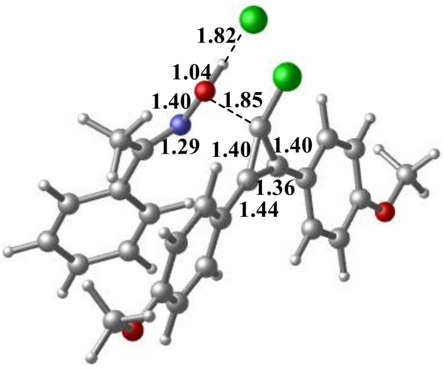
1.82
1.04
1.40
1.85
1.29
1.40
1.40
1.36
1.44

TS2

e.

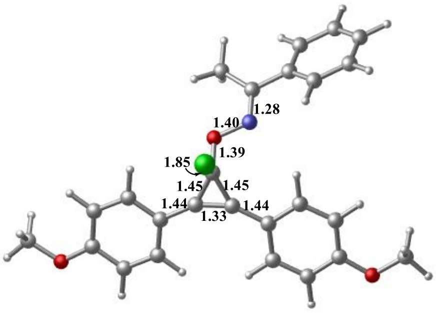
1.28
1.40
1.39
1.85
1.45
1.45
1.44
1.44
1.33

M1

f.

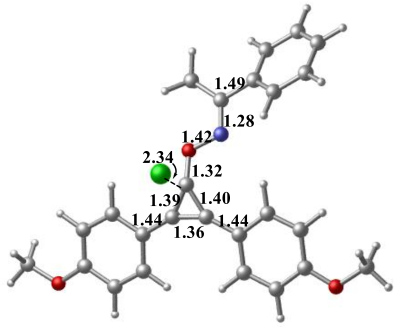
1.49
1.28
1.42
2.34
1.32
1.39
1.40
1.44
1.44
1.36

M_TS3

g.

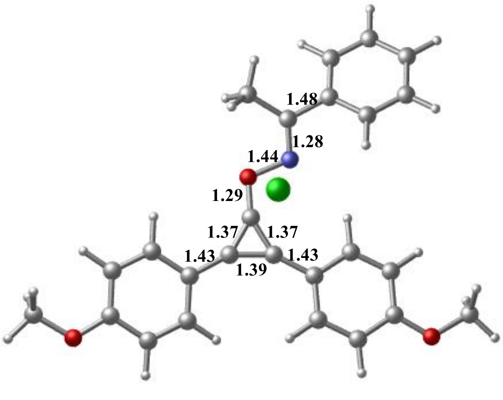
1.48
1.28
1.44
1.29
1.37
1.37
1.43
1.43
1.39

M2

h.

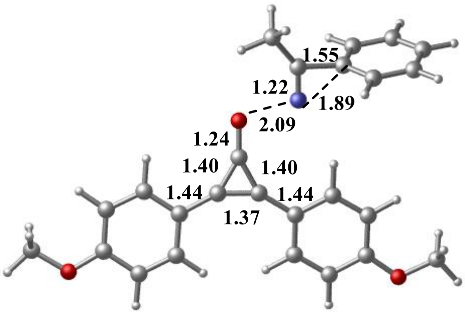
1.55
1.22
1.89
2.09
1.24
1.40
1.40
1.44
1.44
1.37

M_TS4

i.

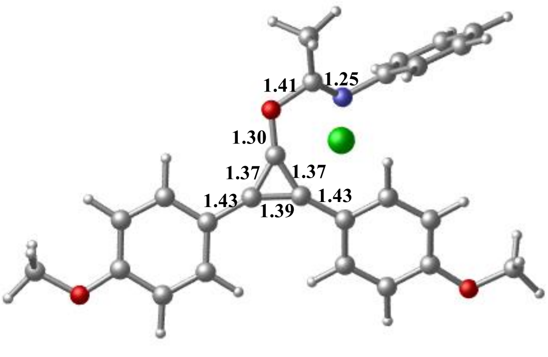
1.41
1.25
1.30
1.37
1.37
1.43
1.43
1.39

M3

j.

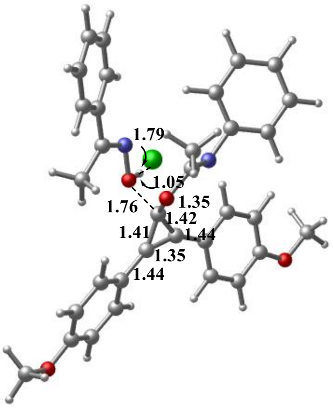
1.79
1.05
1.76
1.35
1.42
1.41
1.44
1.35
1.44

M_TS5

k. l.

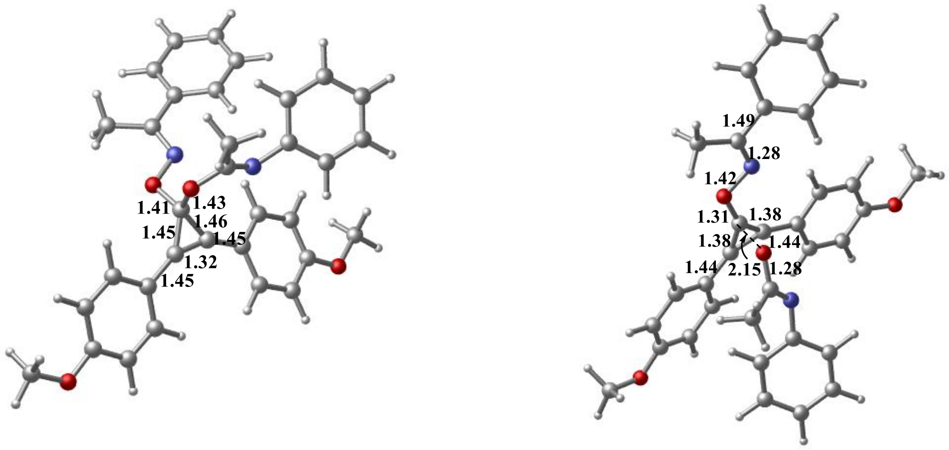

Meisenheimer Complex M_TS6

m.

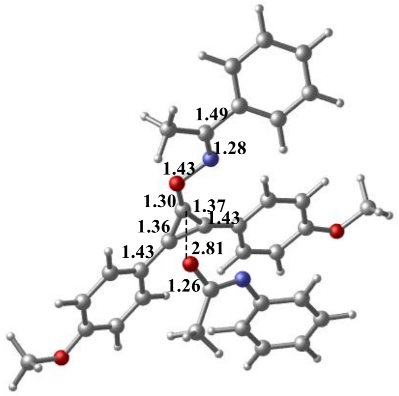

M2 + before_product

Figure 4.17 : Three dimensional structures of intermediates and transition states of the organocatalytic mechanism proceeding via Meisenheimer complex at elevated temperature.

In the thesis, the alternative modelled transition structure for R-migration at elevated temperature in non-existence of chloride ion is called M_TS4_NonCl (Figure 4.18b). In structure M_TS4_NonCl, the distance between O8 and N9 is calculated as 2.10 Å. The transition structure has a relative free energy of 20.7 kcal/mol and 3.6 kcal/mol lower energy than M_TS4 modeled in the presence of chloride ion (Figure 4.16 and Figure 4.19). The formed structures cyclopropenone and nitrilium cation. As it is known, when nitrilium cation and reactant react, the mechanism is called as self-propagating mechanism. Reaction may proceed via self-propagating mechanism due to the fact that reactant molecules exist in the medium.

In the next step, reactant attacks to nitrilium cation with the help of acetonitrile. The attack is modeled via the transition state structure S_TS5 having a relative free energy of -3.2 kcal/mol. It is no matter to overcome such a barrier at an elevated temperature. There is no difference when the transition state S_TS5 and the transition state TS4 of self-propagating mechanism occured at room temperature are geometrically compared (Figure 4.6 and Figure 4.18). Following the reaction, keto - enol tautomer and nitrilium cation are obtained. The obtained nitrilium cation can react with a new reactant again. The last step is modeled via S_TS6 and its has a relative free energy of 2.2 kcal/mol.

R-migration step is the rate determining step of the proposed path. The probability of the path proceeding with self-propagating mechanism is higher than the probability of the path proceeding via Meisenheimer complex. However, the difference between energy barriers is only 3.6 kcal/mol and if it is mentioned about elevated temperature, this value should not be seen as a significant difference. Therefore, the existence of an organocatalytic mechanism proceeding via Meisenheimer complex should not be ignored.

a.

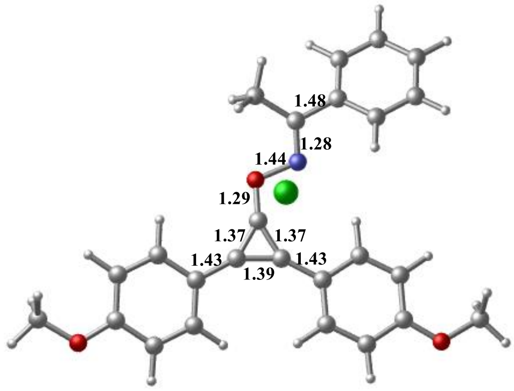

M2

b.

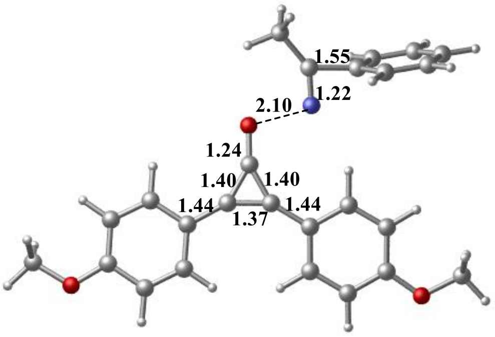

M_TS4 _NonCl

c.

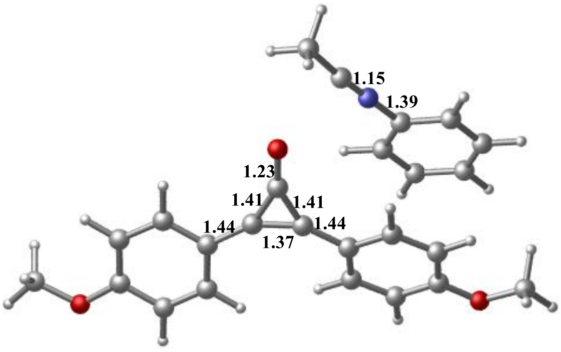

Nitrilium Cation & p-Methoxy-Ph Cyclopropenone

d.

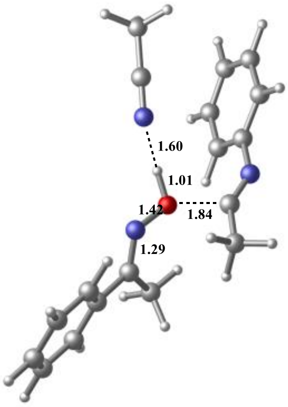

S_TS5

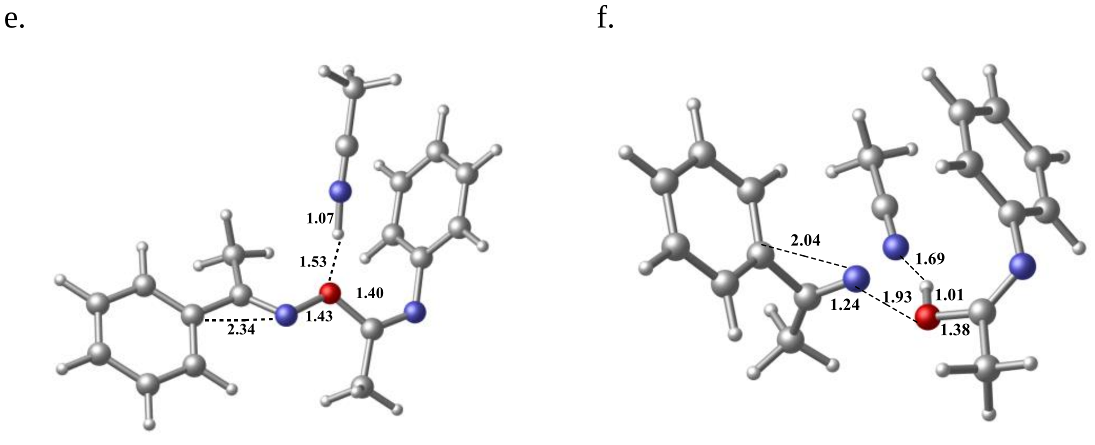

S6 S_TS6

Figure 4.18 : Three dimensional structures of intermediates and transition states for the BKR turning back to self-propagating mechanism during the R-migration at elevated temperature.

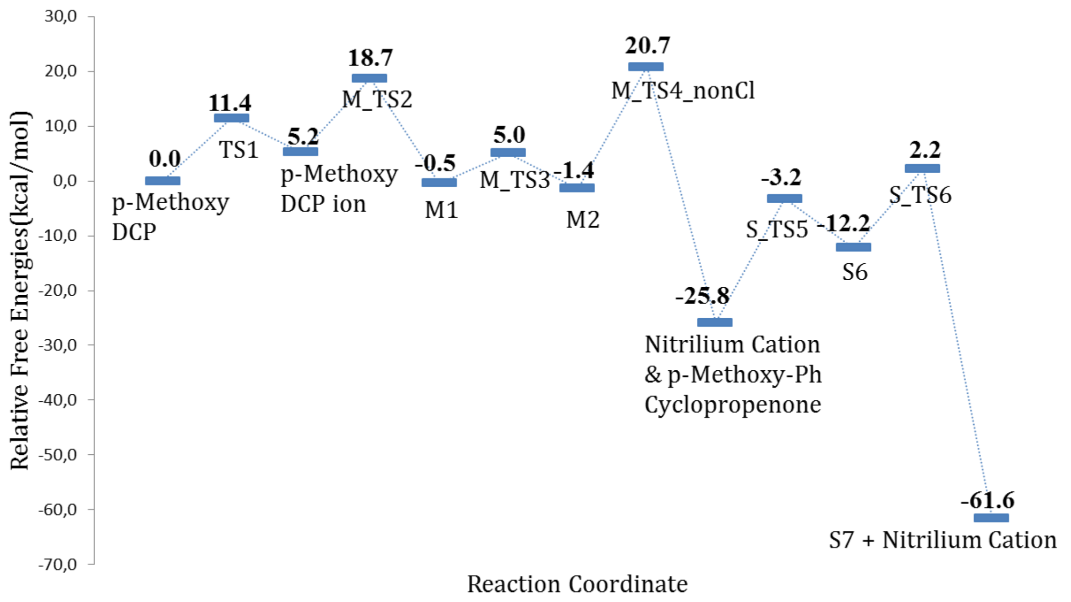

Figure 4.19 : Relative free energy profile of the BKR turning back to self-propagating mechanism during the R-migration at elevated temperature.

4.2 Chlorodehydration of Alcohols

The nucleophilic substitution of alcohols have a great importance in organic synthesis (Comprehensive Organic Synthesis, 1991, Chapter 1.1-1.9). However, the traditional reagents used in the experimental studies suffer from several problems including poor reactivity, hazardous byproduct formations. In recent studies, a new strategy has been developed for the promotion of dehydration reactions of alcohols using cyclopropenones by Lambert et al. (Kelly and Lambert 2009). The new method based on the formation of cyclopropenium cation in situ from the cyclopropenones and the activation of alcohol substrates via nucleophilic displacement mechanism. They have demonstrated the effectiveness of this new methodology in number of dehydration reactions including chlorodehydration, diolcyclodehydration and the Beckmann rearrangements reactions. The reactions ended up with a good yield and high stereoselectivity under mild and convenient conditions. As a result, cyclopropenones have been started to be called as organocatalysts.

Lambert et al. prepared two different experiments and proposed two different reaction mechanisms according to the results of experiments (Vanos and Lambert 2011). In the light of experimental data, at room temperature chlorodehydration mechanism has been investigated in two main titles: Mechanism A and Mechanism B.

In the scope of experimental studies, product distributions were also investigated via changing substituents on phenyl rings of cyclopropenones. It was seen that electron-withdrawing substituent onto the phenyl rings decreases effectiveness of catalyst and provides formation of PRODUCT II. In the contrast, adding electron-donating substituent onto the phenyl rings increases effectiveness of catalyst and provides formation of PRODUCT I (alkyl chloride) with a high yield (Table 4.6).

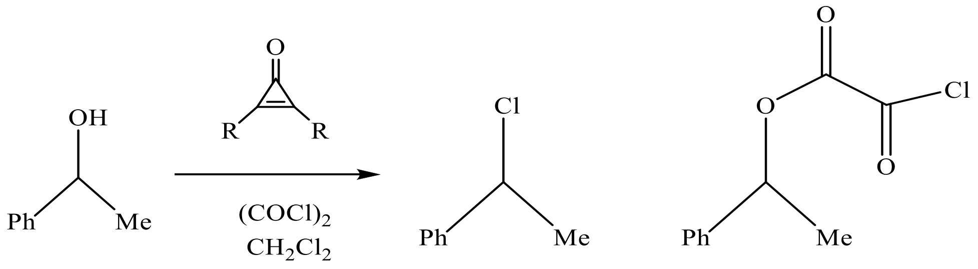

	R	PRODUCT I [%]	PRODUCT II [%]
Set I	p-MeO-Ph	>98	<2
Set II	m-NO$_2$-Ph	14	86

Table 4.6 : Experimental results of cyclopropenone catalyzed chlorodehydration reaction (Vanos and Lambert, 2011).

4.2.1 Mechanism A

4.2.1.1 Chlorodehydration reaction in the presence of p-methoxy-phenyl cyclopropenone

The first experiment by Lambert et al. conducted at room temperature. In the experiment, 1-phenylethanol (reactant) was combined with the cyclopropenone catalyst in CH_2Cl_2 and oxalyl chloride was added to the mixture through a syringe. The first step of the path starts with the chlorination of cyclopropenone in the presence of oxalyl chloride which is stated to be a rapid reaction with an activating agent (Figure 4.20) (Föhlisch and Bürgle 1967; Breslow and Posner 1967).

In the next step, cyclopropenium salt occurs with the loss of chloride of p-methoxydiphenylcyclopropene. Formation of cyclopropenium ion is observed in both of chlorodehydration and Beckmann rearrangement reactions. Thus, the calculations of energy barrier of previously modeled transition structure were repeated in the presence of methylene chloride instead of acetonitrile. The reaction proceeds with the nucleophilic attack of the oxime to DCP ion and a cationic intermediate is obtained (I2). (Figure 4.20) Alkoxy cyclopropenium salt (I3) occurs as the consequence of hydrochloride acid (HCl) separation from the I2 structure. Compound I3 is a species it has been detected by ^{1}H NMR spectroscopy (Kelly and Lambert 2009). Subsequently, nucleophilic substitution reaction occurs with the attack of chloride ion to C9 providing the formation of the PRODUCT I and the regeneration of cyclopropenone.

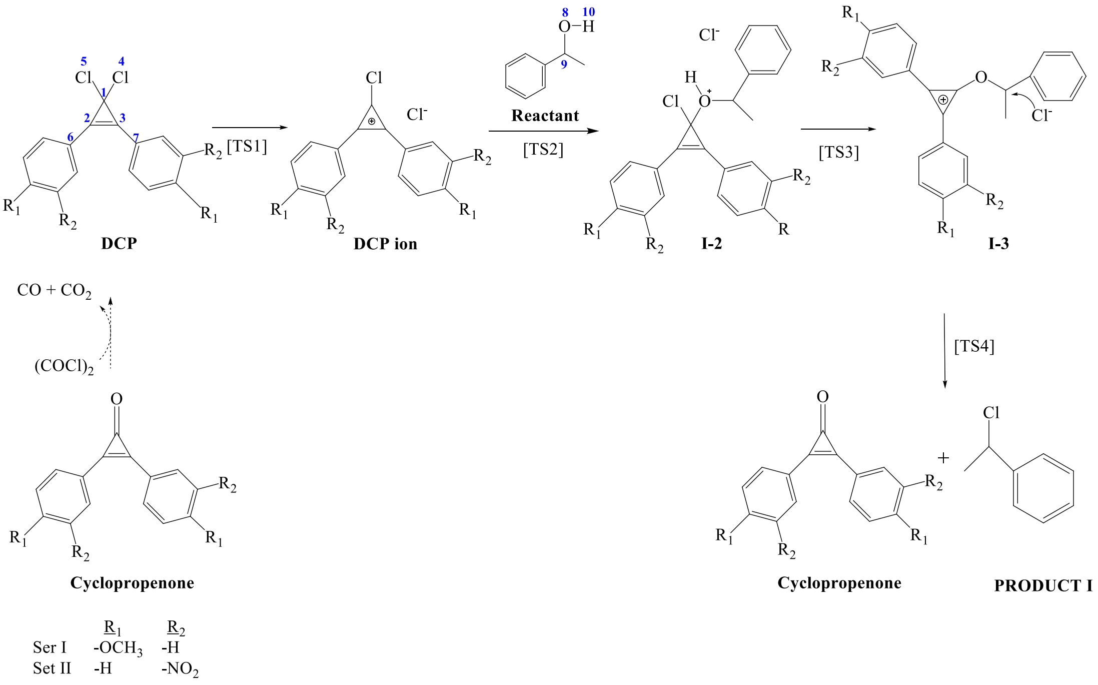

Figure 4.20 : Proposed chlorodehydration mechanism in the presence of oxalyl chloride to obtain PRODUCT I.

A conformer having two methoxy substituents on the phenyl ring of cyclopropenone pointing toward the three membered ring, was found as the lowest energy conformer. Thus, modelings were performed with the structure shown in Figure 4.21a.

The formation of cyclopropenium ion with the loss of chloride ion is modeled via structure TS1 and the free energy activation barrier for the formation of cyclopropenium ion is 13.1 kcal/mol. (Figure 4.22) The distance between C1 and Cl5 is lengthened to 2.53 Å from 1.81 Å and the distance between C1 and Cl4 is shortened to 1.69 Å as chlorine leaves and the length of C-C bonds within the three membered ring became almost equal (C-C = 1.38 Å) in structure TS1 (Figure 4.21b).

p-methoxyDCP ion has a relative free energy of -24.7 kcal/mol (Figure 4.22). The stability of p-MethoxyDCP ion is derived from the delocalization of the two-pi electrons over three 2p orbitals as it has been mentioned. There are two identical C-C bonds having a length of 1.36 Å in the ion and the length of the third C-C bond is 1.40Å (Figure 4.21c). The geometrical parameters are an indication of delocalized electrons on the three membered ring system. The structure TS1 is a product-like transition state and this situation is supported by Hammond's postulate. (Hammond, 1955). As chlorine leaves, the hybridization scheme of C1 turns out to be sp^2 facilitating the delocalization on the ring thereby enhancing the stabilization of the cyclopropenium ion (p-MethoxyDCP ion). The NBO charge results are tabulated in Table 4.7. As chlorine, Cl5, leaves the Cl4 which is bound to C1 becomes positively charged (from 0.136 to 0.177) in the p-MethoxyDCP molecule. Not only the chlorine, positive charges on the ring atoms are also increased (Table 4.7).

a.

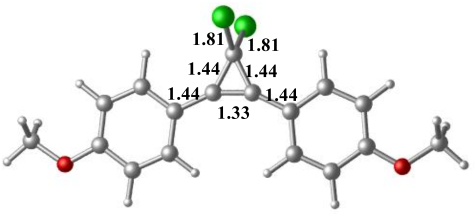
1.81
1.81
1.44
1.44
1.44
1.44
1.33

p-Methoxy DCP

b.

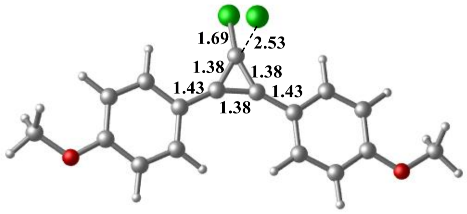
1.69
2.53
1.38
1.38
1.43
1.43
1.38

TS1

c.

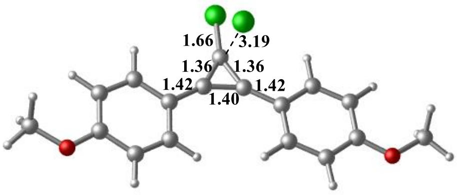
1.66
3.19
1.36
1.36
1.42
1.42
1.40

p-Methoxy DCP Ion

d.

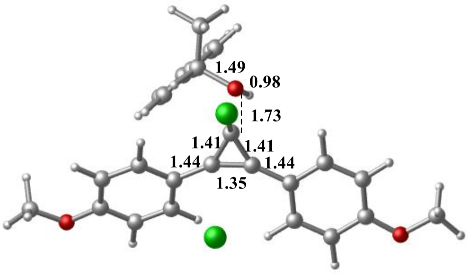
1.49
0.98
1.73
1.41
1.41
1.44
1.44
1.35

TS2

e.

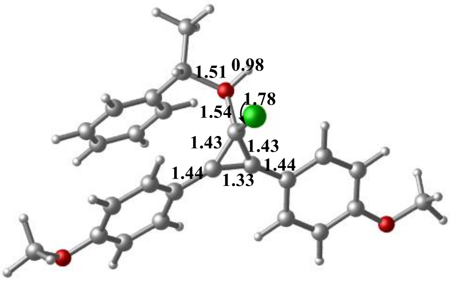
1.51
0.98
1.54
1.78
1.43
1.43
1.44
1.44
1.33

I2

f.

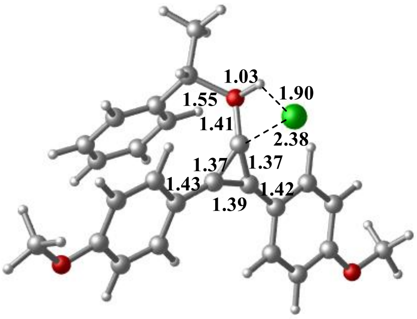
1.03
1.90
1.55
1.41
2.38
1.37
1.37
1.43
1.39
1.42

TS3

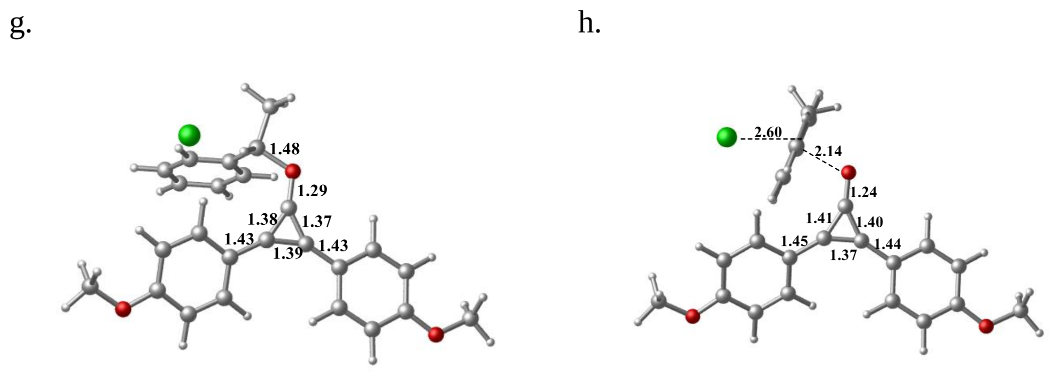

I3 TS4

Figure 4.21 : Three dimensional structures of intermediates and transition states for chlorodehydration mechanism in the presence of p-methoxy-phenyl cyclopropenone.

The free energy activation barrier of formation of p-Methoxy DCP ion is 11.3 kcal/mol and the relative free energy of p-Methoxy DCP ion is calculated to be 5.4 kcal/mol in the presence of acetonitrile. The free energy barrier is increased from 11.3 kcal/mol to 13.1 kcal/mol in the presence of methylene chloride. This free energy barrier difference may stem from the usage of less polar solvent unlike acetonitrile which was utilized in Beckmann rearragement experiments. (dielectric constant of CH_3CN is 37.5 and dielectric constant of CH_2Cl_2 is 8.93). It has not been observed significant differences in terms of the values of distance and angle on three-dimensional geometries of structures.

The second step is the S_N2 type substitution reaction between the oxime and the cyclopropenium ion to form the cationic species. The nucleophilic substitution step is modeled via transition structure TS2 (Figure 4.21d). The distance between negatively charged O8 and positively charged C1 is 1.73 Å. Carbon atom on the ring (C1) on the ring turns out to be tetrahedral geometry. The free energy activation barrier for the formation of the intermediate structure I2 is 25.8 kcal/mol (Figure 4.22).

The transition from intermediate structure I2 to I3 is modeled via TS2 where, the distance between C1 and Cl4 is found to be 2.38 Å as the distance between O8 and H10 is elongated from 0.98 Å to 1.03 Å. As a consequence of interaction between Cl4 and H10, hydrochloric acid (HCl) leaves and intermediate structure I3 having a relative free energy -37.8 kcal/mol is obtained. Transition structure TS3 has a relative free energy of 11.2 kcal/mol (Figure 4.22).

The last step of regeneration of cyclopropenone and formation of product is modeled with TS4. The bond between O8 and C9 is broken with the attack of chlorine to C9. In transition structure TS4, the distance between O8 and C9 is elongated from 1.48 Å to 2.14 Å as the distance between C1 and O8 is shortened from 1.29 Å to 1.2 Å relative to the preceding intermediate. The relative free energy value of transition structure TS4 is -14.9 kcal/mol. Formation of the double bond between C1 and O8 is completed in product and the hybridization scheme of C1 turns out to be sp^2 geometry from tetrahedral geometry. The whole reaction has an exergonic profile. The transition structure TS3 is the rate determining step of the reaction in which HCl leaves as TS3 requires a relative free energy of 11.2 kcal/mol.

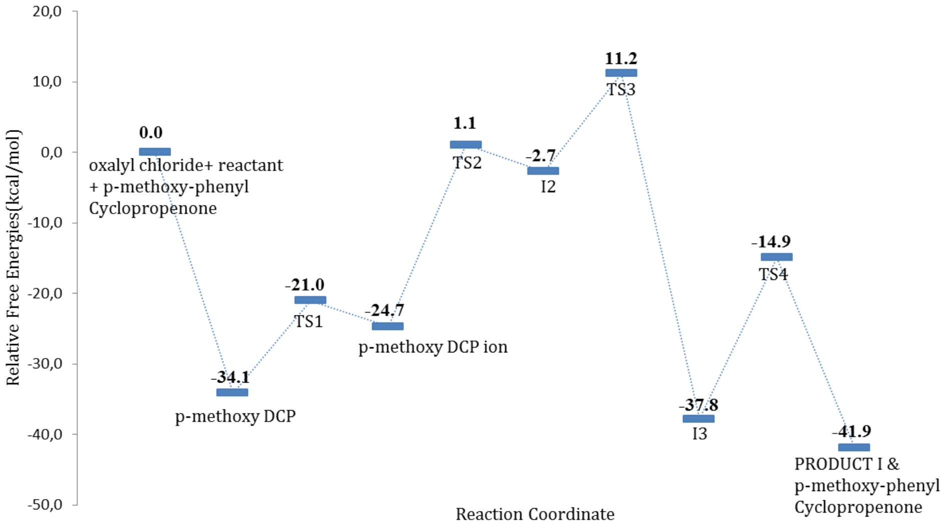

Figure 4.22 : Relative free energy profile of chlorodehydration mechanism in the presence of p-methoxy-phenyl cyclopropenone.

Table 4.7 : NBO charge values of structures located on the reaction coordinate or atoms near to reaction coordinate of chlorodehydration mechanism in the presence of p-methoxy-phenyl cyclopropenone.

	C1	C2	C3	Cl4	Cl5	C6	C7	O8	C9	H10
p-methoxy DCP	-0.124	0.052	0.058	-0.076	-0.076	-0.141	-0.157			
TS1	0.047	0.134	0.140	0.136	-0.794	-0.170	-0.186			
p-methoxy DCP ion	0.037	0.177	0.184	0.177	-0.985	-0.180	-0.196			
Oxime								-0.798	0.053	0.514
TS2	0.119	0.103	0.084	0.069	-0.991	-0.157	-0.150	-0.651	0.066	0.575
I2	0.150	0.062	0.080	-0.005		-0.157	-0.153	-0.598	0.082	0.597
TS3	0.368	0.138	0.134	-0.572		-0.188	-0.177	-0.595	0.094	0.581
I3	0.477	0.114	0.111			-0.198	-0.174	-0.486	0.048	
TS4	0.506	0.019	0.051			-0.172	-0.160	-0.621	0.171	

4.2.1.2 Chlorodehydration reaction in the presence of m-nitro-phenyl cyclopropenone

In the context of this thesis, m-nitro-phenyl cyclopropenone activated chlorodehydration reaction was also modeled at room temperature.

Three different conformers of m-nitro-phenyl cyclopropenone were investigated. The lowest energy conformer is shown in Figure 4.23. The conformers and their relative energy values can be found under the structures.

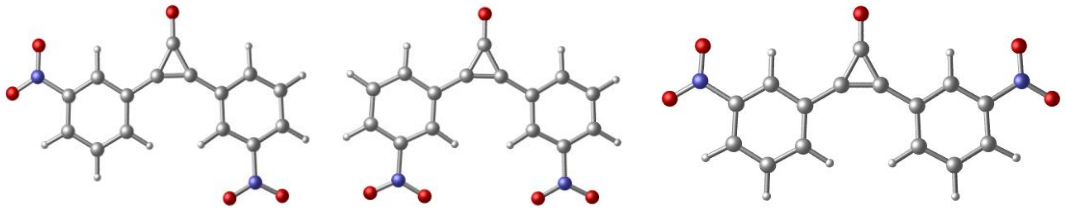

n_C1 (0.00) n_C2 (+0.7) n_C3(+1.4)

Figure 4.23 : Three dimensional structures of the possible conformers of of m-nitrophenylcyclopropenone and their relative energies in kcal/mol.

The whole mechanism was modeled with the lowest energy conformer n_C1.

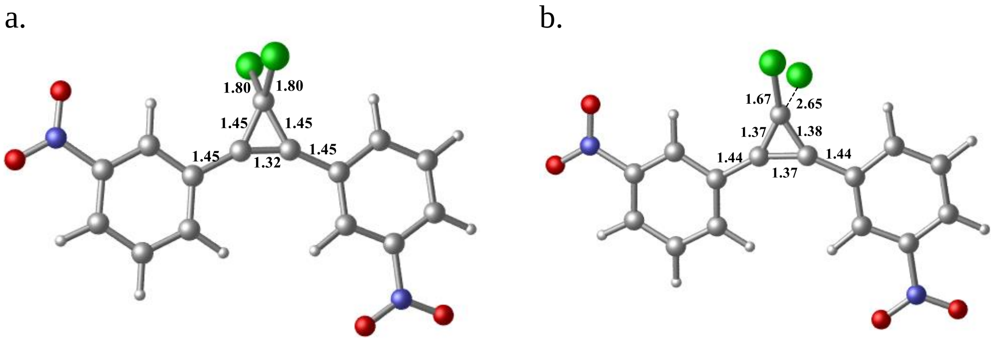
a.
1.80
1.80
1.45
1.45
1.45
1.32
1.45
b.
1.67
2.65
1.37
1.38
1.44
1.44
1.37

m-nitro DCP m-nitro-TS1

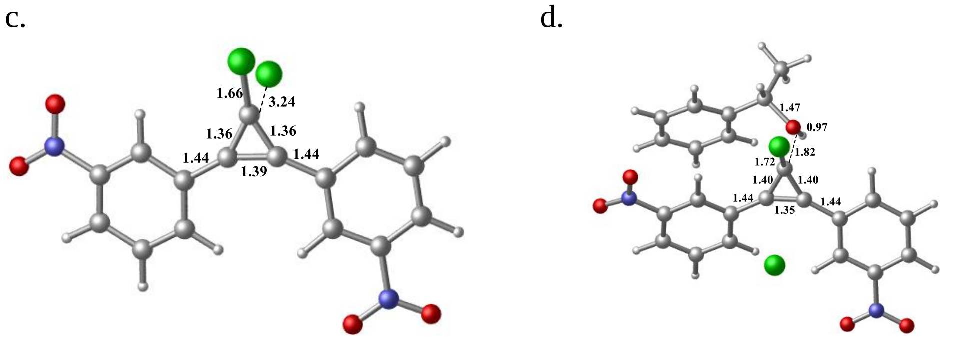
c.
1.66
3.24
1.36
1.36
1.44
1.44
1.39
d.
1.47
0.97
1.72
1.82
1.40
1.40
1.44
1.44
1.35

m-nitro DCP ion m-nitro-TS2

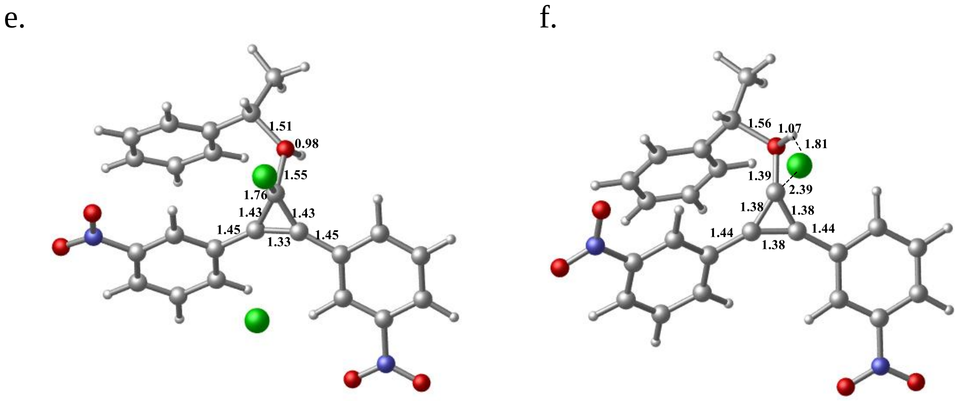
e.
1.51
0.98
1.55
1.76
1.43
1.43
1.45
1.45
1.33
f.
1.56
1.07
1.81
1.39
2.39
1.38
1.38
1.44
1.44
1.38

m-nitro-I2 m-nitro-TS3

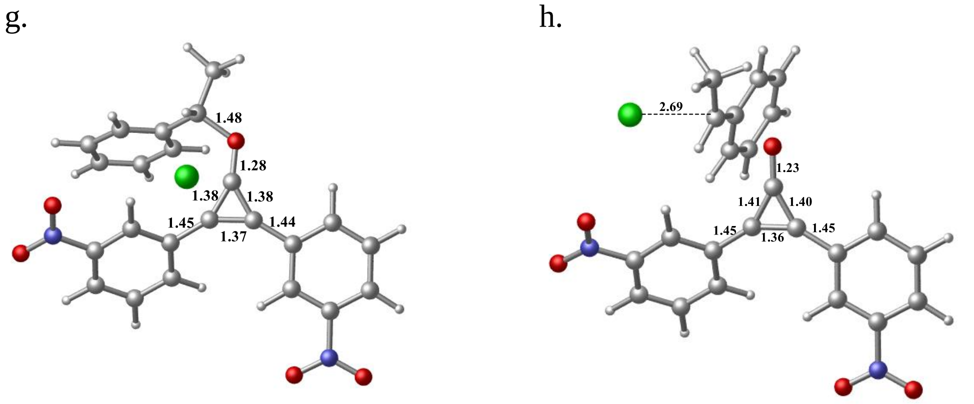
g.
1.48
1.28
1.38
1.38
1.45
1.44
1.37
h.
2.69
1.23
1.41
1.40
1.45
1.45
1.36

m-nitro-I3 m-nitro-TS4

Figure 4.24 : Three dimensional structures of intermediates and transition states for chlorodehydration mechanism in the presence of m-nitro-phenyl cyclopropenone.

When the geometries of the structures were analyzed, it was not observed a notable difference on both geometric parameters of p-methoxy and m-nitro substituted catalyst (Figure 4.21, Figure 4.24). However, the energy profile of the mechanisms show that relative free energy of transition structure m-nitro-TS3 in the presence of m-nitro-phenyl cyclopropenone (22.0 kcal/mol) 10.8 kcal/mol higher than transition structure TS3 in the presence of p-methoxy–phenyl cyclopropenone (11.2 kcal/mol) (Figure 4.22, Figure 4.25). The charges of H and Cl atoms of p-methoxydiphenylcyclopropene which is modeled in the transition structure TS3 are 0.581 and -0.572 respectively. Similarly, the charges of H and Cl atoms of m-nitrodiphenylcyclopropene which is modeled in the transition structure m-nitro-TS3 calculated as 0.556 and -0.532 respectively (Table 4.8). Leaving group HCl from the main structure has stronger electrostatic interactions in the p-methoxydiphenyl substituted structure and it creates an extra stabilization over the transition structure. In addition, the NBO second order perturbation energy values of transition structure TS3 were examined. It is seen that H10 atom interact stronger with orbitals of C1 and O8 atoms of TS3 in the presence of p-methoxy-phenyl cyclopropenone.

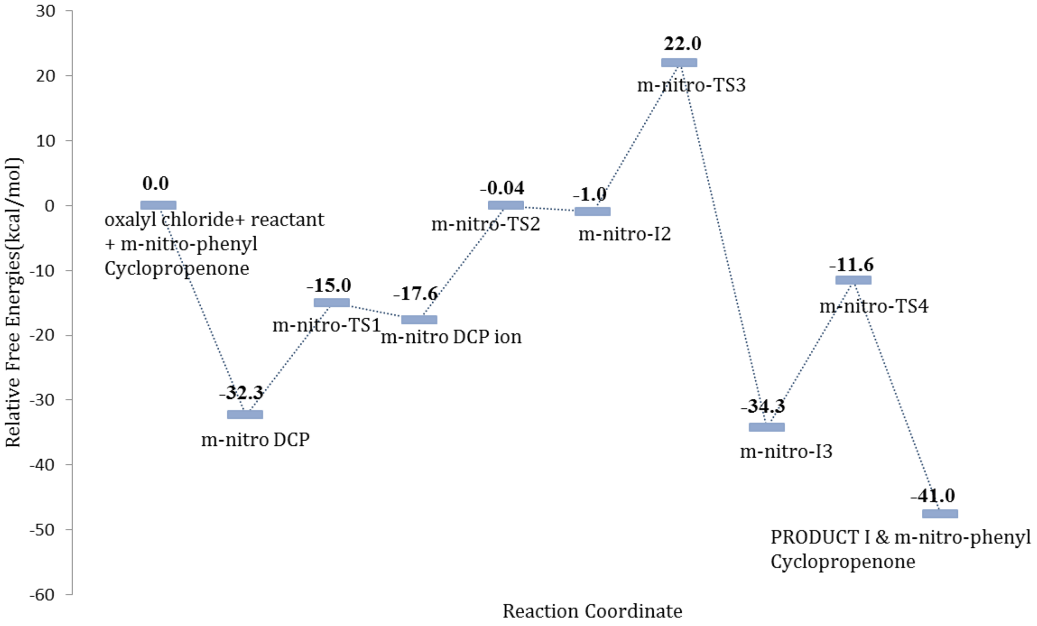

Figure 4.25 : Relative free energy profile of chlorodehydration mechanism in the presence of m-nitro-phenyl cyclopropenone.

Table 4.8 : NBO charge values of structures located on the reaction coordinate or atoms near to reaction coordinate of chlorodehydration mechanism of m-nitro-phenyl substituted cyclopropenone.

	C1	C2	C3	Cl4	Cl5	C6	C7	O8	C9	H10
m-nitro DCP	-0.135	0.066	0.067	-0.047	-0.047	-0.104	-0.121			
m-nitro-TS1	0.076	0.151	0.166	0.192	-0.851	-0.142	-0.139			
m-nitro DCP ion	0.058	0.196	0.200	0.212	-0.964	-0.136	-0.150			
Oxime								-0.798	0.053	0.514
m-nitro-TS2	0.124	0.129	0.111	0.114	-0.980	-0.115	-0.109	-0.671	0.059	0.562
m-nitro- I2	0.154	0.107	0.064	0.038	-0.983	-0.089	-0.116	-0.599	0.073	0.591
m-nitro-TS3	0.402	0.154	0.171	-0.532		-0.145	-0.139	-0.593	0.095	0.556
m-nitro- I3	0.535	0.141	0.112	-0.937		-0.139	-0.125	-0.475	0.059	
m-nitro-TS4	0.536	0.029	0.060			-0.130	-0.118	-0.595	0.188	

4.2.1.3 Benchmark study

To be able to evaluate adequateness of preferred method and basis set during the studies, single point energy values of transition structure TS3 which was determined as a rate determining step of the whole mechanism were calculated using different methods and higher basis sets (Table 4.9). A higher basis set did not have an important effect on the barriers as BMK functional increased the barriers. When MP2 were used, the barriers decreased. In conclusion, a different functional wB97XD gave similar results to M062X functional.

Table 4.9 : Energy values ($\Delta E^{\#}$: Relative electronic energy values kcal/mol) of the rate determing steps of chlorodehydration mechanisms in the presence of m-nitro–phenyl and p-methoxy-phenyl cyclopropenones.

	$m-NO_2$ (RDS: TS 3) $\Delta E^{\#}$kcal/mol	$p-OCH_3$ (RDS: TS 3) $\Delta E^{\#}$kcal/mol
M062X/6-31+G(d,p)	25.7	16.8
M062X/6-311+G(d,p)	22.4	13.7
BMK/6-31+G(d,p)	32.7	21.7
MP2/6-31+G(d,p)	17.4	9.4
wB97XD/6-31+G(d,p)	25.2	16.1

4.2.2 Mechanism B (alternative mechanism)

4.2.2.1 Alternative chlorodehydration reaction in the presence of p-methoxy-phenyl cyclopropenone

The experiment that was done by Lambert et al. oxalyl chloride and alcohol are added in the presence of dichloromethane at room temperature after 30 minutes and cyclopropenone are added as a catalyst. According to this experiment's results, a possible S_N2 mechanism that chlorodehydration reactions follow is proposed shown in Figure 4.26 (Vanos and Lambert, 2011). This alternative mechanism has some similarities with the mechanism that was proposed for triphenyl phosphide oxide catalyzed chlorodehydration reactions and subsequently was disproved by Denton et al. (Denton et al, 2011). In reaction mechanism shown in Figure 4.26, alcohol substrate reacts with oxalyl chloride and hydrochloride acid (HCl) separates, and as a result of that, chloroxalate - in other terms, PRODUCT II (I-5) is obtained. The reaction then proceeds with the nucleophilic attack of the cyclopropenone to the chloroxalate forming an intermediate structure I-6 and a chloride ion. In the last step, PRODUCT I, CO_2, CO ve cyclopropenone are obtained as the consequence of a nucleophilic attack of Cl^- to C1 atom of structure I-6.

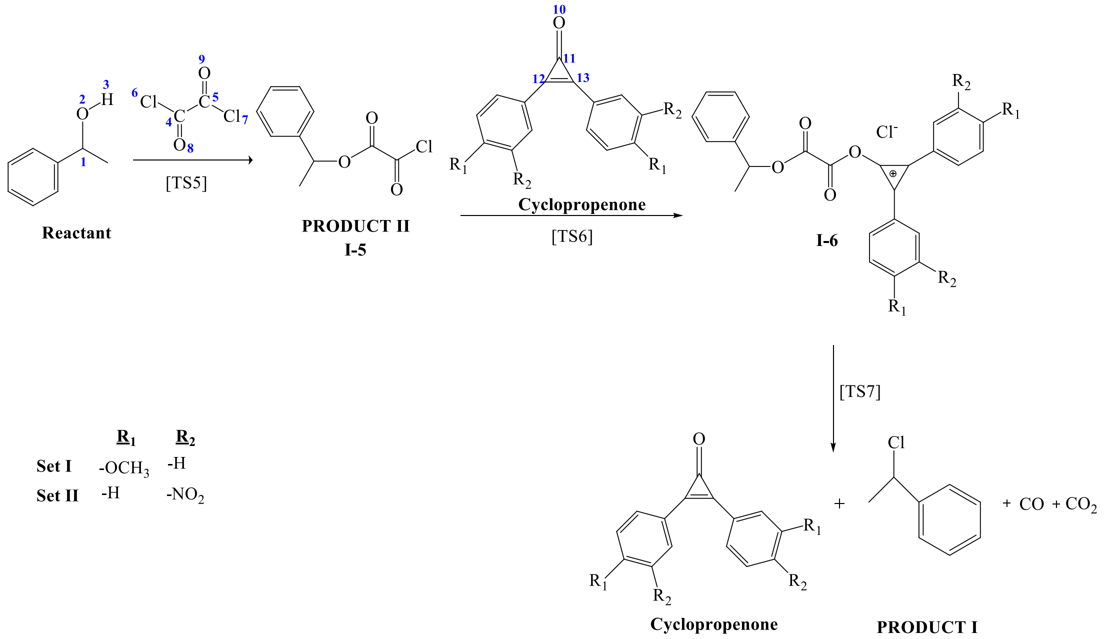

Figure 4.26 : The proposed intermediates for Mechanism B (Vanos and Lambert, 2011).

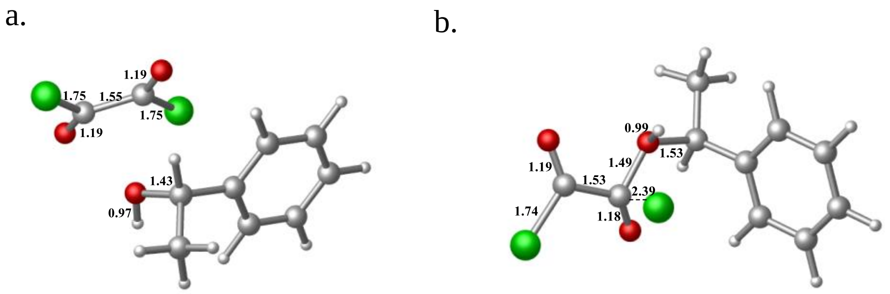
a.
1.19
1.75
1.55
1.75
1.19
1.43
0.97
b.
0.99
1.53
1.49
1.19
1.53
2.39
1.74
1.18

Reactant & oxalyl chloride

TS5

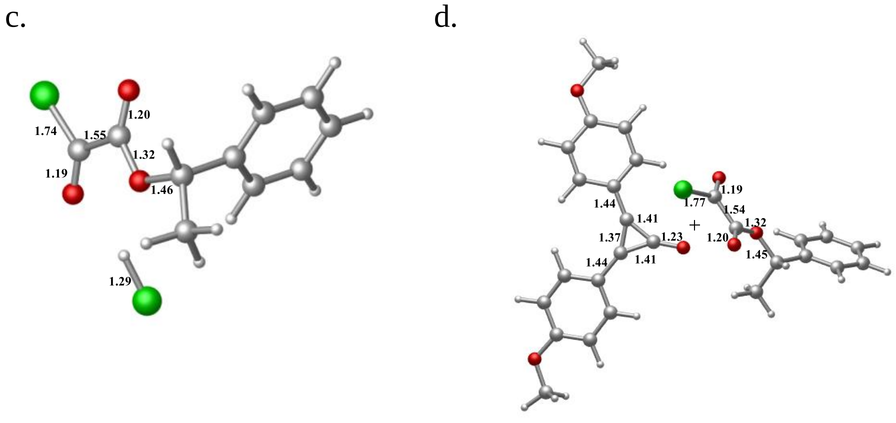
c.
1.20
1.74
1.55
1.32
1.19
1.46
1.29
d.
1.19
1.77
1.44
1.54
1.41
1.32
+
1.37
1.23
1.20
1.45
1.44
1.41

I-5 (PRODUCT II)

cyclopropenone-chloro oxalate complex

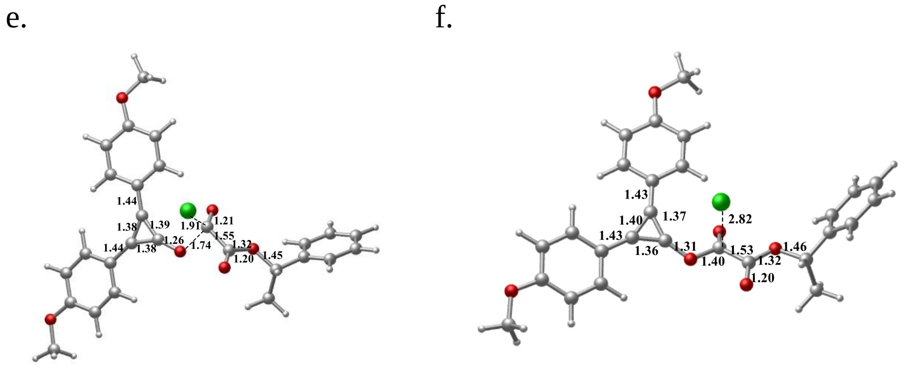
e.
1.44
1.21
1.38
1.39
1.91
1.55
1.26
1.74
1.44
1.38
1.32
1.20
1.45
f.
1.43
1.37
1.40
2.82
1.43
1.31
1.53
1.46
1.36
1.40
1.32
1.20

TS6

I6

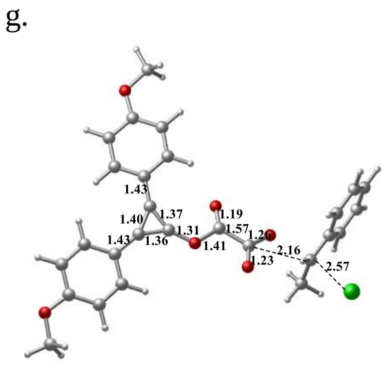
g.
1.43
1.37
1.19
1.40
1.31
1.57
1.43
1.36
1.41
1.26
2.16
1.23
2.57

TS7

Figure 4.27 : Three dimensional structures of intermediates and transition states for Mechanism B in the presence of p-methoxy-phenyl cyclopropenone.

The formation of chloroxalate and separation of HCl is modeled via transition structure TS5 having a relative free energy of 19.5 kcal/mol. (Figure 4.27b, Figure 4.28). In transition structure TS5, the bond between Cl6 and C4 is broken and the relative distance lengthens to 2.39 Å from 1.75 Å. Furthermore, the distance between H3-Cl6 is found to be 2.32 Å as the distance between O2 atom of alcohol substrate and C4 atom of oxalyl chloride is decreased from 2.65 to 1.49 Å in transition structure TS5. Formation of PRODUCT II is an exergonic process. Following the formation of PRODUCT II, PRODUCT I is obtained in Mechanism B.

In the second step of the path, cyclopropenone-chloroxalate complex is obtained with the addition of cyclopropenone to the medium. Subsequently, nucleophilic attack of cyclopropenone to oxalyl chloride occurs as chloride ion leaves. The interaction between cyclopropenone and chloroxalate is modeled via transition state structure TS6 (Figure 4.27). The transition structure TS6 has a free energy barrier of 8.8 kcal/mol. In transition structure TS6, the distance between O8-C5 is shortened from 2.63 Å to 1.74 Å where the C5-Cl7 bond length is elongated from 1.77 Å to 1.91 Å. These bond lengths are found to be 1.40 Å and 2.82 Å, respectively in intermediate structure I-6 which has a relative free energy of -12.7 kcal/mol (Figure 4.28).

In the last step, formation of PRODUCT I and regeneration of cyclopropenone occur as the consequence of a nucleophilic attack of chloride ion to O2 of structure I-6. Formation of chlorodehydration product is modeled via transition structure TS7 having a relative free energy of 19.5 kcal/mol. In structure TS7, the distance of C1 atom to chloride ion and C4 atom is measured as 2.57 Å and 2.16 Å, respectively. The reaction has a high exergonicity and products have relative free energy of -50.3 kcal/mol (Figure 4.28).

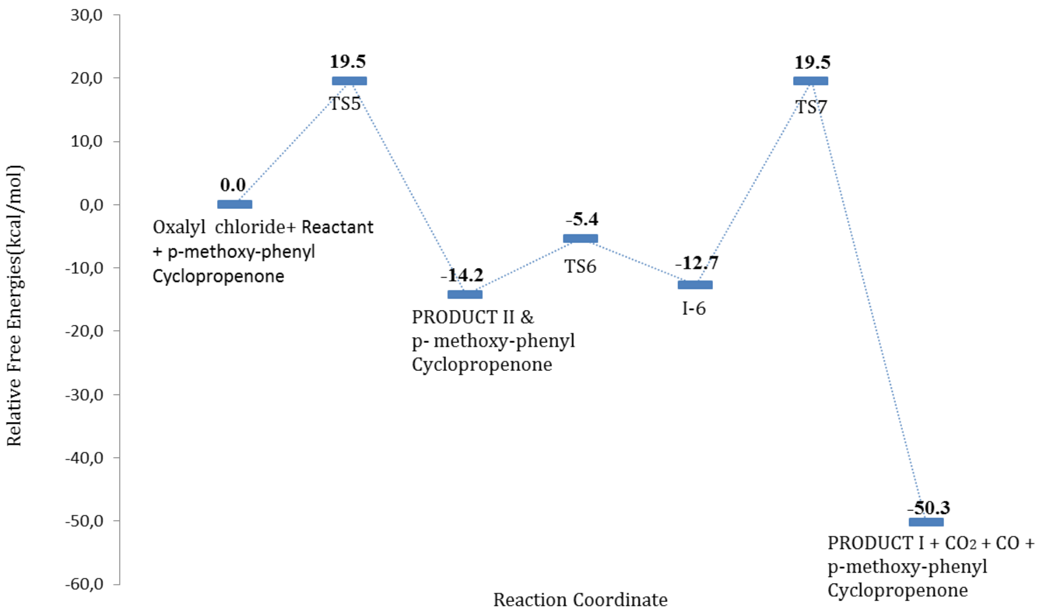

Figure 4.28 : Relative free energy profile of Mechanism B in the presence of p-methoxy-phenyl cyclopropenone.

Table 4.10 : NBO charge values of structures located on the reaction coordinate or atoms near to reaction coordinate of Mechanism B in the presence of p-methoxy-phenyl cyclopropenone.

	C1	O2	H3	C4	C5	Cl6	Cl7	O8	O9	O10	C11	C12	C13
Reactant & oxalyl chloride	0.049	-0.806	0.527	0.458	0.463	0.016	0.010	-0.487	-0.487				
TS5	0.072	-0.622	0.604	0.711	0.451	-0.636	0.029	-0.539	-0.499				
I-5	0.058	-0.560	0.317	0.773	0.456	-0.329	0.020	-0.567	-0.501				
complex	0.056	-0.546		0.791	0.479		-0.032	-0.598	-0.502	-0.693	0.519	-0.001	0.015
TS6	0.053	-0.551		0.800	0.523		-0.223	-0.615	-0.667	-0.566	0.505	0.082	0.074
I-6	0.056	-0.545		0.793	0.780		-0.903	-0.600	-0.534	-0.491	0.467	0.149	0.128
TS7	0.153	-0.685		0.732	0.772		-0.770	-0.705	-0.546	-0.501	0.454	0.137	0.133

4.2.2.2 Alternative chlorodehydration reaction in the presence of m-nitro-phenyl cyclopropenone

Since the initial steps of m-nitro-phenyl cyclopropenone and p-methoxy-phenyl cyclopropenone activated alternative chlorodehydration mechanisms are the same, initial structures (Reactant & oxalyl chloride, TS5) were not modeled again.

When three dimensional geometries of the structures have been analyzed, a notable difference is not seen on both geometric parameters of p-methoxy-phenyl and m-nitro- phenyl substituted catalysts. However, it is seen that the relative free energy of m-nitro-TS7 (28.6 kcal/mol) is 9.1 kcal/mol higher than TS7 (19.5 kcal/mol) similar to Mechanism A. (Figure 4.28, Figure 4.30).

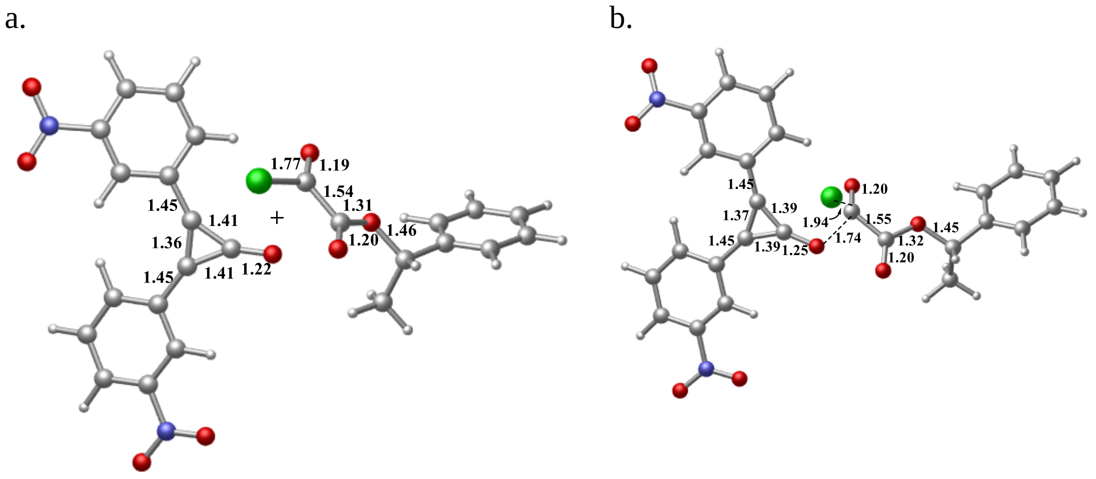
a.
b.
1.77
1.19
1.54
1.31
+
1.45
1.41
1.36
1.20
1.46
1.45
1.41
1.22
1.45
1.39
1.37
1.94
1.20
1.55
1.45
1.45
1.39
1.25
1.74
1.32
1.20

m-nitro-phenyl cyclopropenone chloroxalate complex

m-nitro-TS6

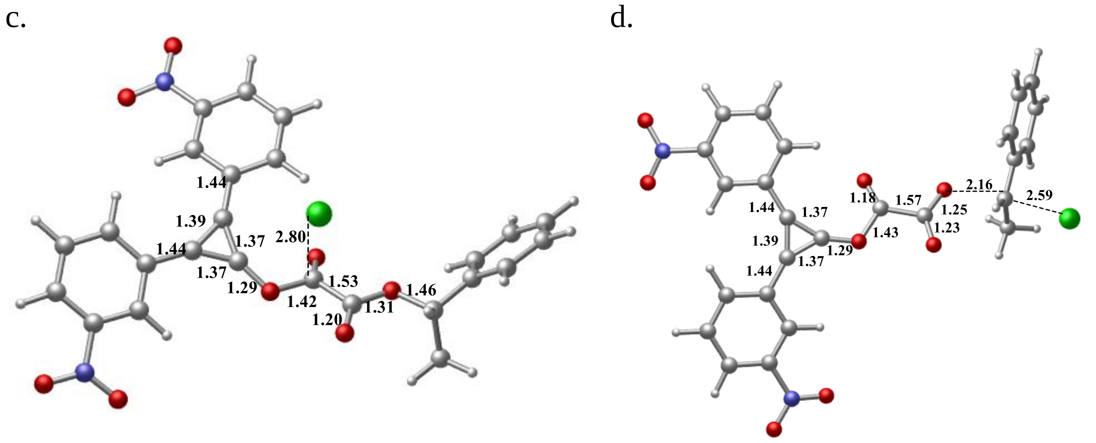
c.
d.
1.44
1.39
1.44
1.37
2.80
1.37
1.29
1.53
1.42
1.46
1.20
1.31
2.16
2.59
1.18
1.57
1.25
1.23
1.44
1.37
1.43
1.39
1.29
1.37
1.44

m-nitro-I6

m-nitro-TS7

Figure 4.29 : Three dimensional structures of intermediates and transition states for Mechanism B in the presence of m-nitro-phenyl cyclopropenone.

This time m-nitro-phenyl cyclopropenone is added to chloroxalate called as structure I-5. Following the formation of chloroxalate complex, chloride ion separates. It is modeled via transition structure TS6 overcoming an energy barrier of 12.5 kcal/mol (Figure 4.29b). Subsequently, I-6 structure is obtained as an intermediate. Finally, the nucleophilic attack of Cl^- to O2 atom on the structure I-6 is modeled via TS6.

p-methoxy-phenyl substituted structures and m-nitro-phenyl substituted structures structures have quite similar geometric parameters. Comparing relative free energies, m-nitro substituted structures have higher values (Figure 4.28, Figure 4.30). However, TS7 structures for both of the substituents have similar energy barriers of approximately 33.0 kcal/mol. This situation stems from that relative free energy of I-6 is lower than m-nitro-I6 although TS7 and m-nitro-TS7 structures have different relative free energies. As it is expressed, there is a high similarity between three dimensional structures, thus electronic effects may cause these energy differences. Dipole moment of I-6 is found to be 12.88 Debye as dipole moment of structure m-nitro-I6 is 8.46 Debye. The comparison related to charges was done with APT charges since NBO charge of m-nitro-I6 structure could not be calculated. The charges can be seen in Figure 4.31. Significant charge differences are observed especially on the aromatic ring parts of the structures. Electron withdrawing and electron donating characters of m-nitro-phenyl substituent and p-methoxy-phenyl substituent, respectively, affect the distribution of charges on the ring. Consequently, electronic properties of aryl substituents play an important role on relative stability of the structures. All electronic effects cause getting similar energy barrier values for both of the substituents, although TS7 has a lower relative free energy.

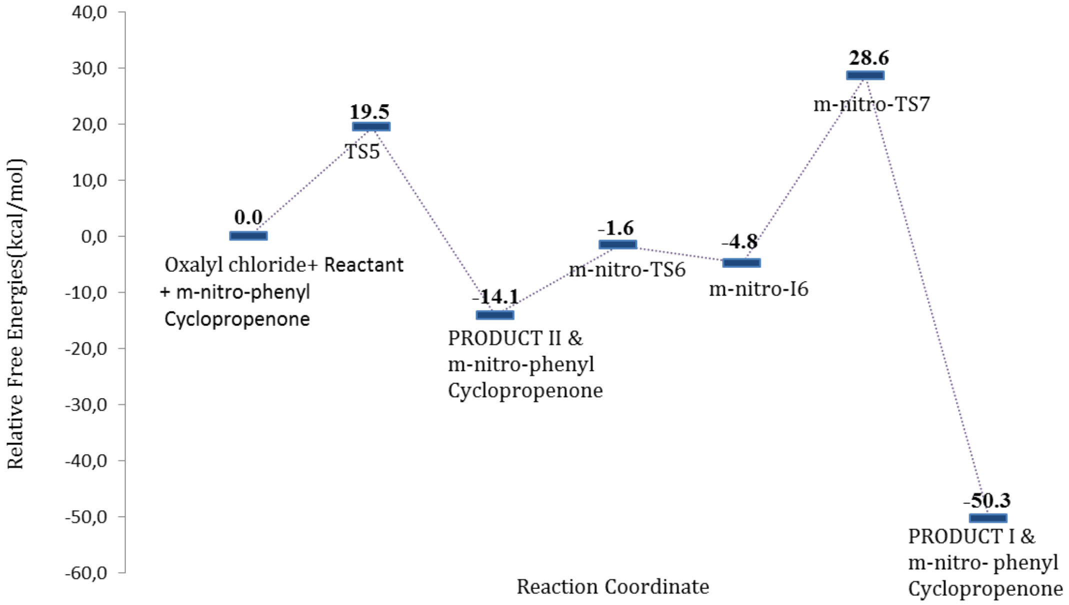

Figure 4.30 : Relative free energy profile of Mechanism B in the presence of m-nitro-phenyl cyclopropenone.

Table 4.11 : NBO charge values of structures located on the reaction coordinate or atoms near to reaction coordinate of Mechanism B in the presence of m-nitro-phenyl cyclopropenone.

	C1	O2	C4	C5	Cl7	O8	O9	O10	C11	C12	C13
Complex	0.056	-0.545	0.787	0.477	-0.032	-0.595	-0.499	-0.659	0.531	0.042	0.013
m-nitro-TS6	0.054	-0.550	0.797	0.535	-0.245	-0.609	-0.661	-0.538	0.533	0.092	0.086
m-nitro-I6	N/A	N/A	N/A	N/A	N/A	N/A	N/A	N/A	N/A	N/A	N/A
m-nitro-TS7	0.185	-0.925	-0.505	0.554	-0.804	0.814	-0.307	-0.491	0.494	0.146	0.143
m-nitro-I7	-0.716	-0.740	0.712	0.773	-0.117	-0.736	-0.551	-0.498	0.500	0.142	0.142

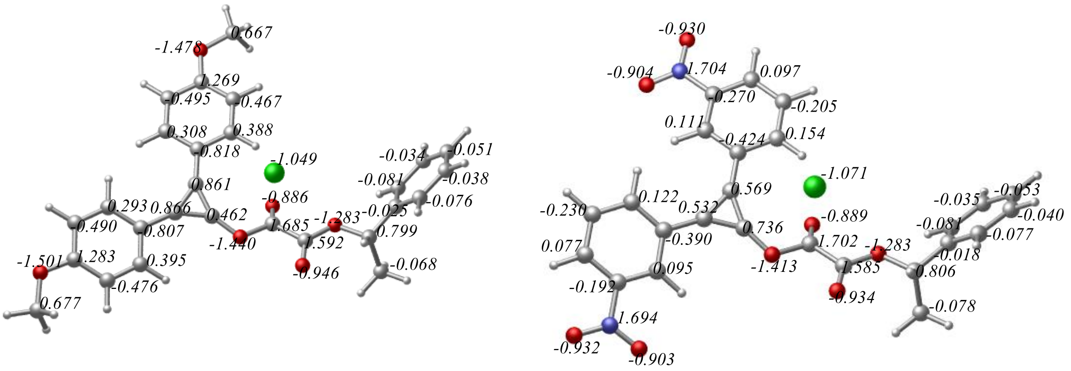
-1.478
0.667
1.269
-0.495
-0.467
0.308
0.388
-0.818
-1.049
0.861
-0.886
0.293
0.866
0.462
1.685
-1.283
-0.025
-0.490
-0.807
-1.440
1.592
0.799
-1.501
1.283
0.395
-0.946
-0.068
-0.476
0.677
-0.034
-0.051
-0.081
-0.038
-0.076
-0.930
-0.904
1.704
0.097
-0.270
-0.205
0.111
-0.424
0.154
-1.071
0.569
0.122
-0.230
0.532
-0.889
0.736
-0.390
1.702
-1.283
0.077
-1.413
1.585
0.806
0.095
-0.192
-0.934
-0.078
1.694
-0.932
-0.903
-0.035
-0.053
-0.081
-0.040
-0.077
-0.018

I-6 m-nitro-I6

Figure 4.31 : Charge distribution of I-6 and m-nitro-I6 structures.

4.2.2.3 Benchmark study

Benchmark analyze was also performed for the alternative chlorodehydration mechanisms (Table 4.12). The barriers were not effected by an increase in basis set. It is known that the barriers are well defined with BMK functional where the kinetic energy density is included together with a large value of the exact exchange missing coefficients (Boese and Martin, 2004). The calculated energy barriers with BMK functional were not different from the M062X barriers. Although barriers were increased as the methodology has changed from DFT to post-HF, the energy difference between two barriers were not effected. Lastly, wB97XD functional is used for a better dispersion effect definition and again the energy difference between two barriers were not remained unchanged.

Table 4.12 : Energy values ($\Delta E^{\#}$: Relative electronic energy values kcal/mol) of the rate determing steps of alternative chlorodehydration mechanisms in the presence of m-nitro–phenyl and p-methoxy-phenyl cyclopropenones.

	$m\text{-}NO_2$ (RDS: TS 7) $\Delta E^{\#}$kcal/mol	$p\text{-}OCH_3$ (RDS: TS 7) $\Delta E^{\#}$kcal/mol
M062X/6-31+G(d,p)	27.9	19.2
M062X/6-311+G(d,p)	29.7	21.1
BMK/6-31+G(d,p)	27.0	17.4
MP2/6-31+G(d,p)	36.4	28.5
wB97XD/6-31+G(d,p)	24.3	15.8

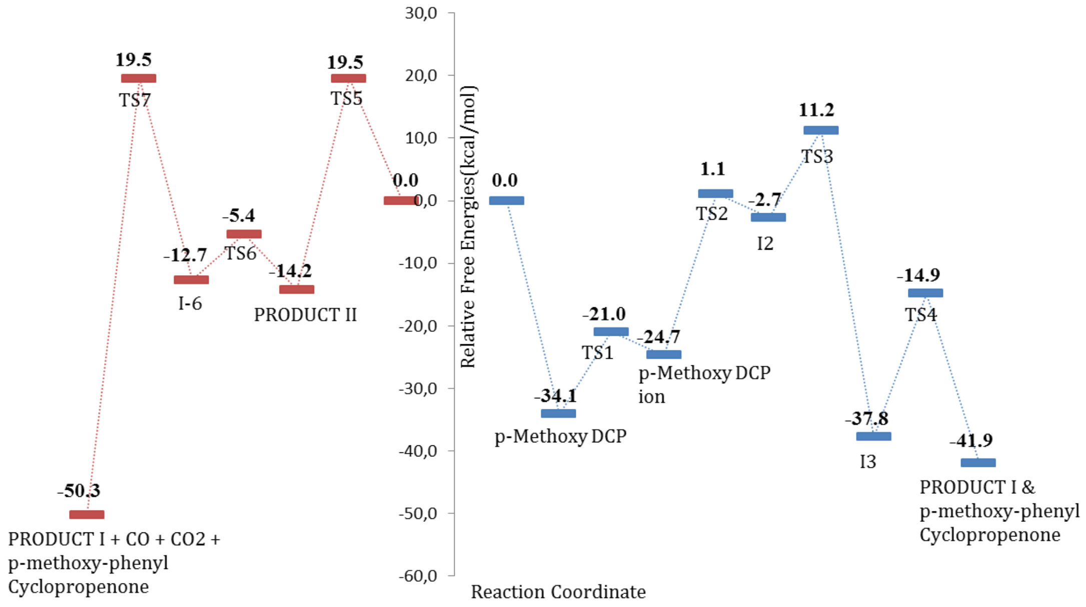

Figure 4.32 : Relative free energies of Mechanism A and Mechanism B in the presence of p-methoxy-phenyl cyclopropenone.

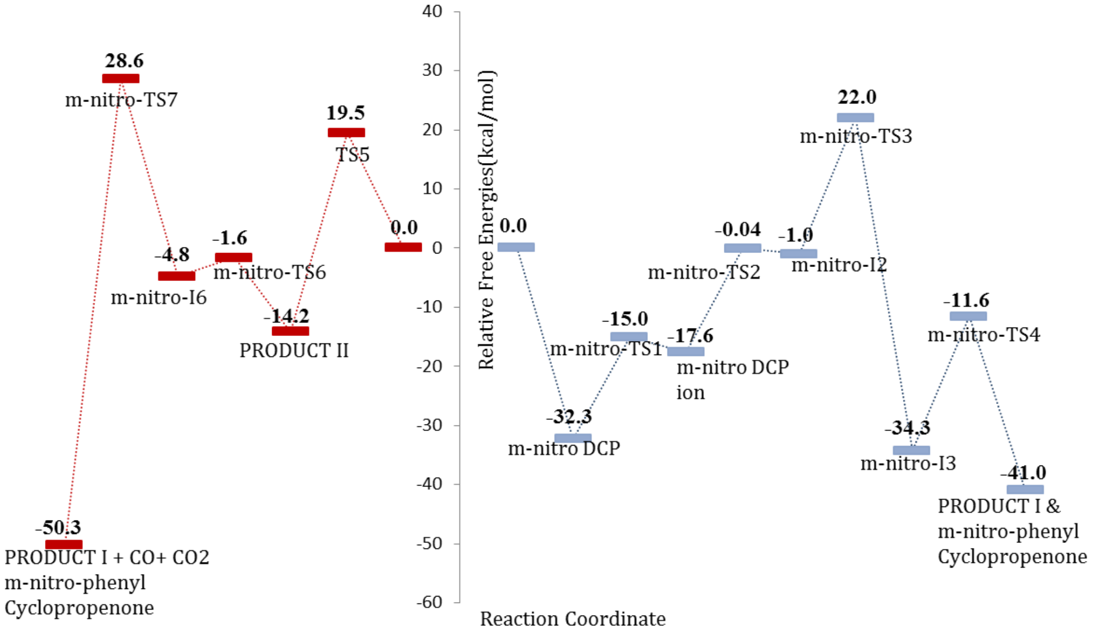

Figure 4.33 : Relative free energies of Mechanism A and Mechanism B in the presence of m-nitro-phenyl cyclopropenone.

In order to explain the product distribution difference obtained in experiments, relative free energies of the rate determining steps of Mechanism A (structure TS3) and Mechanism B (structure TS7) are compared (Figure 4.32 and Figure 4.33). PRODUCT I can be obtained both from Mechanism A and Mechanism B. In addition, PRODUCT II can only be obtained via Mechanism B.

In experiments, the m-nitro substitution on the phenyl ring of cyclopropenone alters the product distribution on behalf of the PRODUCT II (Table 2.1). When the calculated rate determining step barriers are compared, Mechanism A is more probable for the formation of PRODUCT I whichever substituents are added to cyclopropenones.

For the p-methoxy-phenyl cyclopropenone case, TS7 of Mechanism B has relative free energy value of 19.5 kcal/mol which could be exceeded at room temperature easily. However for Mechanism A, the calculated rate determining step has a barrier of 11.2 kcal/mol which leads to the formation of PRODUCT I with a higher percent yield. For the m-nitro-phenyl cyclopropenone case, the barriers of both mechanisms are higher relative to the previous case due to the electron-withdrawing characteristic of the substituent. Formation of PRODUCT I via Mechanism B is not possible having a relative free energy value 28.6 kcal/mol (Structure m-nitro-TS7). In

Mechanism B, m-nitro-phenyl cyclopropenone does not play a role at the beginning of the path hence the free energy of activation did not change for the formation of PRODUCT II. Formation of PRODUCT I via Mechanism A requires 22.0 kcal/mol of free energy which is 2.5 kcal/mol higher than energy required for the formation of PRODUCT II via Mechanism B. The difference in required free energy to overcome the activation barrier explains the PRODUCT II and PRODUCT I distribution (the ratio of 86/14 in Table 2.1) qualitatively.

5. CONCLUSIONS

In the scope of the thesis, two different cyclopropenium activated reactions were modeled and explained the product distribution differences based on electronic properties. In the first part of the study, BKR mechanism was modeled based on experimental findings proposed by Lambert et al. (2010). In the literature, two different mechanisms; self-propagating or organocatalytic were proposed for experiments conducted at room temperatures. The initialization part, which contains a R-migration step is common for all proposed reaction mechanisms. R-migration step has the highest overall relative free energy (40.9 kcal/mol), which can be considered as the rate determining step. As a consequence of R-migration step, nitrilium cation and cyclopropenium are obtained and then, the reaction path branches off. Nitrilium cation is a common intermediate both for self-propagating and organocatalytic mechanisms. The rate determining step of organocatalytic mechanism (13.9 kcal/mol) has a lower free energy value relative to self-propagating mechanism (19.1 kcal/mol), hence organocatalytic path is more probable for the BKR mechanism. In addition, a qualitative agreement is seen between relative free energy values and experimental yield values.

In the second part of the study BKR reactions at elevated temperatures based on a mechanism suggested by Yadav et al. (2010) was modeled. Although the initiation step still proceeds over a R-migration, organocatalytic mechanism has a Meisenheimer complex as an intermediate. Our results showed that, the reaction mechanism may proceed via organocatalytic mechanism as well as the reaction mechanism may turn back to self-propagation mechanism after R-migration step. As it has been mentioned, the relative free energy value of the rate determining step in Lambert’s proposed mechanism was found 40.9 kcal/mol. It is approximately 20 kcal/mol higher than the relative free energy value of the rate determining step in Yadav’s mechanism. Although these energy values are the consequences of the calculations at elevated temperature, similar energy values were obtained when the energies recalculated at room temperature. After modelling Yadav's path, it has been noticed that, a self-propagating mechanism after R-migration occurs is more probable. The relative free energy value of the rate determining (20.7 kcal/mol) in the self-propagating mechanism is lower than the relative free energy value of the rate determining (24.3 kcal/mol) in the organocatalytic mechanism. On the other hand, existence of an organocatalytic mechanism proceeding via Meisenheimer complex should not be ignored. It is noteworthy that, the mechanism proceeding via Meisenheimer complex has been modeled for the first time.

In the last part of the thesis, cyclopropenone activated chlorodehydration reactions were studied. The mechanisms were modeled in the presence of p-methoxy and m-nitro substituents in order to elucidate the reaction mechanism and product distribution based on the experiments done by Lambert et. al (2011).

The obtained results showed that Mechanism A is more probable for the formation of PRODUCT I. PRODUCT II can not be obtained via Mechanism A based on experimental findings. PRODUCT I can be obtained via both Mechanism A and Mechanism B. Our results indicate that formation of PRODUCT I is more probable via Mechanism A for both of the substituents. However, p-methoxy-phenyl substituted case, PRODUCT II formation in trace amount should not be disregarded. At room temperature, the free energy value of 19.5 kcal/mol is not impossible to overcome. This situation enables us to interpret the experimental percent ratio of 98 to 2 qualitatively.

In experiments, an increase in yield is observed in the formation of PRODUCT II for the case of m-nitro-phenyl cyclopropenone case. The obtained free energy values showed that the possibility of formation of PRODUCT II in Mechanism B is more than the possibility of formation of PRODUCT I in Mechanism A for the case of m-nitro-phenyl cyclopropenone case.

Choising suitable computational parameters are quite important in order to obtain correct results. For this reason, studies were done with different methods and basis sets, too. As a consequence of benchmark studies, the DFT method employing the M062X functional with the 6-31+G** basis set is found to be appropriate in the context of this study.

The obtained results throughout this thesis enabled us to explain the details of reaction mechanisms of cyclopropenium activated BKR and chlorodehydration reactions. Moreover, organocatalytic mechanism via Meisenheimer complex is modeled for the first time. At elevated temperature, possibility of self-propagating mechanism should not be disregarded.

REFERENCES

An, N., Tian, B.-X., Pi, H.-J., Eriksson, L.A., Deng, W.-P. (2013). Mechanistic insight into self- propagation of organo-Mediated Beckmann Rearrangement: A combined experimental and computational study. *J.Org. Chem.***,** *78,* 4297-4302.

Boga, C., Del Vecchio, E., Forlani, L., Mazzanti, A., Todesco, P. E. (2005). Evidence for carbon-carbon Meisenheimer-Wheland complexes between superelectrophilic and supernucleophilic carbon reagents. *Angew. Chem. Int. Ed, 44*, 3285−3289.

Boese, A. D., and Martin, J. M. L. (2004). Development of density functionals for thermochemical kinetics, *J. Chem. Phys., 121,* 3405-3416.

Breslow, R., Haynie, R. R., Mirra, J. (1959). The synthesis Of diphenylcyclopropenone. *J. Am. Chem. Soc., 81,* 247.

Breslow, R., and Peterson, R. (1960). Dipropylcyclopropenone. *J. Am. Chem. Soc., 82*, 4426.

Breslow R., and Posner J. (1967). Diphenylcyclopropenone. *Org. Synth., 47,* 62.

Chai D., and Head-Gordon, M. (2008). Long-range corrected hybrid density functionals with damped atom-atom dispersion corrections. *Phys. Chem. Chem. Phys., 10*, 6615-20.

Chapman, A. W. (1935). *J. Chem. Soc.*, 1223−1229.

Constable D. J. C., Dunn P. J., Hayler J. D., Humphrey G. R., J. L. Leazer Jr., Linderman R. J., Lorenz K., Manley J., Pearlman B. A., Wells A., Zaks A., Zhang T. Y. (2007). Key green chemistry research areas- a perspective from pharmaceutical manufacturers. *Green Chem., 9,*411.

Cramer C. J., (1961). Essentials of computational chemistry (2nd ed.) (pp. 166,252,253,254). John Wiley & Sons Ltd.

CYLview, version 1.0b, 2009, Legault, C. Y., Université de Sherbrooke.

Denton, R. M., An, J.; Adeniran, B. (2010). Phosphine oxide-catalysed chlorination reactions of alcohols under Appel conditions. *Chem Commun., 46,* 3025.

Denton, R. M., Tang, X., Przeslak, A. (2010). catalysis of phosphorus(v)-mediated transformations: dichlorination reactions of epoxides under appel conditions. *Org. Lett., 12,* 4678-4681.

Denton, R. M., An, J., Adeniran, B., Blake, A. J., Lewis, W., Poulton, A. M. (2011). Catalytic Phosphorus(V)-Mediated nucleophilic substitution reactions: Development of a catalytic Appel Reaction. *J. Org. Chem., 76,* 6749-6767.

Eck, J. C., Marvel, C. S. (1939). ε-Benzoylaminocaproic acid. *Org. Synth., 19,* 20.

Eck, J. C., Marvel, C. S. (1943). E-Benzoylaminocaproic acid. *Org. Synth., 2,* 76.

Fernandez, I., Frenking, G., Uggerud, E. (2010). Rate-determining factors in nucleophilic aromatic substitution reactions. *J. Org. Chem. 75,* 2971−2980.

Föhlisch B., and Bürgle P. (1967). Cyclopropenyliumsalze und Chinocyclopropene. *Justus Liebigs Ann. Chem., 701,*67-87.

Frisch M. J., Head-Gordon M., Pople J. A. (1990). *Chem. Phys. Lett., 166,* 275-280.

Frisch, M. J., Trucks, G. W., Schlegel, H. B., Scuseria, G. E., Robb, M. A., Cheeseman, J. R., Scalmani, G., Barone, V., Mennucci, B., Petersson, G. A., Nakatsuji, H., Caricato, M., Li, X., Hratchian, H. P., Izmaylov, A. F., Bloino, J., Zheng, G., Sonnenberg, J. L., Hada, M., Ehara, M., Toyota, K., Fukuda, R., Hasegawa, J., Ishida, M., Nakajima, T., Honda, Y., Kitao, O., Nakai, H., Vreven, T., Montgomery, Jr., J. A.; Peralta, J. E.; Ogliaro, F.; Bearpark, M.; Heyd, J. J., Brothers, E., Kudin, K. N., Staroverov, V. N.; Kobayashi, R.; Normand, J.; Raghavachari, K.; Rendell, A.; Burant, J. C., Iyengar, S. S., Tomasi, J.; Cossi, M.; Rega, N., Millam, J. M., Klene, M., Knox, J. E., Cross, J. B., Bakken, V., Adamo, C., Jaramillo, J., Gomperts, R., Stratmann, R. E., Yazyev, O., Austin, A. J., Cammi, R., Pomelli, C., Ochterski, J. W., Martin, R. L., Morokuma, K., Zakrzewski, V. G., Voth, G. A., Salvador, P., Dannenberg, J. J., Dapprich, S., Daniels, A. D., Farkas, Ö., Foresman, J. B., Ortiz, J. V., Cioslowski, J., Fox, D. J. (2009). *Gaussian, Inc.,* Wallingford CT.

Fukui K. (1970). Formulation of the reaction coordinate. *J. Phys. Chem., 74,* 4161.

Fukui K. (1981). The path of chemical reactions- the IRC approach *Acc. Chem. Res., 14*, 363.

Furuya, Y., Ishihara, K., Yamamoto H. (2005). Cyanuric chloride as a mild and active Beckmann rearrangement catalyst. *J. Am. Chem. Soc., 127,* 11240-11241.

Fernandez, I., Frenking, G.; Uggerud, E. (2010). Rate-determining factors in nucleophilic aromatic substitution reactions. *J. Org. Chem., 75,* 2971−2980.

Glukhotsev, M. N., Bach, R. D., Laiter, S. (1997). Single-step and multistep mechanisms of aromatic nucleophilic substitution of halobenzenes and halonitrobenzenes with halide anions: Ab initio computational study. *J. Org. Chem., 62*, 4036−4046.

Gonzalez C., Schlegel H. B. (1989). An improved algorithm for reaction path following. *J. Chem. Phys.90*,2154.

Gonzalez, C.; Schlegel, H. B. (1990). Reaction path following in mass-weighted internal coordinates, J. Phys. Chem., 94, 5523-5527.

Grimme, S. (2011). Density functional theory with London dispersion corrections. *WIREs Comput. Mol. Sci., 1*, 211-228.

Hammond, G. S. (1955). A correlation of reaction rates. *J. Am. Chem. Soc., 77,* 334–338.

Jones Gavin O. , Saoma Ali Al, O'Brien Jeannette M., Albishi Hassan, Al-Megren Hamid A., Alabdulrahman Abdullah M., Alsewailem Fares D., Hedrick James L., Rice Julia E., Horn Hans W. (2013). Computational investigations on base-catalyzed diaryl ether formation. *J. Org. Chem*., 78 (11), 5436–5443.

Ma H., Bao Z., Bai L., Cao W. (2012). A new facile route to chlorination of alcohols via lewis acid $AlCl_3$. *Int. J. of Org. Chem., 2*, 21-25.

Jones, G. O., Al Somaa, A., O'Brien, J. M., Albishi, H., Al-Megren, H. A., Alabdulrahman, A. M., Alsewailem, F. D., Hedrick, J. L., Rice, J. E., Horn H. W. (2013). Computational investigations on base-catalyzed diaryl ether formation. *J. Org. Chem., 78*, 5436–5443.

Kelly, B.D., and Lambert, T. H. (2009). Aromatic cation Activation of alcohols: Conversion to alkyl chlorides using dichlorodiphenylcyclopropene. *J. Am. Chem. Soc., 131*, 13930-13931.

Kelly, B. D., and Lambert, T. H. (2011). Cyclopropenium-activated cyclodehydration of diols. *Organic Letters, 13,* 740-743.

Kopple, K. D., and Katz, J. J. (1959). Beckmann rearrangement in hydrogen fluoride , J. Org. Chem., 24, 1975-1977.

Kursanov, D. N., Volpin, M. E., Koreshkov, Y. D. (1959). Diphenylcyclopropenone: A three membered analog of tropone, *Izv. Acad. Nauk SSSR, Otd. Khim. Nauk.,3,* 560.

Levine I. N. (2009). Physical chemistry (6th ed.) (pp. 711, 712, 713, 714, 715) McGraw- Hill Companies Inc.

Maeda S., Harabuchi Y., Ono Yuriko, Taketsugu T., Morokuma K. (2015). Intrinsic reaction coordinate: calculation, bifurcation and automated search. *Int. J. Quantum Chem., 115*, 258 - 269.

Miertus, S., Scrocco, E., Tomasi (1981). Electrostatic interaction of a solute with a continuum - a direct utilization of abinitio molecular potentials for the prevision of solvent effects. *J. Chem. Phys., 55,* 117-129.

Mitsunobu, O. and Yamada, Y. (1967). Preparation of esters of carboxylic and phosphoric acid via quaternary phosphonium salts. *Bulletin of the Chemical Society of Japan, 40,* 2380–2382.

Nguyen, T. V., and Bekensir, A. (2014). Aromatic cation activation: Nucleophilic substitution of alcohols and carboxylic acids. *Org. Lett., 16,* 1720–1723.

Ramachandran K. I., Deepa G., Namboori K. (2008). Computational chemistry and molecular modeling (pp.124) Springer.

Reed, A. E., Curtiss, L. A., Weinhold, F. (1988). Intermolecular interactions from a natural bond orbital. Donor-Acceptor Viewpoint. *Chem. Rev., 88,* 899-926.

Ritz, J., Fuchs H., Kieczka H., Moran W. C. (2005). Caprolacatam. *Ullmann's Encyclopedia of Industrial Chemistry. Weinheim: Wiley-VCH.*

Srivastava, V. P., Patel, R., Garima, Yadav, L. D. S. (2010). Cyclopropenium ion catalysed Beckmann rearrangement. *Chem. Commun., 46,* 5808-5810.

Tian, B.-X., An, N., Deng, W.-P., Eriksson, L.A. (2013). Catalysts or initiators? Beckmann rearrangement revisited. *J.Org. Chem., 78,* 6782-6785.

Trost, B. M., Fleming, I. (1991). Comprehensive Organic Synthesis, Vol. 6, Chapter 1.1-1.9, (pp. 1-284). Pergamon Press: New York,.

Vanos, C.M., and Lambert, T. H. (2010). Cyclopropenium-activated Beckmann rearrangement. Catalysis versus self-propagation in reported organocatalytic Beckmann rearrangements. *Chem. Sci., 1,* 705-708.

Vanos C. M., Lambert, T. H. (2011). Development of a catalytic platform for nucleophilic substitution: Cyclopropenone-catalyzed chlorodehydration of alcohols, *Angew. Chem. Int. Ed., 50,*12222-12226.

Young, D. C., (2001). Computational chemistry: a practical guide for applying tehniques to real-world problems, (pp. 42, 43, 81, 82). John Wiley & Sons Inc.

Zhao, Y., Truhlar, D. G. (2008). The M06 suite of density functionals for main group thermochemistry, thermochemical kinetics, noncovalent interactions, excited states, and transition elements: two new functionals and systematic testing of four M06-class functionals and 12 other functionals. *Theor. Chem. Acc., 120,* 215-41.

Zhao, Y., Truhlar, D. G. (2006). A new local density functional for main-group thermochemistry, transition metal bonding, thermochemical kinetics, and noncovalent interactions. *J. Chem. Phys., 125,* 1-18.

Zhao, Z. X., Wang, H.Y., Guo, Y. L. (2011). ESI-MS study on transient intermediates in the fast cyclopropenium-activated chlorination reaction of alcohols. *Journal of Mass Spectrometry, 46,* 856–858.

CURRICULUM VITAE

Name Surname **:** Muammer Melin Demirkızak

Place and Date of Birth : Bursa 18/02/1989

E-Mail **:** demirkizak@itu.edu.tr

EDUCATION **:**

B.Sc. **:** Yıldız Technical University, 2011, Faculty of Science and Letters, Department of Mathematics

PUBLICATIONS, PRESENTATIONS AND PATENTS ON THE THESIS:

- **Demirkızak M. M., Sungur F. A.** : An Insight Into Cyclopropenium Activated Beckmann Rearrangement Mechanisms : A Computational Study. *International Congress – 11th Chemical Physics*, October 17-18, 2014 İstanbul, Turkey.
- **Demirkızak M. M., Sungur F. A., Başaran Kınalı A**. : A Computational Approach to Cyclopropenone Activated Chlorodehydarion of Alcohols. *International Congress – 10th European Conference on Computational Chemistry*, August 31 - September 3, 2015 Fulda, Germany.
- **Sungur F. A., Demirkızak M. M.** : Computational Insight to Cyclopropenium Activated Beckmann Rearrangement. *International Congress – 10th European Conference on Computational Chemistry*, August 31 - September 3, 2015 Fulda, Germany.